

IDENTIFICATION OF EPITOPES AND BINDING AFFINITY OF
MONOCLONAL ANTIBODIES AGAINST HUMAN
APOLIPOPROTEIN B-100



A Thesis submitted in Partial Fulfillment of the Requirements for the
Degree of Master of Science in Biochemistry and Biochemical Technology
Suranaree University of Technology
Academic Year 2023

การระบุตำแหน่งอีพิโทปและสัมพรรคภาพการจับของโมโนโคลนอลแอนติบอดี
ต่ออะโปไลโปโปรตีนบี-100 ของมนุษย์



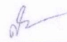
นางสาวทาริกา ศรีตระกูล

วิทยานิพนธ์นี้เป็นส่วนหนึ่งของการศึกษาตามหลักสูตรปริญญาวิทยาศาสตรมหาบัณฑิต
สาขาวิชาชีวเคมีและเทคโนโลยีชีวเคมี
มหาวิทยาลัยเทคโนโลยีสุรนารี
ปีการศึกษา 2566

IDENTIFICATION OF EPITOPES AND BINDING AFFINITY OF MONOCLONAL ANTIBODIES AGAINST HUMAN APOLIPOPROTEIN B-100

Suranaree University of Technology has approved this thesis submitted in
partial fulfillment of the requirement for a Master's Degree.

Thesis Examining Committee



(Assoc. Prof. Dr. Saengduen Moonsom)

Chairperson



(Assoc. Prof. Dr. Panida Khunkaewla)

Member (Thesis Advisor)



(Prof. Dr. James R. Ketudat-Cairns)

Member



(Assoc. Prof. Dr. Jaruwan Siritapetawee)

Member



(Assoc. Prof. Dr. Yupaporn Ruksakulpiwat)

Vice Rector for Academic Affairs
and Quality Assurance



(Prof. Dr. Santi Maensiri)

Dean of Institute of Science

ทาริกา ศรีตระกูล : การระบุตำแหน่งอีพิโทปและสัมพรรคภาพการจับของโมโนโคลนอลแอนติบอดีต่ออะโปไลโปโปรตีนบี-100 ของมนุษย์ (IDENTIFICATION OF EPITOPES AND BINDING AFFINITY OF MONOCLONAL ANTIBODIES AGAINST HUMAN APOLIPOPROTEIN B-100). อาจารย์ที่ปรึกษา : รองศาสตราจารย์ ดร.พนิดา ชันแก้วหล้า, 109 หน้า.

คำสำคัญ: ตำแหน่งจับ (binding site) โมโนโคลนอลแอนติบอดีต่อ แอล ดี แอล (mAb-LDL) อะโปไลโปโปรตีนบี-100 สัมพรรคภาพการจับ

ไลโปโปรตีนความหนาแน่นต่ำ ในระดับสูงเป็นหนึ่งในสาเหตุหลักของภาวะหลอดเลือดแข็ง มอนอโคลนอลแอนติบอดีต่อไลโปโปรตีนความหนาแน่นต่ำ ได้รับการรายงานว่าสามารถลดขนาดของคราบพลัคในผนังหลอดเลือด ซึ่งอาจนำไปใช้สำหรับการพัฒนารักษาโรคได้ มอนอโคลนอลแอนติบอดีที่จำเพาะต่อ ไลโปโปรตีนความหนาแน่นต่ำของมนุษย์ถูกผลิตขึ้นและพบว่าจับแบบจำเพาะกับอะโปไลโปโปรตีนบี-100 ในการศึกษานี้ มอนอโคลนอลแอนติบอดีสามโคลน คือ hLDL-E8 (IgG₁) hLDL-2D8 (IgG_{2b}) และ hLDL-F5 (IgG₁) ได้ถูกแสดงคุณลักษณะเฉพาะสำหรับบริเวณ ซึ่งกำหนดส่วนจำเพาะต่อแอนติเจน (CDRs) อีพิโทปสำหรับจับ และสัมพรรคภาพในการจับ การทดลอง RT-PCR ระบุว่าบริเวณที่แปรผันได้ของแอนติบอดีเหล่านี้ประกอบด้วยโปรตีนสายน้ำหนักร้อยตัวแคปปา และสายหนักแกมมา การหาลำดับดีเอ็นเอแสดงว่าบริเวณที่แปรผันมีขึ้นที่แปรผันได้ในเฟรมที่เหมาะสม ลำดับโปรตีนถูกวิเคราะห์โดยโปรแกรม IMGT เพื่อพิสูจน์เอกลักษณ์ของ CDR โดยเปอร์เซ็นต์ความเหมือนกันที่ยอมรับได้มากกว่า 50% เมื่อเปรียบเทียบกับฐานข้อมูล โครงสร้างส่วนแปรผัน (Fv) ของมอนอโคลนอลแอนติบอดี ถูกสร้างขึ้นโดย SWISS-MODEL โดยมีค่าคะแนน QSQE ที่ยอมรับได้สูงกว่า 0.7 มุมไดฮีดรัลได้รับการวิเคราะห์โดยแผนภาพรามจันทัน และพบว่า 99% ของกรดอะมิโนอยู่ในบริเวณที่ยอมรับได้ อะโปไลโปโปรตีนบี-100 ถูกย่อยด้วยทรมอบินเพื่อสร้างชิ้นส่วนย่อยของอะโปไลโปโปรตีนบี-100 ที่แตกต่างกัน 4 ชิ้น ได้แก่ T1 T2 T3 และ T4 จากการทำให้ Western blot บ่งชี้ว่า hLDL-E8 และ hLDL-F5 จับอย่างจำเพาะกับ T3 ที่กรดอะมิโน 1297-3249 ในขณะที่ hLDL-2D8 จับกับปลาย N ของ T4 ที่กรดอะมิโน 1-1297 ผลลัพธ์เหล่านี้สอดคล้องกับการสอบวิเคราะห์การจับอีพิโทปโดยใช้การสอบวิเคราะห์เอนไซม์-ลิงค์อิมมูโนซอร์เบนต์แอสเสซ (ELISA) แบบยับยั้งพบว่า hLDL-E8 จับที่อีพิโทปที่ต่างกันจาก hLDL-2D8 และมีการทับซ้อนกันบางส่วนกับ hLDL-F5 จากนั้นฐานข้อมูล IEDB ถูกใช้เพื่อทำนายบริเวณการจับหรืออีพิโทปเชิงเส้นของมอนอโคลนอลแอนติบอดีที่จำเพาะต่อไลโปโปรตีนชนิดความหนาแน่นต่ำของมนุษย์

ตามการคาดการณ์ เปปไทด์ 53 ชิ้นของชิ้นส่วน T4 และ 70 เปปไทด์ของชิ้นส่วน T3 ถูกเลือกมาเพื่อทำการคัดกรองเสมือนจริง GOLD และ Autodock Vina ถูกนำมาใช้ในการศึกษาเชิงคำนวณเกี่ยวกับการจำลองการจับกับระดับโมเลกุล เพื่อทำนายอิทธิพลที่จับของ Fv ของแอนติบอดีต่อไลโปโปรตีนชนิดความหนาแน่นต่ำของมนุษย์ และอะโปไลโปโปรตีนบี-100 มอนอโคลนอลแอนติบอดี hLDL-E8 และ hLDL-F5 แสดงการจับสูงสุดกับลำดับกรดอะมิโน ¹⁵⁷⁴EYQADYE¹⁵⁸⁰ และ ²¹⁵⁷YIKDSYD²¹⁶³ ของอะโปไลโปโปรตีนบี-100 แบบเต็มความยาว ในขณะที่ มอนอโคลนอลแอนติบอดี hLDL-2D8 มีคะแนน GOLD สูงที่สุดเมื่อจับกับลำดับกรดอะมิโน ⁶⁴⁵DPNNYLPKES⁶⁵⁴ ของ อะโปไลโปโปรตีนบี-100 ตำแหน่งการจับอิทธิพลที่คาดการณ์ไว้ของมอนอโคลนอลแอนติบอดีกับเปปไทด์อะโปไลโปโปรตีนบี-100 ได้ทำการยืนยันโดยการทดลองด้วยวิธี ELISA ผลลัพธ์บ่งชี้ว่า มอนอโคลนอลแอนติบอดี hLDL-E8 จับกับอะโปไลโปโปรตีนบี-100 ที่ลำดับกรดอะมิโนในช่วง 2050 ถึง 2166 โดยมีค่า OD 0.24343 ถึง 0.31347 hLDL-2D8 จับกับโอลิโกเปปไทด์ที่กรดอะมิโนเรซิดูว 712 ถึง 722 ในขณะที่ใช้ hLDL-F5 ไม่มีการสังเกตสัญญาณที่มีปฏิสัมพันธ์กับโอลิโกเปปไทด์ใด ซึ่งอาจเกิดจากการทำนายผิดหรือสัมพรรคภาพการจับของแอนติบอดีต่ำ สุดท้าย สัมพรรคภาพการจับของมอนอโคลนอลแอนติบอดีกับไลโปโปรตีนความหนาแน่นต่ำ ได้ถูกตรวจวัดโดยเทคนิค ELISA และคำนวณจากสมการของ Beatty ถูกใช้เพื่อวัดหาค่าคงที่สัมพรรคภาพ ผลลัพธ์ชี้ให้เห็นว่า มอนอโคลนอลแอนติบอดี hLDL-2D8 hLDL-E8 และ hLDL-F5 มีค่าคงที่สัมพรรคภาพเฉลี่ยอยู่ที่ $1.51 \pm 0.69 \times 10^9 \text{ Mol}^{-1}$ $7.25 \pm 3.56 \times 10^8 \text{ Mol}^{-1}$ และ $4.39 \pm 2.63 \times 10^6 \text{ Mol}^{-1}$ ตามลำดับ นอกจากนี้ คุณลักษณะของความเข้มข้นของแอนติบอดีที่ OD=50 บนเส้นกราฟการตอบสนองต่อปริมาณของแอนติบอดี เผยให้เห็นว่า มอนอโคลนอลแอนติบอดี hLDL-F5 มีแนวโน้มที่จะจดจำสองอิทธิพลบนอะโปไลโปโปรตีนบี-100 ในขณะที่ hLDL-2D8 และ hLDL-E8 จดจำอิทธิพลเดียวบนอะโปไลโปโปรตีนบี-100 การค้นพบเหล่านี้ได้ให้การสนับสนุนที่จะเป็นประโยชน์สำหรับการใช้งานมอนอโคลนอลแอนติบอดีเหล่านี้ต่อไปสำหรับการวิจัยในห้องปฏิบัติการและทางคลินิก

TARIGA SRITRAKARN : IDENTIFICATION OF EPITOPES AND BINDING AFFINITY OF
MONOCLONAL ANTIBODIES AGAINST HUMAN APOLIPOPROTEIN B-100. THESIS
ADVISOR : ASSOC. PROF. PANIDA KHUNKAEWLA, Ph.D. 109 PP.

Keywords: Binding epitope, Monoclonal antibody, Apolipoprotein B-100, Binding affinity

A high level of low-density lipoprotein (LDL) is known as one of the major causes of atherosclerosis. Some monoclonal antibodies (mAbs) to LDL were reported to reduce atherosclerotic plaque size, which may be applicable for therapeutic drug development. In-house mAbs that are specific to human LDL were produced and found to specifically bind to apolipoprotein B-100. In this study, three mAb clones hLDL-E8 (IgG₁), hLDL-2D8 (IgG_{2b}) and hLDL-F5 (IgG₁) were characterized for their complementarity determining regions or CDRs, binding epitopes and binding affinity. RT-PCR experiment indicated that the variable regions of these antibodies are composed of kappa light chains and gamma heavy chains. DNA sequencing revealed that variable regions have a proper in-frame variable gene. The protein sequence was analyzed by IMGT for CDR identification with an acceptable percentage identity more than 50% compared to databases. The variable fragment (Fv) structures of the mAbs were constructed by SWISS-MODEL with an acceptable QSQE score value above 0.7. The backbone dihedral angle was analyzed by Ramachandran plot and it was found that 99% of the amino acid residues are in acceptable regions. ApoB protein was digested with thrombin to generate 4 different apoB-100 fragments including T1, T2, T3 and T4. Western blot indicated that hLDL-E8 and hLDL-F5 specifically bind to T3 which includes amino acid residues 1297-3249, while hLDL-2D8 binds to the N-terminus of T4 which includes amino acid residues 1-1297. These results are consistent with epitope binding assay using an inhibition enzyme-linked immunosorbent assay (ELISA), in which hLDL-E8 binds at different epitopes from hLDL-2D8 and has some overlap with hLDL-F5. The IEDB database was used to predict a binding region or linear epitope of the hLDL-specific mAbs. According to the prediction, 53 peptides of T4 fragment and 70 peptides of T3 fragment were chosen for virtual screening.

GOLD and Autodock Vina were used for computational studies on molecular docking to predict the binding epitope of hLDL-mAbs Fv and apoB-100 peptides. The mAbs hLDL-E8 and hLDL-F5 showed highest binding to the amino acid sequences ¹⁵⁷⁴EYQADYE¹⁵⁸⁰ and ²¹⁵⁷YIKDSYD²¹⁶³ of full-length apoB-100, while mAb hLDL-2D8 had the highest GOLD score with the sequence ⁶⁴⁵DPNNYLPKES⁶⁵⁴ of apoB-100. The predicted epitope binding sites of the mAbs to apoB-100 peptides was experimentally confirmed by ELISA. The results indicated that mAb hLDL-E8 binds to apoB-100 at amino acid residues in the range of 2050 to 2166 with OD values 0.24343 to 0.31347. The mAb hLDL-2D8 bound to a peptide including amino acid residues 712 to 722. No interacting signal to any peptide was observed for mAb hLDL-F5, which may be caused by either misprediction or low binding affinity of the antibody. Finally, the binding affinity of monoclonal antibodies to apoB-100 was determined by the ELISA technique, and Beatty's equation was used to determine the affinity constant. The results suggested that mAbs hLDL-2D8, hLDL-E8 and hLDL-F5 have an average affinity constant value of $1.51 \pm 0.69 \times 10^9 \text{ Mol}^{-1}$, $7.25 \pm 3.56 \times 10^8 \text{ Mol}^{-1}$ and $4.39 \pm 2.63 \times 10^6 \text{ Mol}^{-1}$, respectively. In addition, the antibody concentration at OD-50 on the dose-response curve revealed that mAbs hLDL-F5 tend to recognize two epitopes of apoB-100, while hLDL-2D8 and hLDL-E8 recognized a single epitope of apoB-100. These findings contribute valuable information for further use of these mAbs for laboratory and clinical research.

ACKNOWLEDGEMENTS

I would like to express my deepest appreciation to my thesis advisor Assoc. Prof. Dr. Panida Khunkaewla for providing me with a great opportunity to work on this project. Without her valuable time for guiding, unconditional support, inspiration and encouragement, this thesis could not be accomplished.

I am also deeply grateful to all Biochemistry instructors at Suranaree University of Technology for providing me many valuable knowledge and techniques in Biochemistry. Besides, I would like to thank Dr. Kanokwan Lowhalidanon, and Mr. Aekkapot Chamkasem for giving me knowledge required for this work and all friends in Biochemistry-Electrochemistry Research Unit, Suranaree University of Technology for supporting me through this M.Sc. journey.

I would like to thank all committee members, Assoc. Prof. Dr. Saengduen Moonsom, Prof. Dr. James R. Ketudat-Cairns and Assoc. Prof. Dr. Jaruwan Siritapetawee.

My special thanks go to the Development and Promotion of Science and Technology scholarship for the financial support, and Biochemistry-Electrochemistry Research Unit, Suranaree University of Technology for providing research facilities. This research would not have been possible without their support.

Finally, I would like to express my great gratitude to my parents for their love and encouragement through this study.

Tariga Sritrakarn

CONTENTS

	Page
ABSTRACT IN THAI.....	I
ABSTRACT IN ENGLISH.....	III
ACKNOWLEDGMENTS.....	V
CONTENTS.....	VI
LIST OF TABLES.....	IX
LIST OF FIGURES.....	X
LIST OF ABBREVIATIONS.....	XII
CHAPTER	
I INTRODUCTION	1
1.1 Significance of research	1
1.2 Objectives	3
1.3 Literature review	3
1.3.1 Lipoproteins.....	3
1.3.2 Apolipoproteins.....	6
1.3.3 The immune system in atherosclerosis	9
1.3.4 Biochemical structure of antibody.....	11
1.3.5 Antigen-antibody interaction	14
1.3.6 Complementarity-determining regions (CDRs).....	16
1.3.7 Ag-Ab interaction studies	22
II MATERIALS AND METHODS.....	27
2.1 Reagents.....	27
2.2 Software used in the study.....	29

CONTENTS (Continued)

	Page
2.3 Preparation of monoclonal antibodies against human LDL	30
2.3.1 Cultivation of hybridoma cell producing mAbs to human LDL	30
2.3.2 Isotypic determination	30
2.3.3 Monoclonal antibody purification by affinity chromatography	30
2.3.4 Determination of antibody activity by indirect ELISA	31
2.3.5 Purity determination of the purified mAbs by SDS-PAGE	31
2.4 Amplification of monoclonal antibody variable region	32
2.4.1 Total RNA extraction and cDNA synthesis	32
2.4.2 Amplification of cDNA using PCR	32
2.5 DNA sequence analysis	33
2.6 Computational modeling of antibody Fv region	33
2.7 Cleavage of LDL and apoB-100 using thrombin	33
2.7.1 Western blot analysis of mAbs reactivity	34
2.8 Computational docking and simulations of mAb Fv region with apoB-100	34
2.9 Epitope binding analysis by inhibition ELISA	36
2.10 Affinity determination of apoB-100 specific mAbs by indirect ELISA	36
2.10.1 Titration of human apoB-100 concentration	36
2.10.2 Experimental dose-response curves for anti-human LDL mAbs	37
2.10.3 Calculation of affinity constant	37
2.11 Peptide ligand-based indirect ELISA analysis	38
III RESULTS	40
3.1 Production of the purified mAbs against human LDL	40

CONTENTS (Continued)

	Page
3.1.1 Purity of the generated mAbs against human LDL	40
3.1.2 Activity of the purified mAbs	43
3.2 Sequencing of the variable region of hLDL-mAbs	44
3.3 Computational modeling of antibody Fv region	48
3.4 Screening of mAbs binding regions by thrombin digestion and Immune Epitope Database (IEDB) prediction	53
3.5 Characterization of the mAb epitope binding	57
3.6 Computational docking and simulations of mAbs Fv region with apoB-100	59
3.7 Confirmation epitope binding sites on apoB-100 by ELISA	62
3.8 Binding affinity determination of apoB-specific mAbs by indirect ELISA	66
IV DISCUSSION AND CONCLUSION	76
REFERENCES	82
APPENDICES	91
APPENDIX A PERMISSION LETTER	92
APPENDIX B LIST OF CHEMICALS AND MATERIALS	95
APPENDIX C LIST OF INSTRUMENTS	98
APPENDIX D REAGENTS AND BUFFER PREPARATION	100
CURRICULUM VITAE	109

LIST OF TABLES

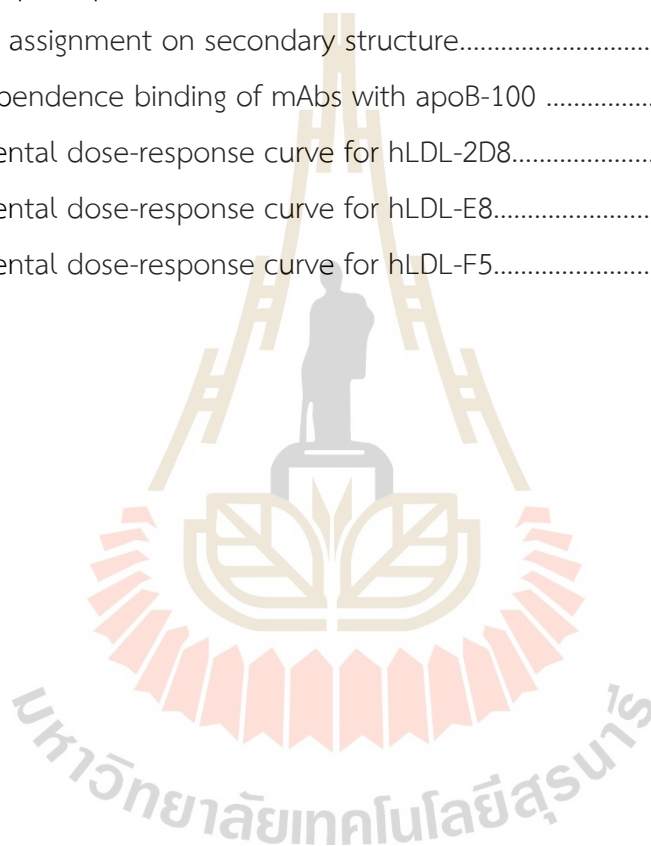
Table	Page
1.1 Types and functions of human apolipoproteins.....	6
1.2 Antibody isotypes and their functions.....	13
1.3 List of amino acids in CDRs.....	18
1.4 Databases containing information on antibody structure and sequence.....	21
2.1 Mouse IgG (mIgG) primers.....	28
2.2 List of software containing information biological databases.....	29
2.3 Synthetic peptides fragments of the human apoB-100.....	39
3.1 Production yield of the purified hLDL-mAbs.....	41
3.2 Complementarity-determining region.....	47
3.3 SWISS-MODEL Homology Modelling Report.....	49
3.4 Scoring values of T3 and T4 apoB-100 fragments	57
3.5 Summary of inhibition analysis of the generated mAbs against human LDL.....	59
3.6 Calculated affinity constants (K_{aff}) of mAb hLDL-2D8.....	72
3.7 Calculated affinity constants (K_{aff}) of mAb hLDL-E8	73
3.8 Calculated affinity constants (K_{aff}) of mAb hLDL-F5.....	74
3.9 Conclusion of characteristics of three mAbs on apoB-100.....	75

LIST OF FIGURES

Figure	Page
1.1 Composition and main physical-chemical properties.....	4
1.2 Metabolism of apoB-containing lipoproteins.....	5
1.3 Schematic of human apoB-100.....	7
1.4 Amino acids sequence of eight putative glycosaminoglycan.....	8
1.5 The atherosclerotic plaque progression.....	10
1.6 Antibody structure and genetic encoding.....	12
1.7 Types of non-covalent interactions.....	14
1.8 The nature of antigenic determinants.....	15
1.9 The Ab Fv region.....	17
1.10 Theoretical ELISA curve response.....	24
2.1 Monoclonal antibody Fv modeling and molecular docking simulations.....	35
3.1 Purity of purified mAbs against human LDL.....	42
3.2 Binding activity of the purified mAbs against human LDL.....	43
3.3 Agarose gel electrophoresis.....	46
3.4 Sequence alignment.....	47
3.5 Computational modeling Fv structure hLDL-2D8.....	50
3.6 Computational modeling Fv structure hLDL-E8.....	51
3.7 Computational modeling Fv structure hLDL-F5.....	52
3.8 The amino acid residues thrombin cleavage site.....	53
3.9 Immunoblots of thrombin fragments of LDL and apoB-100.....	54
3.10 The linear epitope prediction generated by the IEDB server of T3.....	55
3.11 The linear epitope prediction generated by the IEDB server of T4.....	56

LIST OF FIGURES (Continued)

Figure	Page
3.12 Percent inhibition among each mAb analyzed by inhibition ELISA.....	58
3.13 The docking score.....	61
3.14 Epitope binding region confirmation.....	63
3.15 Linear map of apoB-100.....	64
3.16 Epitopes assignment on secondary structure.....	65
3.17 Dose dependence binding of mAbs with apoB-100	68
3.18 Experimental dose-response curve for hLDL-2D8.....	69
3.19 Experimental dose-response curve for hLDL-E8.....	70
3.20 Experimental dose-response curve for hLDL-F5.....	71



LIST OF ABBREVIATIONS

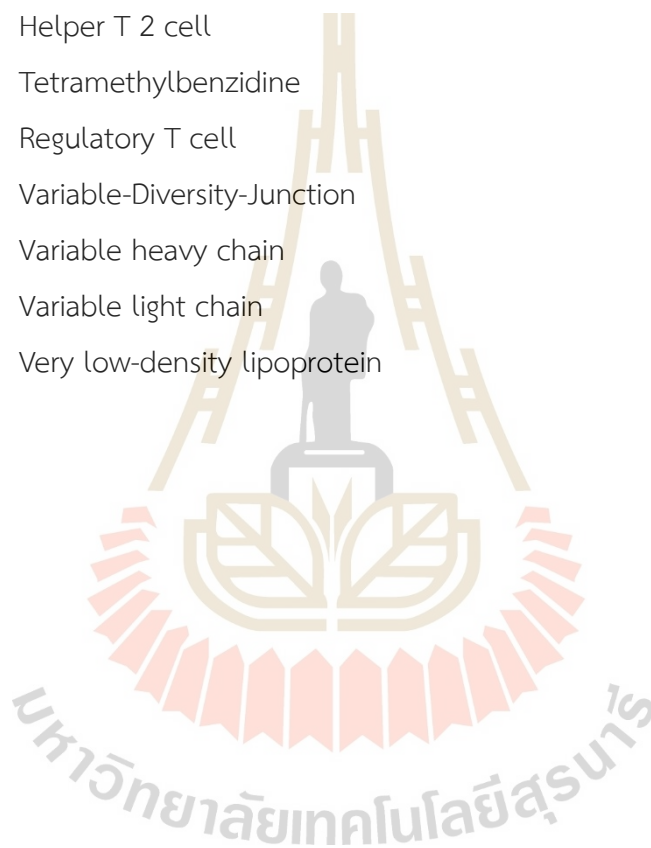
Ab	Antibody
AbRSA	Antibody Region-Specific Alignment
ADCC	Antibody-Dependent Cellular Cytotoxicity
Ag-Ab	Antigen-Antibody
ANARCI	Antigen receptor numbering and receptor classification
Apo	Apolipoprotein
BCA	Bicinchoninic acid
CDC	Complement-Dependent Cytotoxicity
cDNA	complementary DNA
CDRs	Complementarity-Determining Regions
CH	Constant domains (heavy chain)
CL	Constant domains (light chain)
CM	Chylomicron
CVD	Cardiovascular disease
DC	Dendritic cells
dNTPs	Deoxy nucleotide triphosphates
EDTA	Ethylenediaminetetraacetic acid
ELISA	Enzyme-linked immunosorbent assay
Fab	Fragment antigen binding domain
FBS	Fetal Bovine Serum
Fv	Variable fragment
GAGs	Glycosaminoglycans
HCS	Heavy chains
HDL	High density lipoprotein
HRP	Horseradish peroxidase

LIST OF ABBREVIATIONS (Continued)

HSPG	Heparan sulfate proteoglycan
IDL	Intermediate density lipoprotein
IEDB	Immune epitope database
Ig	Immunoglobulin
IMDM	Iscoe's Modified Dulbecco's Medium
IMGT	ImMunoGeneTics information system
ITC	Isothermal titration calorimetry
K_a	Association constant
K_d	Dissociation constant
kDa	Kilo Dalton
LCAT	Lecithin cholesterol acyl transferase
LCs	Light chains
LDL	Low density lipoprotein
LDLR	Low density lipoprotein receptor
LPL	Lipoprotein lipase
LRP	Lipoprotein receptor-related protein
mAb	Monoclonal antibody
mIGK	Immunoglobulin G kappa light chain
mIGL	Immunoglobulin G lambda light chain
mIGHG	Immunoglobulin G heavy chain
oxLDL	Oxidized low density lipoprotein
PBS	Phosphate buffer saline
PBST	Tween20 in phosphate buffer saline
PDB	Protein Data Bank
PGs	Proteoglycans
PyIgClassify	Phyton-based immunoglobulin classification
RMSD	Root-mean-square deviation
RT	Room temperature

LIST OF ABBREVIATIONS (Continued)

RT-PCR	Reverse transcription polymerase chain reaction
SDS-PAGE	Sodium dodecyl sulfate polyacrylamide gel electrophoresis
SPR	Surface plasmon resonance
TG	Triglyceride
Th1	Helper T 1 cell
Th2	Helper T 2 cell
TMB	Tetramethylbenzidine
Treg	Regulatory T cell
V-D-J	Variable-Diversity-Junction
VH	Variable heavy chain
VL	Variable light chain
VLDL	Very low-density lipoprotein



CHAPTER I

INTRODUCTION

1.1 Significance of research

According to the World Health Organization report in 2021, cardiovascular disease (CVD) caused 17.9 million deaths in 2019, representing 32% of total global deaths (WHO, 2021). Low-density lipoprotein (LDL) is a major cholesterol carrier in circulation, which is considered as one of the major risk factors that promote the progression of atherosclerotic cardiovascular disease.

Initiation of atherosclerosis involves the accumulation of LDL in the subendothelial extracellular space within the arterial wall. Plasma LDL particles can bind to proteoglycans of the extracellular matrix through ionic interactions, which trap them in the arterial wall to promote the atherogenic process. LDL oxidation plays a crucial role in atherosclerotic plaque formation as oxidized LDL (oxLDL) can be taken up by smooth muscle cells, endothelial cells and macrophages (Tian et al., 2020). Thus, plasma LDL concentration is used in determining the level of circulating atherogenic lipoproteins and their metabolism. LDL particle contains apolipoprotein B-100 (apoB-100), which acts as a principal ligand that can be recognized by the LDL receptor leading to LDL-receptor mediated endocytosis.

ApoB can be categorized into two major forms, full-length apoB-100 containing 4536 amino acid residues found as an integral component of LDL and a truncated form consisting of the N-terminal 2152 amino acids (apoB-48), which is found mainly in chylomicrons (Behbodikhah et al., 2021). The amino acid sequence of apoB-100 has been deduced from its mRNA sequence, leading us to map the epitopes defined by their specific antibodies (Krul et al., 1988).

Several studies revealed that the binding regions of apoB-100 by mAbs or LDL-receptor consist of a small linear sequence of about 10 amino acids, which is a proteoglycan-binding region. Additionally, the principal proteoglycan binding site of apoB-100 was also identified and named as the site B (residues 3359-3369) (Flood et al., 2002).

According to the growing number of monoclonal antibodies (mAbs) produced against human LDL, current information about epitope mapping on the amino acid sequence of apoB-100 has been characterized and suggests that this molecule contains several epitope binding sites.

Several pharmacological and clinical studies on atherosclerosis revealed that antibodies specific to the epitope of oxLDL show atheroprotective effects, such as abatement of atherosclerotic plaque size and inflammation (Ji and Lee, 2021; Smeets et al., 2022). Therefore, the recognition site for LDL that directly interacts with antibodies is important for research and medical applications.

In our laboratory, monoclonal antibodies against human LDL have been generated and bound specifically to apoB-100 of LDL particles, however their specific binding sites on apoB-100 have not been identified.

In general, a mAb contains two variable regions that are composed of six hypervariable loops of complementarity-determining regions (CDRs). Therefore, antibody sequence analysis of our newly generated mAbs against human LDL will provide more information about their structure and specific binding mode of these antibodies, which is a critical point for further study on the apoB-antibody interaction at the molecular level.

Firstly, the antigen-binding site or paratope was identified according to numbering of amino acid residues of antibodies or CDR regions on the variable fragment (Fv). Several methods, based on the random automatic learning techniques with specificity as high as 80% and implemented on free and easy-to-use servers (AbRSA, IMG2, IgBLAST) have been exploited to correctly define these CDRs of the antibody recognition site (Olimpieri et al., 2013).

Rational design for prediction of the antigen-antibody interaction using computational molecular docking is one of the foremost methods for potential

therapeutic antibody development. However, accurate estimation is challenging due to computational inaccuracy and unreliable binding predictors. Therefore, the information obtained from the computational prediction needs to be confirmed by various experimental assays such as enzyme-linked immunosorbent assay (ELISA) and Western blot.

The obtained results will be useful for further development of therapeutic antibodies or diagnostic tools for atherosclerotic plaque progression.

1.2 Objectives

1.2.1 To identify CDRs of in-house monoclonal antibodies against human LDL and their binding epitopes on apoB-100.

1.2.2 To study the binding affinity of monoclonal antibodies on human apoB-100.

1.3 Literature review

1.3.1 Lipoproteins

Lipoproteins are amphiphilic particles containing a central hydrophobic core of non-polar lipids, cholesteryl esters, and triglycerides. The hydrophobic core is surrounded by a monolayer of phospholipids containing free cholesterol and apolipoproteins, which facilitate lipoprotein formation and functions. Lipoproteins are synthesized mainly in the liver and to a lesser extent in the intestine to transport dietary triglyceride and cholesterol to various cells of the body. Based on their size and lipid components, plasma lipoproteins can be categorized into five different groups; chylomicrons (CM) (<0.94 g/ml), very low density (VLDL) (0.94-1.006 g/ml), intermediate density lipoprotein (IDL) (1.006-1.019 g/ml), low density (LDL) (1.019-1.063 g/ml), and high density (HDL) (1.063-1.210 g/ml) lipoproteins (Figure 1.1) (Feingold, 2021).

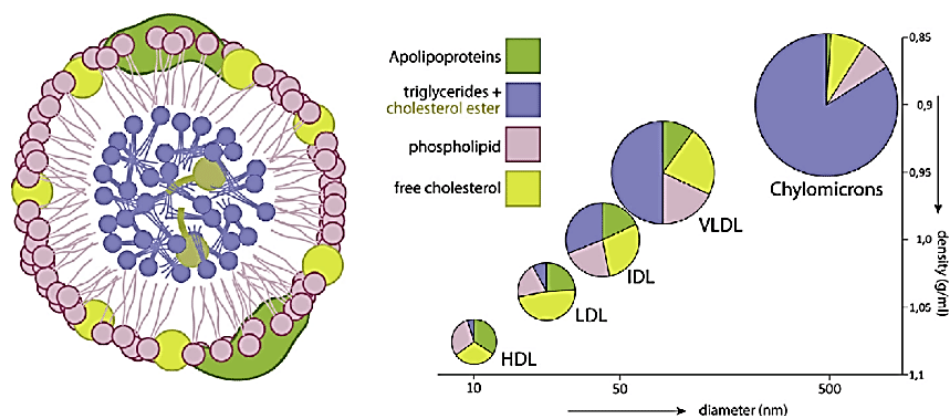


Figure 1.1 Composition and main physical-chemical properties of major lipoprotein classes. The outer shell of lipoproteins consists of phospholipid and cholesterol combined with apolipoproteins that define the type, function and/or destination of the lipoprotein. Hydrophobic lipids (triglycerides, cholesteryl esters) are in the core of the lipoprotein. Adapted from (van Leeuwen et al., 2018).

Transportation of lipids in our body can be divided into two major pathways. The exogenous pathway is involved in transporting dietary fats from the small intestine to peripheral tissues in the form of chylomicrons and disassembly into chylomicron remnants, which will then be taken up by the liver. The endogenous pathway is involved in transporting synthesized lipids from the liver to the extrahepatic tissues as VLDL. Triglycerides of VLDL are transported to the tissues by the action of lipoprotein lipase (LPL), leading to transformation of VLDL to IDL and cholesterol-rich LDL, respectively. These LDL particles mainly contain cholesteryl esters and apoB-100 that deliver cholesterol to peripheral tissues and the liver. HDL picks up excess cholesterol and delivers it to the liver for use or disposal (Figure 1.2). A high level of LDL particles in circulation is principally pro-atherogenic to decrease affinity for the LDL receptor-mediated uptake and removal, while a high level of HDL is protective against atherosclerosis.

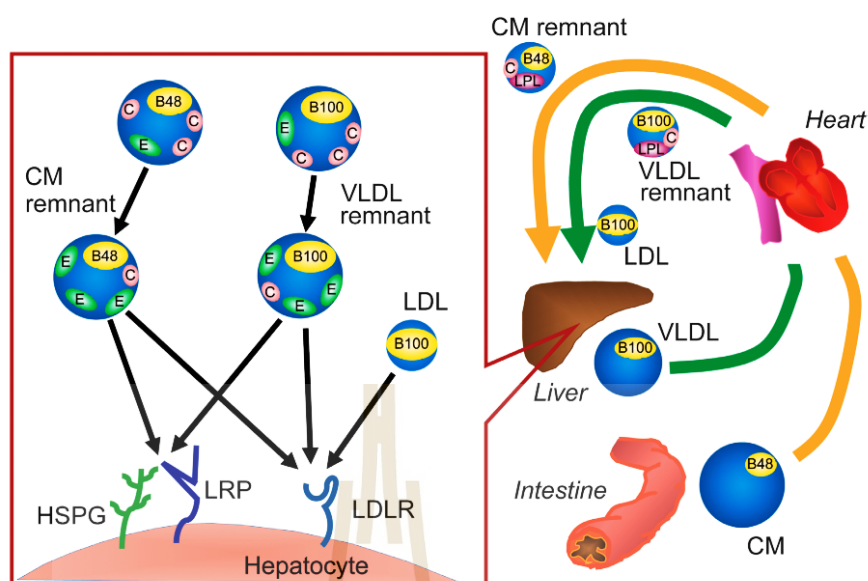


Figure 1.2 Metabolism of apoB-containing lipoproteins. CM with apoB-48 and VLDL with apoB-100 are secreted from the intestine and liver, respectively. In the bloodstream, CM remnants are formed by the LPL-mediated lipolysis, which is activated by apoC-II. The lipolysis converts VLDL to VLDL remnants and subsequently to LDL. LDL is taken up into the hepatocytes by low-density lipoprotein receptor (LDLR). ApoE-enriched lipoprotein remnants are internalized by hepatocytes through LDLR or heparan sulfate proteoglycan (HSPG)-lipoprotein receptor-related protein (LRP) pathways. ApoCs prevent the apoE-mediated hepatic uptake of lipoprotein remnants. Adapted from (Morita, 2016).

1.3.2 Apolipoproteins

Apolipoproteins are proteins of the various lipoproteins that regulate lipoprotein metabolism and determine the unique roles of lipoproteins in lipid metabolism. Functions of apolipoproteins are involved in transportation and redistribution of lipids among various tissues via recognition of specific apolipoproteins by cell surface lipoprotein receptors and maintenance of the structure of the lipoprotein particles. The major apolipoproteins include the exchangeable apolipoproteins; apoA-I, apoA-II, apoA-IV, apoC-I, apoC-II, apoC-III and apoE. Non-exchangeable is apolipoprotein apoB (apoB-100 and apoB-48), which is larger and more water soluble than the exchangeable type. Information about apolipoproteins is shown in Table 1.1 (Mahley et al., 1984).

Table 1.1 Types and functions of human apolipoproteins.

Apolipoprotein	Molecular weight (Da)	Function(s)
apoA-I	28,000	- Structural component of HDL - Lecithin: cholesterol acyl transferase (LCAT) activation
apoA-II	17,400	- Structural component of HDL
apoB-100	512,000	- Structural component of VLDL, LDL, IDL - Ligand for LDL receptor
apoB-48	264,000	- Structural component of CM and CM remnant
apoC-II	8,900	- Lipoprotein lipase (LPL) activation cofactor
apoC-III	8,800	- Inhibition of LPL
apoE	33,000	- Receptor ligand for LDL VLDL and CM remnant

ApoB-100 is a major protein component of LDL that plays an important role in lipid transport and maintenance of cholesterol homeostasis. The secondary structure of apoB-100 is characterized by a large content of alpha-helix (~50%), beta-sheet (~11%), beta-turn (~27%) and random coil (~13%) (Morita et al., 2003). An apoB exists in two distinct forms, apoB-100 and apoB-48. Both forms are products of the same structural gene located on chromosome 2 (Young et al., 1986). Human apoB-100 is a large glycoprotein comprising 4536 amino acids synthesized in the liver, which is a constituent of VLDL, IDL and LDL. ApoB-100 is responsible for the hepatic clearance of LDL via low-density lipoprotein receptor (LDLR) or heparan sulfate proteoglycan (HSPG)-lipoprotein receptor-related protein (LRP) pathways. HSPG is a remnant receptor acting either independently or in concert with LRP in the clearance of cholesterol-rich lipoproteins (Figure 1.2). ApoB-100 also plays a certain role in maintaining the structural integrity of lipoprotein particles and in controlling their interaction with LDLR (Esser et al., 1988). ApoB-48 is synthesized in the intestine where the mRNA undergoes editing, resulting in a premature stop codon resulting in a shorter protein of 2152 amino acids within chylomicrons. The existing evidence suggests that apoB-48 neither participates in the particle interaction with the hepatic remnant receptor nor contains an LDL receptor-binding domain (Cooper, 1997; Goldberg et al., 1998).

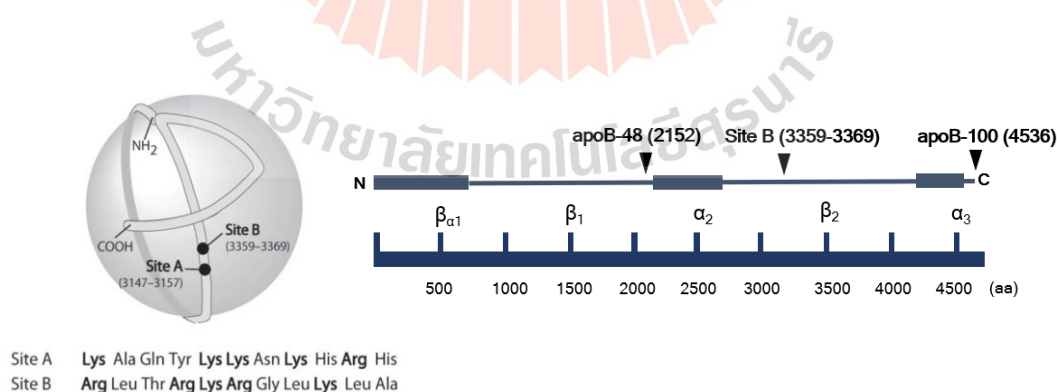


Figure 1.3 Schematic of human apoB-100. The left hand is an LDL particle consisting of two sites (A and B) involved in the binding of apoB-100 (and LDL) to proteoglycans. Adapted from (Olofsson et al., 2007). The right hand is a linear structure of apoB-100 indicating five structural domains.

LDL particles can bind to proteoglycans (PGs) in the subendothelial layer to internalize its particles into the intima of blood vessels. The binding is mediated through ionic interactions between the negatively charged (sulfate and carboxyl groups) of the glycosaminoglycans (GAGs) and the positively charged (lysine and arginine residues) in apoB-100. Two clusters of basic residues (A; 3147–3157 and B; 3359–3369) are presented on the surface of the LDL particle. Site B is the interacting domain of apoB-100 with LDLR, whereas site A is not the primary LDLR binding site. However, apoB-48 is capable of binding proteoglycans despite lacking site B. In addition to LDLR binding, apoB-100 contains at least eight potential proteoglycan binding sites (Figure 1.4).

Site (amino acids)	Amino acid sequence										
B-Ia (15–25) ^a	Asp	Ala	Thr	Arg	Phe	Lys	His	Leu	Arg	Lys	Tyr
B-Ib (84–94) ^a	Ala	Leu	Leu	Lys	Lys	Thr	Lys	Asn	Ser	Glu	Glu
B-II (222–232)	Leu	Asp	Ala	Lys	Arg	Lys	His	Val	Ala	Glu	Ala
B-III (900–910)	Pro	Ser	Pro	Lys	Arg	Pro	Val	Lys	Leu	Leu	Ser
B-IV (2079–2089)	Gln	Phe	Val	Arg	Lys	Tyr	Arg	Ala	Ala	Leu	Gly
B-V (2117–2127)	Ala	Leu	Thr	Lys	Lys	Tyr	Arg	Ile	Thr	Glu	Asn
B-VI (3148–3158)	Ala	Gln	Tyr	Lys	Lys	Asn	Lys	His	Arg	His	Ser
B-VII (3359–3369)	Arg	Leu	Thr	Arg	Lys	Arg	Gly	Leu	Lys	Leu	Ala
B-VIII (3668–3678)	Ser	Ile	Gly	Arg	Arg	Gln	His	Leu	Arg	Val	Ser

^a The first putative glycosaminoglycan binding region was divided into B-Ia (15–25) and B-Ib (84–94).

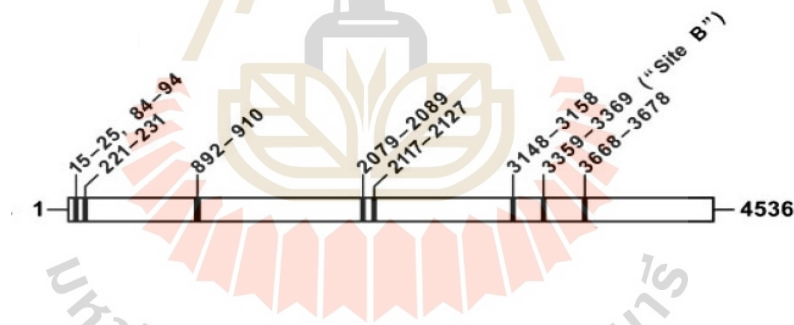


Figure 1.4 Amino acids sequence of eight putative glycosaminoglycan binding regions of apoB-100. Adapted from (Flood et al., 2002).

1.3.3 The immune system in atherosclerosis

The atherosclerotic process begins with apoB-containing LDL cholesterol bound to proteoglycans. When LDL particles are trapped in the intima, they are prone to oxidative modification. Oxidized LDL (oxLDL) can activate endothelial cells and macrophages to produce adhesion molecules and chemokines. The adhesion molecules endothelial surface were upregulated leading to the accumulation of monocytes at the subendothelial space. Under chemokine activation, monocytes become macrophages and upregulate their receptors that finally remove these oxLDL by phagocytosis of oxLDL. This leads to accumulation of remnant cholesterol that leads to the macrophage developing to foam cells that are characteristic of the atherosclerotic lesion, as shown in Figure 1.5. Moreover, several types of immune response cells, such as T cells, B cells, mast cells, and dendritic cells (DC), are also activated and produced during plaque progression.

The immune mechanisms and inflammatory processes are directly involved in the formation of atherosclerotic plaques (Shoenfeld et al., 2001). T cells are more prevalent in the atherosclerotic plaque, where they identify antigenic peptides produced from lipid and endothelial cells and release cytokines that promote inflammation. Although effector T cells in mouse models of atherogenesis promote atherogenesis, regulatory T (Treg) cells transfer is protective. For B cells, their main functions are the generation of humoral immunity in form of antigen-specific antibodies, antigen presentation, and co-stimulation of T cells as well as secretion of a variety of cytokines. Th1 and Th2 cells have also been postulated to play different roles in promoting the inflammatory response (Roselaar et al., 1996). Interestingly, high titers of IgM and IgG antibodies to oxLDL have been found to be associated with cardiovascular disease. Some reports review that the oxLDL-IgG antibody titers were lower, while the oxLDL-IgM antibody titers were higher in atherosclerotic cardiovascular diseases than in the normal group (Li et al., 2016).

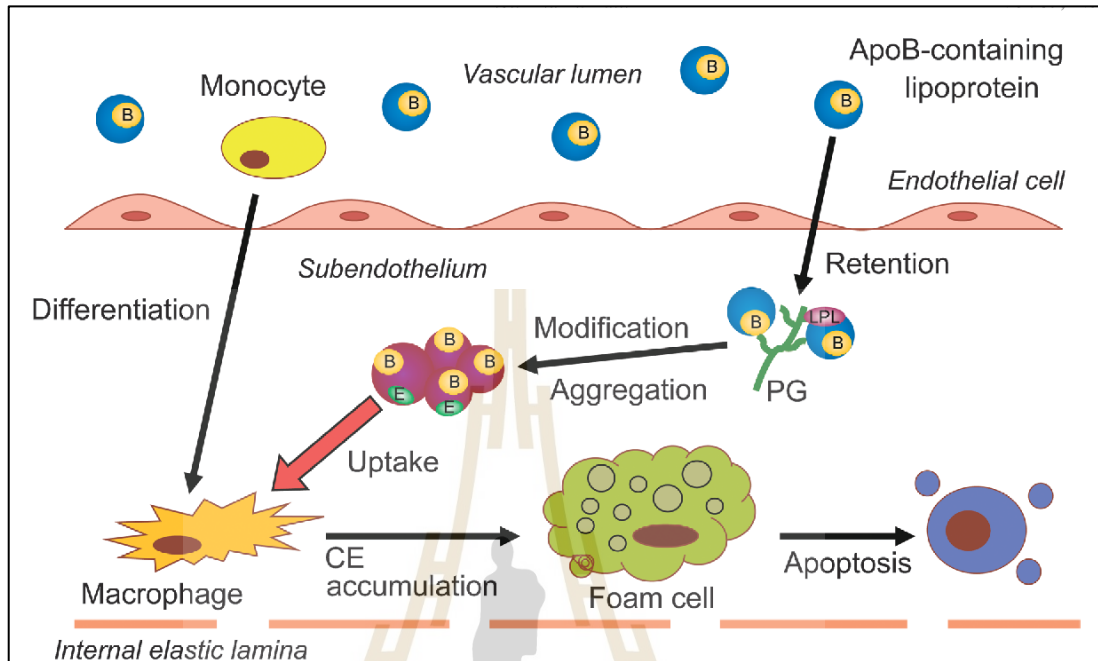


Figure 1.5 The atherosclerotic plaque progression. Starting from the interaction between apolipoprotein B-100 (apoB-100) and proteoglycans increases the possibility that LDL undergo modification. Modified LDL induces endothelial and smooth muscle cells to express monocyte chemotactic activity. LDL that has been aggregated or modified is avidly taken up by macrophages leading to foam cell formation. The conversion of macrophages to foam cells stimulates the release of many proteins including proinflammatory cytokines and bridging molecules. Adapted from (Morita, 2016).

1.3.4 Biochemical structure of antibody

Antibodies (Abs) are secreted by plasma cells derived from B cells, constituting about 20% of the total protein in plasma by weight (Chaffey, 2003). General structures are composed of two identical heavy chains (HCs) and two identical light chains (LCs), which can be one of two functionally similar classes, kappa or lambda. The two HCs and LCs are connected by disulfide bonds to form the arms of a Y-shaped structure. The fragment antigen binding domain (Fab) is composed of two variable domains (variable light chain, VL and variable heavy chain, VH) and two constant domains (CH1 and CL). In the pairing of light and heavy chains, the two variable domains dimerize to form the variable fragment (Fv). Fv contributes to the antigen-binding site that is defined by six hypervariable loops known as complementarity-determining regions (CDRs), three in the light chain (L1, L2, and L3) and three in the heavy chain (H1, H2, and H3). Both VL and VH fold in a manner that brings the hypervariable loops close together to create the antigen-binding site or paratope. The constant (CH2, CH3) regions of heavy chains determine the isotype and effector function of the secreted immunoglobulin. In humans, antibodies are categorized into five classes; IgG, IgM, IgA, IgE, and IgD (Table 1.2) (Amzel and Poljak, 1979).

Antibody (Ab) repertoire biology

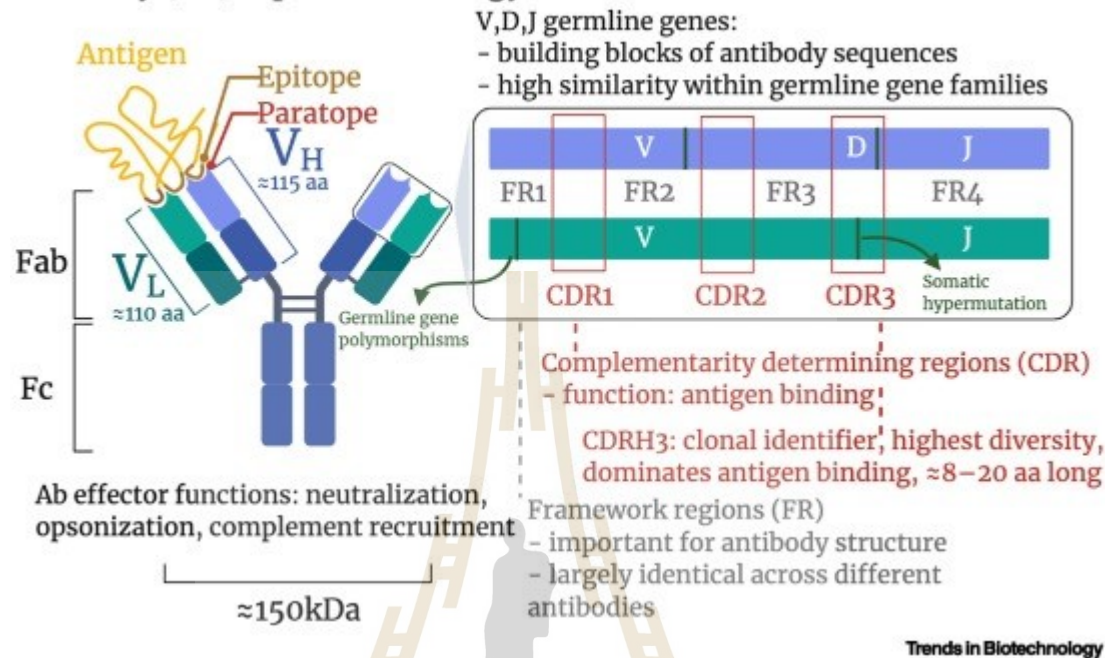


Figure 1.6 Antibody structure and genetic encoding. Stepwise rearrangement of the germline DNA results in the joining of a heavy chain D and J gene segments, followed by joining of a V segment to the D-J product to generate the DNA encoding for the heavy chain variable region. The constant regions of the heavy and light chains (domains CH1, CH2, and CH3 for the heavy chain, and CL for the light chain) are encoded by downstream exons that are joined to the rearranged V(D)J gene by mRNA splicing. Disulfide bridges joining protein chains in the full antibody structure are shown with black dark blue line segments. Adapted from (Snapkov et al., 2022).

Table 1.2 Antibody isotypes and their functions. Adapted by (McComb et al., 2019).

Antibody	Functions	Locations
IgM	<ul style="list-style-type: none"> - Naïve B cell receptor - Early antibody production - Activates the complement system 	<ul style="list-style-type: none"> - Membrane bound, released as a pentamer
IgD	<ul style="list-style-type: none"> - Naïve B cell receptor 	<ul style="list-style-type: none"> - Membrane bound
IgG	<ul style="list-style-type: none"> - Directly neutralize target proteins - Mark targets for phagocytosis - Mark targets for neutrophil degranulation - Aid in complement activation 	<ul style="list-style-type: none"> - Most common antibody in the bodily fluids - Found in monomeric form - Low levels at mucosal sites
IgA	<ul style="list-style-type: none"> - Specialized for neutralization of targets, weakly induces phagocytosis, or complement 	<ul style="list-style-type: none"> - The main antibody found at mucosal site (e.g. intestine and lung) in the dimeric form
IgE	<ul style="list-style-type: none"> - Specialized for activating mast cell which can induce rapid responses, such as in allergies 	<ul style="list-style-type: none"> - Bound to surface receptors upon mast cells

Immunoglobulin gamma (IgG) antibodies comprise 75% of antibodies in circulation, followed by IgA at 15%, IgM at 10%, and IgD and IgE are the least abundant. IgG can be split into 4 subclasses, IgG₁, IgG₂, IgG₃, and IgG₄, in which various heavy chains give a distinctive conformation to the hinge and tail regions of antibodies. Each subclass has its own characteristic properties (Schroeder Jr and Cavacini, 2010) and these four IgG subclasses have almost 90% sequence identity. Each subclass mediates effector activities, including antibody-dependent cellular cytotoxicity (ADCC) and complement-dependent cytotoxicity (CDC), placental transport, long half-life, high antigen binding, and therapeutic antibodies are currently

exclusively found in the IgG class. To investigate novel targets and utilize the effector capabilities of various immune cells, there is interest in creating therapeutic IgG antibodies. However, the expression, purification, and characterization of these have a few difficulties (Vattepu et al., 2022).

1.3.5 Antigen-antibody interaction

The antigen-antibody interaction is a bimolecular reversible association with various non-covalent interactions between the epitope (antigenic determinant) and paratope, a part of the variable region domain of the antibody. Non-covalent interactions consist of electrostatic interactions, hydrogen bonds, hydrophobic interactions, and van der Waals bonds or weak interactions (Figure 1.7), the binding capacity of which is reversible in high ionic strength or extreme pH.

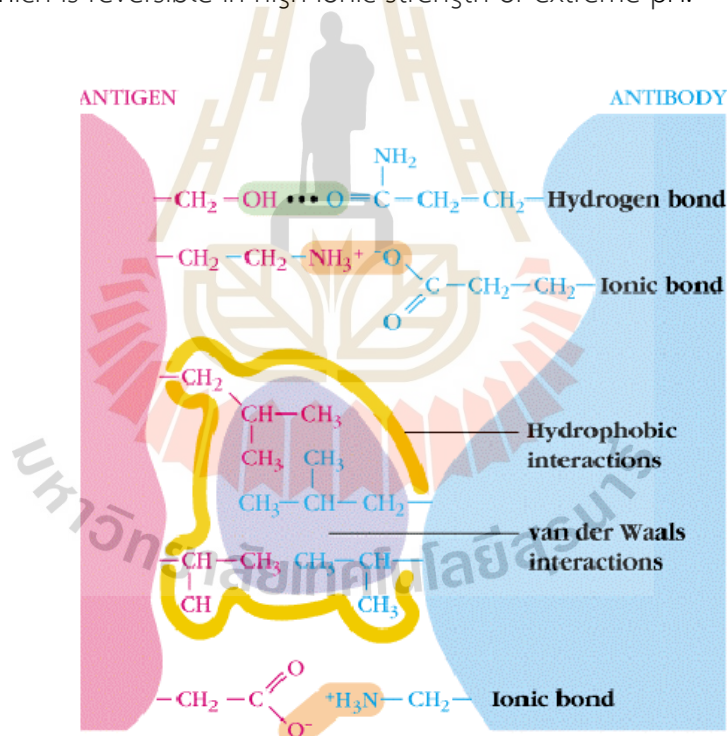


Figure 1.7 Types of non-covalent interactions that form the basis of antigen-antibody (Ag-Ab) binding. Adapted from (Kim et al., 2003).

The Ag-Ab interaction is a type of highly specific binding, and with closely related antigens, the better recognition depends on shapes, geometry, and chemical

characteristics. The antigenic determinants or epitopes are surface areas of antigen that are specifically recognized by an antibody (paratope). Epitopes are commonly classified as either linear or conformational. Linear epitopes are made up continuously of five to ten amino acids that appear when a protein is denatured or digested into several segments. Conformational epitopes are discontinuous and dependent on the native structure and the determinant can be lost by denaturation. Some protein modifications (glycosylation, phosphorylation, ubiquitination, acetylation, and proteolysis) can generate new epitopes called neo-antigenic determinants to be recognized by its specific antibodies (Figure 1.8).

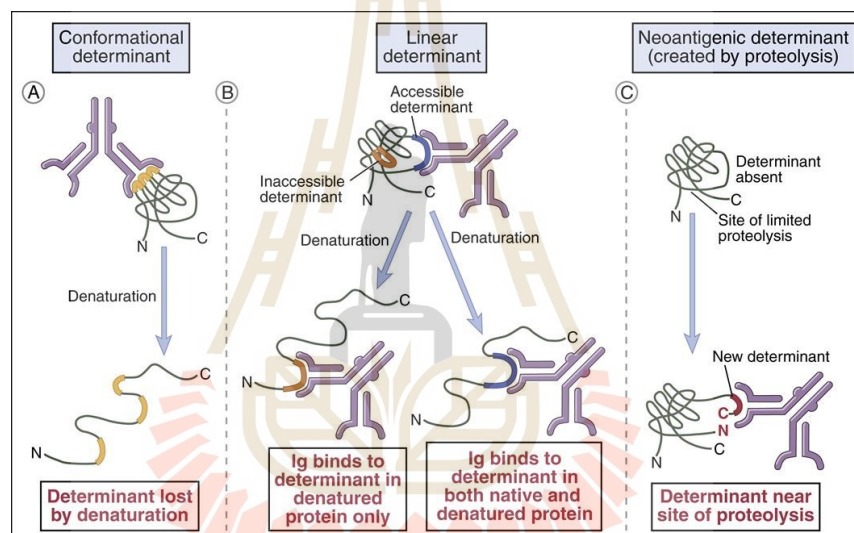


Figure 1.8 The nature of antigenic determinants. Antigenic determinants (shown in orange, red, and blue) may depend on protein folding (conformation) as well as on primary structure. Some determinants are accessible in native proteins and are lost on denaturation (A), whereas others are exposed only on protein unfolding (B). Neo-determinants arise from post synthetic modifications such as peptide bond cleavage (C). Adapted from (Abbas et al., 2010).

For the strength of antigen-antibody interactions including affinity force is defined by the basic thermodynamic principle to describe how much antigen-antibody complex according to the following equation.

$$K_a = \frac{[Ag-Ab]}{[Ab][Ag]}$$

K_a is an association constant and shows the correlations between associated concentration $[Ag-Ab]$, and the dissociated concentrations of antibody $[Ab]$ and antigen $[Ag]$, respectively. K_a can therefore vary widely for antibodies from below $10^5 M^{-1}$ to above $10^{12} M^{-1}$ and other factors can influence it, including temperature, pH, and buffer composition. Antigens and antibodies interactions are categorized as multivalent interactions (binding more than one site). The total binding strength of an antibody is also determined by avidity, including the relation of singular binding (binding affinity), total number of sites involved or valency, and depends on the isotypes switching or structural arrangement, such as IgG is bivalent, and IgM is decavalent to which a greater amount of antigen can bind.

1.3.6 Complementarity-determining regions (CDRs)

The binding site is formed by amino acids located in the CDRs from VL and VH which interact with amino acids of the epitope. The specificity of an antibody to its target is determined by CDRs of beta-sheets with six loops that constitute the CDRs. Each domain contributes three CDRs, consisting of CDR-L1, CDR-L2, and CDR-L3 for VL and CDR-H1, CDR-H2, and CDR-H3 for VH (Figure 1.9). Genetic recombinant of the V, D, and J gene segments for VH and VL (excepted the D segment) with subsequent somatic hypermutation in mature B cells accounting for antibody CDR sequence diversity (Figure 1.6). The underlying assumption of this approach was that CDRs are the most variable residues in the antibody sequence (Wu and Kabat, 1970; Johnson and Wu, 2000). CDRs have unusual sequences that typically lack sequence motifs, or similar elements and are hard to align, therefore leading to misidentifying CDRs loops.

Some residues within CDRs may not contact directly with the antigen but are important to maintain the conformational structure.

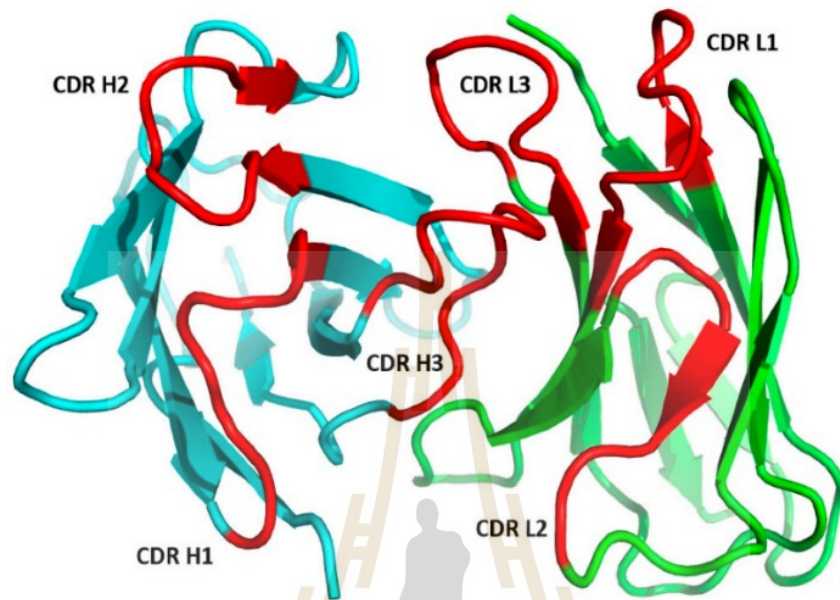


Figure 1.9 The Ab Fv region with the variable heavy chain (VH) in cyan color, the variable light chain (VL) in green color and six complementarity-determining regions (CDR) for both chains in red color. Adapted by (Chiu et al., 2019).

Table 1.3 List of amino acids in CDRs (separating heavy, H and light, L chains). For each amino acid corresponding (X) epitope residues of 140 protein-antibody complexes from the Protein Data Bank (PDB). Adapted from (Ofra et al., 2008).

Amino acid	CDR-L1	CDR-H1	CDR-L2	CDR-H2	CDR-L3	CDR-H3
Tyrosine, Y	x	x	x	x	x	X
Serine, S	x	x	x	x	x	
Asparagine, N	x		x	x	x	X
Tryptophan, W	x	x	x	x	x	X
Threonine, T		x	x	x		
Aspartic acid, D		x		x		X
Histidine, H	x		x		x	
Glycine, G				x		X
Arginine, R			x		x	X
Phenylalanine, F					x	X

Based on the current definitions of CDRs, general antigenic epitope amino acids residues are present in all available protein-antibody complexes, as shown in Table 1.3. Various amino acid residues that constitute the CDRs were identified based on their high variability as compared to the other regions of the antibody. Although the CDR boundaries are free and not limited by the common definitions, two important factors should be considered. First, the CDRs should be as short as possible to minimize the number of amino acid residues affecting species-associated residues. Second, the CDRs should include at least all residues in direct contact with the antigen. All definitions have advantages and disadvantages in terms of CDR grafting. However, the specific interaction pattern of each antibody is important to maintain the correct three-dimensional conformation and specify the physicochemical environment of antibodies (Narciso et al., 2011). Knowing the specific residue is a key aspect in antibody rational design, engineering, and prediction of the conformational structure.

Currently, several existing bioinformatic tools are used to search for antigen-binding sites. Paratome is a tool for identification of antigen-binding regions that define CDRs, but does not provide direct information about binding interaction type of the specific residue (hydrogen bond, hydrophobic, and other non-bonded interactions) (Kunik et al., 2012). Prediction of Antibody Contact (proABC) is a developed server to identify amino acid residues of an antibody that are involved in the probability that its interaction with the cognate antigen. It also builds a 3D model of the antibody, in which residues are colored according to their contact probability (Ambrosetti et al., 2020). IgBLAST is used to approach the germline sequence alignment against pre-annotated databases of germline genes and perform a map of numberings to the query sequence (Ye et al., 2013). Antibody region specific alignment (AbRSA) is another immunoinformatic analysis tool, which is easy-to-use. This method can identify whether a query sequence is heavy or light chain, how the sequence is numbered, and which region is the CDR. AbRSA also improves robustness when numbering the antibodies with diverse patterns according to benchmark test (Li et al., 2019).

Furthermore, computationally predicted structural models can be used to reduce time, cost, and provide a rapid accurate method for prediction. Various methods have revolutionized the field of computational protein structure prediction. For examples, AlphaFold is the top-ranked protein structure prediction that has achieved near experimental accuracy for a large number of proteins (Jumper et al., 2021). ABodyBuilder2 is used to perform an antibody specific model with accuracy of the antibody-specific tools and consistently predicts structure with correct stereochemistry. The SWISS-MODEL is a web server for structural bioinformatics devoted to 3D protein structure homology modeling (Schwede et al., 2003; Biasini et al., 2014), methods of homology (or comparative) modeling using experimental protein structures (also known as "templates") to construct models for proteins that are evolutionary related (also known as "targets"). Other software choices are listed in Table 1.4. The root-mean square deviation (RMSD) between predicted and true structure for each Fv was computed by aligning each antibody chain to the crystal structure and then calculating the RMSD (Abanades et al., 2022). These servers use

for antibody modeling provide a paratope residue prediction (Krawczyk et al., 2013), epitope patch prediction (Krawczyk et al., 2014), and aid decisions about which mutation can be made to enhance or at least not disrupt binding properties. Moreover, correct identification of B-cell epitope within an antigenic protein may permit the design of molecules and could be used to raise specific antibodies to promote protective immunity (Sela-Culang et al., 2013).



Table 1.4 Databases containing information and servers providing predictions and analysis on antibody structure and sequence.

Method	Definition	Weblink	Ref
proABC	Predict CDR, 3D models of antibody	https://wenmr.science.uu.nl/proabc2/	(Ambrosetti et al., 2020)
ANARCI	Align sequence of variable domain from several species	https://opig.stats.ox.ac.uk/webapps/newsabdab/sabpred/anarci/	(Dunbar and Deane, 2016)
AbRSA	Query sequence is an antibody heavy or light chain	http://cao.labshare.cn/AbRSA/	(Li et al., 2019)
IgBLAST	Germline sequence alignment against databases	https://www.ncbi.nlm.nih.gov/igblast/	(Ye et al., 2013)
IMGT/DomainGapAlign	Aligning the closest germline V-region or C-domain	https://www.imgt.org/3DStructure-DB/cgi/DomainGapAlign.cgi	(Giudicelli et al., 2022)
PyIgClassify	Databases of CDR canonical classes	http://dunbrack2.fccc.edu/PyIgClassify/User/UserPdf.aspx	(Adolf-Bryfogle et al., 2015)
ABodyBuilder2	Build model and predict accurate conformation for segment of models.	https://opig.stats.ox.ac.uk/webapps/newsabdab/sabpred/abodybuilder2/	(Leem et al., 2016)
SWISS-MODEL	A fully automated protein structure homology-modelling server	https://swissmodel.expasy.org/	(Schwede et al., 2003)

1.3.7 Ag-Ab interaction studies

1.3.7.1 Ag-Ab interaction study by computational analysis

Computational methods provide a fast and inexpensive route for generated homology models for antigen-antibody interactions study. The construction of accurate homology models for antibodies can correctly describe the affinity of the Ag-Ab interactions. Molecular docking is carried out for the binding free-energy simulations of the complex. The vital factor of molecular docking is the scoring function that is composed of three major functions; the first is to determine the binding mode and site of ligand binding to a protein, the second is to predict the absolute binding affinity between the protein and ligand, and the third is used to identify potential of drug design by searching from a large ligand database. An available free program that is widely used to study protein-ligand interaction is AutoDock Vina. This program can dock simultaneously multiple ligands, which is an alternative method for binding mode predictions based on force-field analysis. The procedure attempts to predict noncovalent binding of macromolecule (receptor) and small molecule (ligand), starting with their unbound structure obtained from the Protein Data Bank (PDB) or homology modeling. Additionally, docking assumes all the receptor is rigid, the covalent lengths and the free energy of binding (Huey et al., 2012). In addition, GOLD docking is another popular program to predict the binding affinity between ligand and protein. It provides speed for ligands screening using Goldscore as an original scoring function based on the energy of hydrogen bonds, van der Waals energy, metal interactions and torsion deformations (Verdonk et al., 2003).

1.3.7.2 Ag-Ab Interaction and mapping on apoB studies by experimental analysis

Specificity and affinity are qualities that make antibodies an important tool in experimental biology, biomedical research, diagnostics, and therapeutic drugs. Biochemical assays are used to understand antigen-antibody interactions by measuring bioactivity, affinity, kinetics, and thermodynamics of binding.

There are several studies that report about antibody mapping on apoB-100. Bacterial expression of apolipoprotein cDNA constructs have been used to map a series of mAbs to apoB by immunoblotting (Pease et al., 1990). Electron microscopy has been used to visualize pairs of mAbs binding to the LDL surface (Chatterton et al., 1991). Surface plasmon resonance (SPR)-based biosensor (BIA-technology) has been used to study the interaction of different murine monoclonal antibodies (all IgG₁ isotype) against the main protein constituent of human LDL (Robbio et al., 2001). Mapping antibody specificities to smaller regions along the linear sequence has been done with thrombin generated fragment apoB-100 (Marcel et al., 1987; Krul et al., 1988; Fantappie et al., 1992).

1.3.7.2.1 Enzyme-linked immunosorbent assay (ELISA)

ELISA is a rapid, simple, and reliable method for determining the affinity of an interaction by enzyme-labeled antibody or antigen binding followed by enzyme activity measurement by colorimetry. ELISA is performed in polystyrene plates, typically in 96-well plates with protein with high strong binding. The secondary detection system uses a common enzyme, typically horseradish peroxidase (HRP) to catalyze the oxidation of substrate by hydrogen peroxide resulting in a colored product.

There are four major types of ELISA including direct ELISA, indirect ELISA, sandwich ELISA, and competitive ELISA. These immunoassays can also be applied for quantification based on the Law of Mass Action to provide the basis for calculation of antibody affinity constants, K_{aff} (M^{-1}) in a solution phase assay (Beatty et al., 1987). The affinity constant is analyzed by a sigmoidal serial dilution curve and optical

density (OD) showing a direct reflection of the amount of antibody bound to the antigen in the well as shown in Figure 1.10.

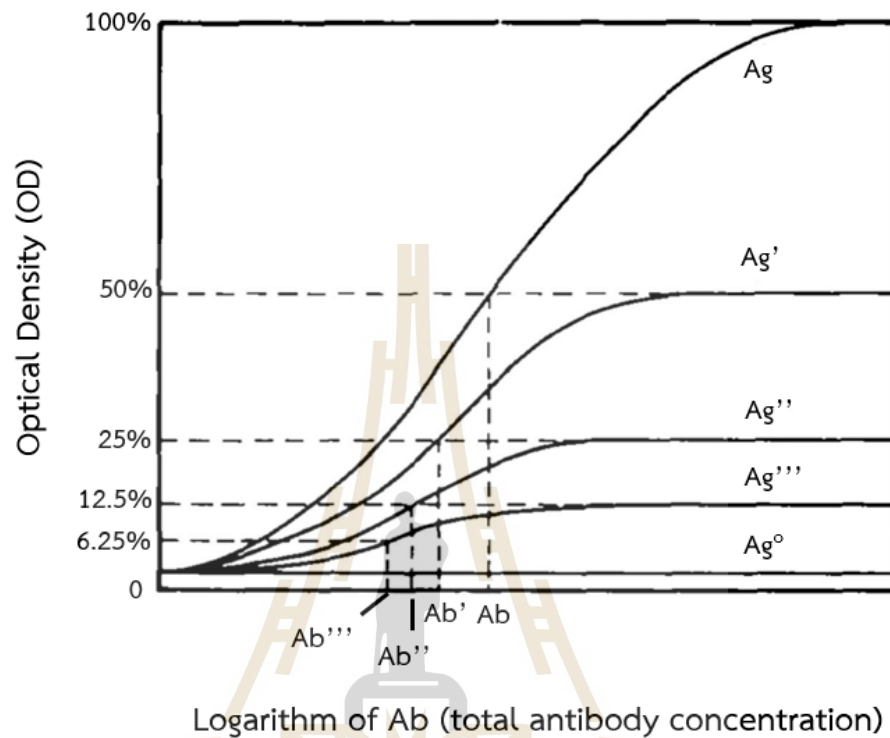


Figure 1.10 Theoretical ELISA curve response at different concentrations of coated antigen. The corresponding OD-50 points move to the left on the graph as the coating concentration decreases indicating $[Ab] > [Ab'] > [Ab''] > [Ab''']$ (Beatty et al., 1987).

According to the obtained sigmoidal curve, one-half of the amount of antibody bound to antigen at 50% of OD-100 is the K_{aff} of the antibody. The following equation was derived from the Law of Mass Action for two identical antibody binding sites and used to calculate the K_{aff} .

$$K_{aff} = \frac{1}{2([Ab']_t - [Ab]_t)}$$

K_{aff} = Affinity constant, (M^{-1})

$[Ab]_t$ = total antibody concentration, (M)

$[Ab']_t$ = one-half concentration of $[Ab]_t$, (M)

1.3.7.2.2 Surface plasmon resonance (SPR) method

SPR is an optical technique for detecting the interactions between immobilized molecules on the sensor chip (e.g. gold film) and molecules flowing over the chip in real-time. Binding affinity can be obtained from the ratio of protein-protein interaction by measuring the change in the refractive index on the sensor surface. Thus, SPR can measure the kinetic binding constant (associated constant (K_a) and dissociated constant (K_d)) and equilibrium binding constant (K_{eq}). Furthermore, this technique can also be applied for detection of protein mass without the labeling of either radioactive or fluorescence. SPR is reported to have been successfully used for mapping distinct epitopes on apoB-100 protein in solution dispensing with labels and secondary tracers. It has been reported that SRP can recognize apoB-100 thrombolytic fragments which have been confirmed by immunoblotting (Robbio et al., 2001).

1.3.7.2.3 Isothermal titration calorimetry (ITC)

Although SPR is very powerful for studying protein-protein interactions, its weak point that affects binding affinity consists of mass transport effect and surface immobilization. Therefore, ITC is one of the techniques that can resolve this problem.

ITC is the best quantitative technique in measuring the thermodynamic properties of protein-protein, protein-drug, protein-carbohydrate, or any biomolecular interaction by using the change of heat as a signal. The binding affinity of each antigen-antibody interaction was defined by precise measurement of its dissociation constant, K_d (small K_d means tight or high binding affinity) by ITC assay. It also provides a direct measurement of the binding enthalpy as well as binding stoichiometry and can aid in the engineering of antibodies (Frasca, 2016). ITC accurately measures K_d from millimolar to nanomolar values. Terms of thermodynamics parameters were calculated by the Gibbs equation.

$$\Delta G = RT \ln K_d = \Delta H - T \Delta S$$

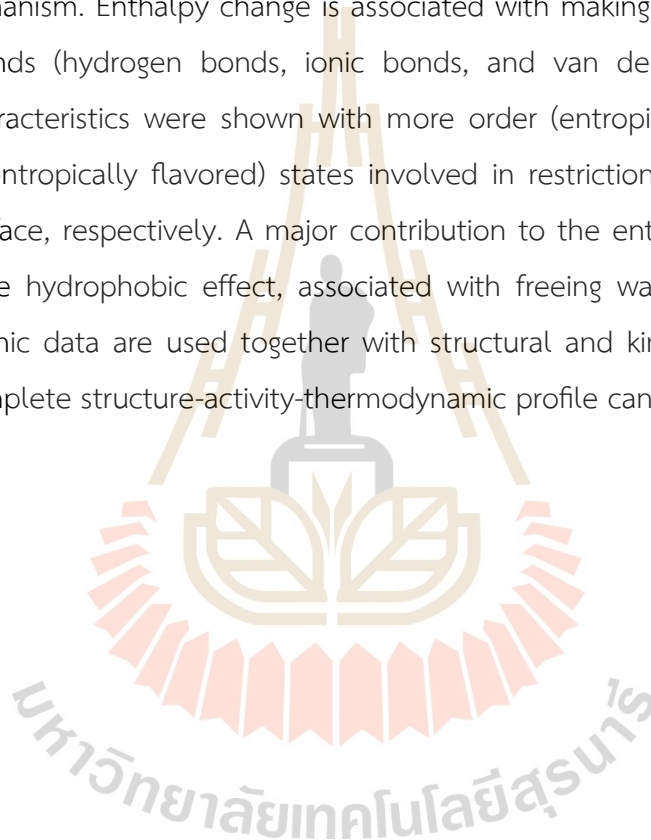
T = temperature (Kelvin)

S = entropy (Joule/Kelvin)

H = enthalpy (Joule)

R = gas constant = $8.314 \text{ J K}^{-1} \text{ mol}^{-1}$

Characterization of binding enthalpy and entropy provide insight into the binding mechanism. Enthalpy change is associated with making and breaking of non-covalent bonds (hydrogen bonds, ionic bonds, and van der Waals interactions). Different characteristics were shown with more order (entropically unflavored) and disordered (entropically flavored) states involved in restriction and freedom at the binding interface, respectively. A major contribution to the entropic contribution for binding is the hydrophobic effect, associated with freeing water molecules. When thermodynamic data are used together with structural and kinetic data from other assays, a complete structure-activity-thermodynamic profile can be obtained.



CHAPTER II

MATERIALS AND METHODS

2.1 Reagents

Iscove's Modified Dulbecco's Medium (IMDM) and fetal bovine serum (FBS) were purchased from Gibco, USA. Serum free media (ISF-1) was purchased from PAN Biotech, Germany. GENEzol™ reagent was purchased from Geneaid, Taiwan. A cDNA synthesis kit was purchased from Vivantis, Malaysia. Phusion™ High-fidelity DNA polymerase, BCA assay kit, SYBR green, horseradish peroxidase conjugated streptavidin, and the Chemiluminescent detection system were purchased from Thermo Scientific, USA. The peptides with purity >90% were synthesized by Genscript, USA. All primer sets for cDNA synthesis and PCR steps are listed in Table 2.1 and were synthesized by ATGC company, Thailand. Streptavidin was purchased from Genscript, USA. Horseradish peroxidase conjugated rabbit anti-mouse immunoglobulins antibody was purchased from Dako, Denmark. Native human LDL protein, human apoB-100, thrombin, and tetramethylbenzidine (TMB) substrate were purchased from Merck, Germany. Coomassie brilliant blue R250 was purchased from AppliChem, Germany.

Table 2.1 Mouse IgG (mIgG) primers Adapted from (Meyer et al., 2019).

Primer name	Description	Primer sequence
mIGK RT	Reverse primer for kappa chain	5' TTGTCGTTCACTGCCATCAATC 3'
mIGL RT	Reverse primer for lambda chain	5' GGGGTACCATCTACCTTCCAG 3'
mIGHG RT	Reverse primer for heavy chain	5' AGCTGGGAAGGTGTGCACAC 3'
ISPCR	Universal forward primer	5' AAGCAGTGGTATCAACGCAGAG 3'
mIGK PCR	Reverse primer for kappa chain	5' ACATTGATGTCTTTGGGGTAGAAG 3'
mIGL PCR	Reverse primer for lambda chain	5' ATCGTACACACCAGTGTGGC 3'
mIGHG PCR	Reverse primer for heavy chain	5' GGGATCCAGAGTTCCAGGTC 3'
IgG _{2b} Heavy PCR	Reverse primer for heavy chain IgG _{2b}	5' GGTGCGGTGTCCTTGTAGTT 3'

2.2 Software used in the study

Open-source software and computer technologies have grown in significance in research and development. These databases allow for the organization of protein sequence, structural and functional analysis. Bioinformatic tools that were used in this study are listed in Table 2.2.

Table 2.2 List of software containing information biological databases.

Tool	Source (URL)	Ref
Uniprot	https://www.uniprot.org/	-
IEDB	http://tools.iedb.org/main/bcell/	(Vita et al., 2019)
IMGT	https://www.imgt.org/3Dstructure-DB/cgi/DomainGapAlign.cgi	(Lefranc et al., 2009)
IgBLAST	https://www.ncbi.nlm.nih.gov/igblast/	(Ye et al., 2013)
Primer-BLAST	https://www.ncbi.nlm.nih.gov/tools/primer-blast/	(Ye et al., 2012)
Structure Validation Server	https://saves.mbi.ucla.edu/	-
SWISS-MODEL	https://swissmodel.expasy.org/	(Waterhouse et al., 2018)
AutoDock Vina	https://autodock.scripps.edu/	(Huey et al., 2012)
GOLD	personal software license	(Verdonk et al., 2003)
MEGA-X	https://www.megasoftware.net/	(Kumar et al., 2018)
Discovery studio	https://www.3ds.com/products/biovia/discovery-studio	(Studio, 2008)

2.3 Preparation of monoclonal antibodies against human LDL

2.3.1 Cultivation of hybridoma cell producing mAbs to human LDL

Three hybridoma cells producing mAbs against human LDL (hLDL-2D8, hLDL-E8, and hLDL-F5) were cultured in Iscove's Modified Dulbecco's Medium (IMDM) (Gibco, USA), supplemented with 10% fetal bovine serum (FBS), 40 mg/ml gentamicin, and 2.5 mg/ml amphotericin B (Gibco, USA) in a humidified atmosphere of 5% CO₂ at 37°C. For high yield production of mAbs, hybridoma cells were cultured in ISF-1 serum free medium (PAN Biotech, Germany).

2.3.2 Isotypic determination

Isotypic determination of the mAbs was performed using the mouse mAb isotyping reagents (Sigma Aldrich, USA) according to the manufacturer procedure. Briefly, antibodies against different isotypes of immunoglobulin (IgA, IgG₁, IgG_{2a}, IgG_{2b}, IgG₃ and IgM) were diluted in coating buffer (carbonate buffer, pH 9.6) at a dilution of 1:100 and coated onto an ELISA plate 50 µl per well and incubated at room temperature (RT) for 2 h. The plate was blocked with 100 µl of 2% skimmed milk in 1X PBS pH 7.2 for an hour at RT. After removing of blocking solution, 50 µl of culture supernatant of each mAb clone was added into each well and incubated at RT for an hour. The plate was washed with 0.05% Tween-20 in PBS (PBST) 3 times before adding 50 µl of horseradish peroxidase conjugated rabbit anti-mouse immunoglobulins antibody (HRP-anti-mouse-Ig) (Dako, Denmark) at a dilution of 1:5,000 into each well and incubating at RT for 1 h. After three times washing with 0.05% PBST, 50 µl of tetramethylbenzidine (TMB; Merck, Germany) substrate was added into each well and incubated at RT for 3 min. The reaction was terminated by adding 100 µl of 1N HCl. The absorbance at 450 nm was measured using a microplate reader (Tecan, Switzerland).

2.3.3 Monoclonal antibody purification by affinity chromatography

Culture supernatant containing mAb in ISF-1 medium were harvested and centrifuged at 1,500 rpm for 5 min to collect clear supernatant. Purification of the mAbs was performed by affinity chromatography using a HiTrap® Protein G Sepharose

column linked to AKTA START protein purification system (GE Healthcare Bio-Science, Sweden) according to the manufacturer's instruction. The eluting fractions were collected, and the buffer exchanged overnight at 4 °C by dialysis against 1X PBS pH 7.2. The concentration of the purified mAbs was measured by the BCA protein assay kit (Thermo Scientific, USA) according to the supplier's instruction. The purity of the purified mAbs was checked by sodium dodecyl sulfate polyacrylamide gel electrophoresis (SDS-PAGE) under non reducing and reducing conditions. The specific activity was analyzed by indirect ELISA as described in 2.3.4.

2.3.4 Determination of antibody activity by indirect ELISA

Fifty microliters of human apoB-100 at concentration 10 µg/ml in coating buffer was coated onto an ELISA plate and incubated at RT for 2 h. The plate was blocked with 100 µl of 2% skimmed milk in 1X PBS pH 7.2. After incubation for 1 h at RT, the blocking solution was discarded, and the plate was washed 3 times with 200 µl of 0.05% PBST. Fifty microliters of the purified mAbs at a final concentration 10 µg/ml was added into each well and incubated at RT for 1 h. Then the plate was washed 3 times with 0.05% PBST before adding 50 µl of HRP-anti-mouse-Ig at a dilution 1:5,000 into each well. After an hour of incubation at RT, the plate was washed with 200 µl per well of 0.05% PBST 3 times. Finally, 50 µl of TMB substrate was added into each well and incubated at RT for 3 min. The reaction was terminated by adding 100 µl of 1 N HCl. The absorbance at 450 nm was measured in a microplate reader (Tecan, Switzerland).

2.3.5 Purity determination of the purified monoclonal antibodies by SDS-PAGE

Five micrograms of the purified mAbs were resolved in 10% SDS-PAGE under reducing and non-reducing conditions. Proteins were separated by applying electricity at 120 volts for 1 h. The separated proteins were visualized by staining the gel with Coomassie brilliant blue R250 staining solution at RT for 1 h and destained using destaining solution until there were clear protein bands with no background.

2.4 Amplification of monoclonal antibody variable region

2.4.1 Total RNA extraction and cDNA synthesis

Total RNA was isolated from hybridoma cells using GENEzol reagent (Geneaid, Taiwan) following the manufacturer's protocol. The concentration of total RNA was measured by a Nanodrop spectrophotometer at 260 nm wavelength. The purity was checked by agarose gel electrophoresis. First strand complementary DNA (cDNA) synthesis was carried out using M-MuLV cDNA synthesis kit (Vivantis, Malaysia) according to the manufacturer's instructions. Briefly, cDNA synthesis was performed in two separated mixtures of 10 µl reaction volumes that consisted of 5 µg extracted RNA, 2 mM template-switch oligo (5' AAGCAGTGGTATCAACGCAGAGTACATGGG 3'), Oligo d(T)₁₈ (1 µl), 0.5 mM dNTPs, and nuclease-free water to the final volume. After incubating at 65 °C for 5 min, the reaction was placed on ice for 2 min and the mixture of 10X Buffer M-MuLV (2 µl) and 100 U/µl M-MuLV reverse transcriptase was added. The reaction mixture was then incubated at 42 °C for 60 min and terminated by incubating at 85 °C for 5 min.

2.4.2 Amplification of cDNA by PCR

The PCR was performed with a total reaction volume of 50 µl, containing 5 ng/µl of first-strand cDNA, 0.5 µM Universal forward primer, 0.5 µM reverse primer (kappa, lambda, heavy), 0.2 mM dNTP Mix, 5X Phusion™ HF Buffer (10 µl), 0.02 U/µl Phusion™ High-fidelity DNA polymerase (Thermo Scientific, USA) and nuclease free water to the final volume. The PCR condition comprised of initial heating at 98 °C for 30 s, followed by 35 cycles of denaturation at 98 °C for 10 s, annealing at 57 °C for 30 s, extension at 72 °C for 30 s and a final extension at 72 °C for 7 min. Immunoglobulin specific primers of VH and VL used for cDNA amplification are listed in Table 2.1. The PCR products (8 µl) loaded on a 1.2% agarose gel in SYBR green dye, and then were visualized by UV exposure in a gel documentation system (Bio-rad, USA).

2.5 DNA sequence analysis

The PCR products of 2.4.2 were submitted for DNA sequenced by Sanger methods (ATGC company, Thailand). The sequence chromatogram of clones representing VL and VH chains was subjected to analysis by FinchTV-v 1.4.0 software (<https://finchtv.software.informer.com/1.4/>). A consensus sequence pattern was built from a set of three clones representing light and heavy chains by multiple sequence alignments using MEGA-X software with forty mouse immunoglobulin nucleotide reference sequences from National Center for Biotechnology Information (NCBI) databases. Nucleotide sequence verification and CDR domain assignment were carried out using the Immunogenetics Information System (IMGT) (<https://www.imgt.org/>) by choosing the default algorithmic parameters with the germline of mouse organisms. The percentage identity of each light and heavy chain variable region was identified by using IMGT.

2.6 Computational modeling of antibody Fv region

The VL and VH nucleotide sequences of each mAb clones were translated into amino acids using the six reading frames by Expasy tool. The pairs of deduced VL and VH chains protein sequences were submitted to the protein structure homology-modeling server, SWISS-MODEL, for homology modeling using the crystal structure as PDB template. The obtained models were evaluated by the Discovery studio program for Ramachandran plot, molecular overlay with the reference crystal structure, and amino acid residues of the Fv structure were evaluated for their backbone properties (phi-psi angles) using the Verify3D bioinformation server (<https://saves.mbi.ucla.edu/>). The CDR loop regions were assigned based on the IMGT numbering system.

2.7 Cleavage of LDL and apoB-100 using thrombin

One hundred and fifty micrograms of either purified human LDL (Merck, Germany) or apoB-100 (Merck, Germany) was solubilized in buffer containing 10 mM Tris-HCl, 0.3 mM EDTA (pH 8) and 3 µg of thrombin (enzyme: substrate =1:50 w/w) in a total volume of 300 µl. The reaction was incubated for 8 h at RT and terminated by

the addition of an electrophoresis sample buffer consisting of 5% (w/v) SDS, 40% (w/v) sucrose, 10% (v/v) mercaptoethanol, and 0.01% (w/v) bromophenol blue, as described in (Cardin et al., 1984; Fantappie et al., 1992).

2.7.1 Western blot analysis of mAbs reactivity to thrombolytic digested apoB-100 fragments

Five micrograms of undigested and thrombolytic digestion proteins were resolved using 6% SDS-PAGE and electrophoretically transferred onto a polyvinylidene fluoride (PVDF) membrane. The blotted membrane was blocked with 5% skimmed milk in PBS pH 7.2 for 1 h at RT. The membrane was incubated with mAbs in 2.5% skimmed milk in PBS pH 7.2: hLDL-E8 (2.5 µg/ml) for 3 h, hLDL-2D8 (10 µg/ml) or hLDL-F5 (5 µg/ml) for overnight. The stained membranes were washed 5 times with 0.1% Tween-20 in PBS (PBST) before incubation with HRP-anti-mouse-Ig at a dilution of 1:5,000 in 2.5% skimmed milk in PBS pH 7.2 for an hour at RT. After 3 times washing with 0.1% PBST and twice with PBS, the protein bands were visualized using an enhanced chemiluminescent detection system (SuperSignal™ West Pico PLUS; Thermo Scientific, USA) and analyzed by Amersham Image Quant™ 500 CCD imaging system (Cytiva, USA).

2.8 Computational docking and simulations of mAb Fv region with apoB-100 peptides

The molecular docking GOLD 5.3.0 and AutoDock Vina programs were used for prediction of the mAb Fv with apoB peptide binding complex. The sequence of apoB-100 was taken from UniProt (human apoB), while the obtained Fv structures from 2.6 were used as the targeting structures for docking studies. Information obtained from Western blot of thrombolytic fragment results and epitope prediction by the Immune Epitope Database (IEDB) server were utilized to scope the binding regions for preliminary analysis. Then, ligands were created and optimized for structure using the Discovery Studio program. Before docking, preparation of the target site by adding hydrogen atoms to the side chains, and charges addition is needed. A receptor grid

with box diameter was generated according to antigen binding region as shown in Figure 2.1. Subsequent docking rounds were performed with a peptide apoB-100 (~7 aa) and mAb Fv structure which passed the initial screen for detailed analysis of interactions. Docking solutions were initially screened based on the $\text{RMSD} \leq 1$ with the lowest energy binding for Autodock Vina and the highest for GOLD fitness score. The binding model was visualized by the Discovery program, which provides information about the bond distance, hydrogen bond and hydrophobic interaction of each binding conformation.

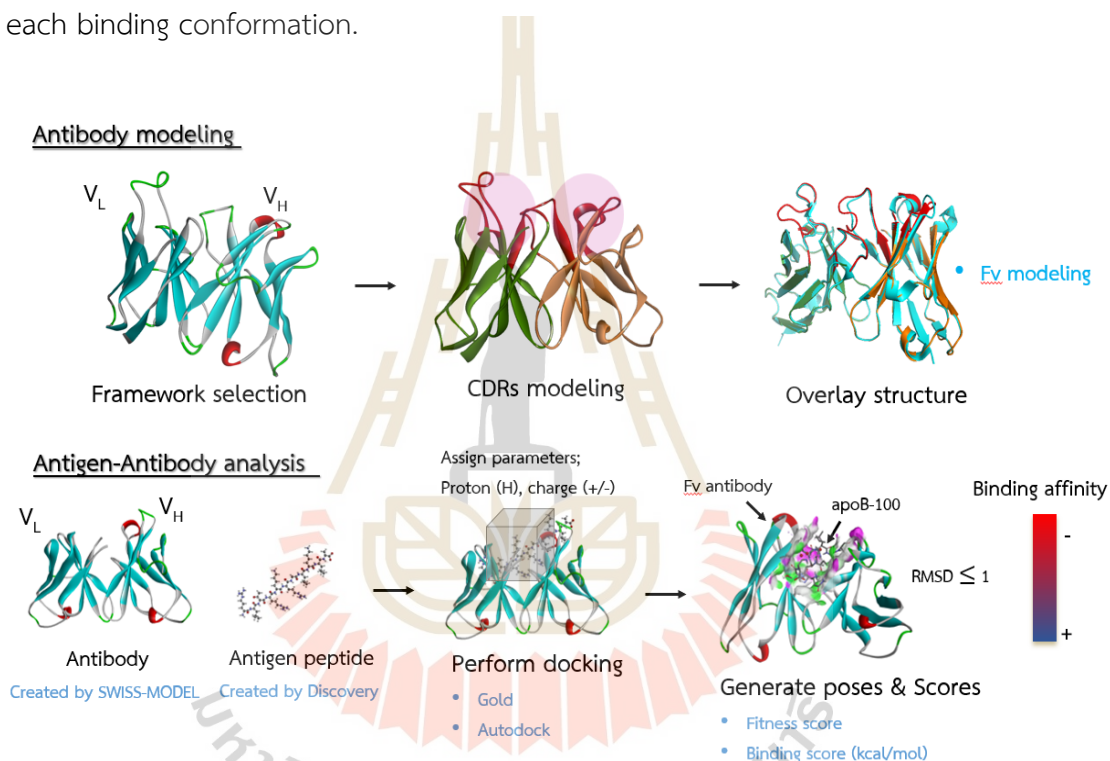


Figure 2.1 Monoclonal antibody Fv modeling and molecular docking simulations.

2.9 Epitope binding analysis by inhibition ELISA

Indirect ELISA was performed to analyze the epitope binding of mAbs clone hLDL-F5, hLDL-E8 and hLDL-2D8. Five hundred nanograms per well of purified human apoB-100 was coated onto the 96-well plate and incubated at RT for 2 h. The plate was then blocked with 100 µl per well of 2% skimmed milk in PBS pH 7.2 at RT for 1 h. The blocking solution was discarded before adding 50 µl of unconjugated anti-human LDL mAb (20 µg/ml). After incubation at RT for 1 h, the plate was washed 3 times with 200 µl per well of 0.05% PBST, then 50 µl of biotinylated anti-human LDL mAb (10 µg/ml) was added and incubated at RT for 1 h. After the plate was washed 3 times with 0.05% PBST, 50 µl of HRP-conjugated streptavidin (Invitrogen, U.S.A.) at dilution 1:5,000 was added to each well. After incubation at RT for 1 h, the plate was washed 3 times with 0.05% PBST before adding 100 µl of TMB substrate and incubating in dark for 3 min. The reaction was stopped by adding 100 µl of 1 N HCl into each well. The optical density (OD) at 450 nm was measured by a microplate reader (Tecan, Switzerland). Percent inhibition was calculated according to the following equation.

$$\text{Inhibition (\%)} = \left(\text{control OD} - \frac{\text{sample OD}}{\text{control OD}} \right) \times 100$$

2.10 Affinity determination of apoB-100 specific mAbs by indirect ELISA

2.10.1 Titration of human apoB-100 concentration

Fifty microliters of human apoB-100 at various concentrations (0.019, 0.039, 0.078, 0.156, 0.312, 0.625, 1.25, 2.5, 5, 10, 20, 40 µg/ml) were coated into ELISA plate in coating buffer, pH 9.6 and incubated RT for 2 h. The wells were blocked with 100 µl of 2% skimmed milk in PBS pH 7.2 for an hour at RT. The plate was washed 3 times with 200 µl of 0.05% PBST and 50 µl of mAb clones hLDL-E8, or hLDL-2D8 or hLDL-F5 (80 µg/ml) in 2% skimmed milk in PBS pH 7.2 was added. After an hour of incubation at RT, the plate was washed 3 times with 200 µl of 0.05% PBST. Fifty microliters of HRP-anti-mouse-Ig at a dilution of 1:5,000 was added to each well and incubated at RT for an hour. The excess conjugated reagent was removed by washing

the plate with 200 μ l of 0.05% PBST for 3 times. The color representative of the binding activity of the mAbs was visualized by adding 50 μ l of the TMB substrate into each well and incubating in dark at RT for 3 min. One hundred microliters of 1 N HCl was added to stop reaction. The absorbance at 450 nm was measured using a microtiter plate reader (Tecan, Switzerland).

2.10.2 Experimental dose-response curves for anti-human LDL mAbs

Fifty microliters of human apoB-100 at four concentrations (1.25, 2.5, 5, 10 μ g/ml), chosen from 2.10.1, were coated into ELISA plate in coating buffer pH 9.6 and incubated RT for 2 h. The wells were blocked with 100 μ l of 2% skimmed milk in PBS pH 7.2 for an hour at RT. The plate was washed 3 times with 200 μ l of 0.05% PBST and 50 μ l of serial 4-fold concentration dilutions of hLDL mAbs (hLDL-2D8 (0.0003 - 5 μ g/ml), hLDL-E8 (0.0009 - 15 μ g/ml), and hLDL-F5 (0.00048 - 500 μ g/ml)) in 2% skimmed milk in PBS pH 7.2 were added. After an hour of incubation at RT, the plate was washed 3 times with 200 μ l of 0.05% PBST. Fifty microliters of HRP-anti-mouse-Ig at a dilution of 1:5,000 was added to each well and incubated at RT for an hour. The excess secondary antibodies were removed by washing the plate with 200 μ l of 0.05% PBST for 3 times. The color representative of the binding activity of the mAb was visualized by adding of 50 μ l of the TMB substrate into each well and incubated in dark at RT for 3 min. One hundred microliters of 1 N HCl was added to stop reaction. The absorbance at 450 nm was measured using a microtiter plate reader (Tecan, Switzerland).

2.10.3 Calculation of affinity constant

A sigmodal curve of optical density at 450 nm (Y axis) versus the logarithm of the antibody concentration (X axis) was plotted to provide the antibody bound to the antigen on the plate. The concentration that produces 50% of the highest absorbance value (OD-50) for a particular concentration of the coated antigen was chosen for affinity constant calculation. The affinity constant (K_{aff}) was calculated according to Beatty equation as follows (Beatty et al., 1987).

$$K_{\text{aff}} = \frac{1}{2 (2[\text{Ab}']_t - [\text{Ab}]_t)} = \frac{n-1}{2 (n[\text{Ab}']_t - [\text{Ab}]_t)}$$

$$\text{where, } n = \frac{[\text{Ag}]}{[\text{Ag}']}$$

K_{aff} = Affinity constant, (M^{-1})

$[\text{Ab}]_t$ = total antibody concentration, (M)

$[\text{Ab}']_t$ = one-half concentration of $[\text{Ab}]_t$, (M)

K_{aff} is an estimated value of the affinity constant of the antigen-antibody interaction that is based on the total antibody concentration at OD-50 of $[\text{Ab}]_t$, total antibody concentration and $[\text{Ab}']_t = 1/2[\text{Ab}]_t$. When different concentrations of $[\text{Ag}]$ ($[\text{Ag}] = n [\text{Ag}']$) are used, one being half the other (e.g., $\text{Ag} = 2\text{Ag}' = 4\text{Ag}'' = 8\text{Ag}'''$)

2.11 Peptide ligand-based indirect ELISA analysis

Seven different oligopeptide fragments of human apoB-100 (11 amino acid length) with N-terminal biotinylation were synthesized with a purity of 90% as shown in Table 2.3 were used as antigen for the studied mAbs. The ELISA plate were coated with 20 $\mu\text{g/ml}$ streptavidin (Genscript, USA) in coating buffer (100 $\mu\text{l/well}$) and incubated at 37°C for 2 h. Then, 100 μl of each oligopeptide at 20 $\mu\text{g/ml}$ were added and incubated at 37°C for 1 h. The non-specific binding surface on the plate was blocked by adding 100 μl 5% BSA-PBS solution pH 7.2. After washing with 0.1% PBST, 100 μl of anti-human LDL mAbs (hLDL-2D8, hLDL-E8, or hLDL-F5) at concentration 10 $\mu\text{g/ml}$ were added. After an hour of incubation at 37 °C, the plate was washed 3 times with 200 μl of 0.1% PBST. One hundred microliters of HRP-anti-mouse-Ig at a dilution of 1:5,000 was added to each well and incubated at 37 °C for an hour. The excess conjugated reagent was removed by washing the plate with 200 μl of 0.1% PBST 3 times. Finally, 100 μl of the TMB substrate was added into each well and the plate was incubated in dark at RT for 3 min. One hundred microliters of 1 N HCl was

added to stop reaction. The absorbance at 450 nm was measured using a microtiter plate reader (Tecan, Switzerland).

Table 2.3 Synthetic peptide fragments of the human apoB-100 used in this study.

Peptide name	Sequence (N' - C')	pI	Range on apoB-100	Purity	N' terminal labeling	Solvent
P1	DPNNYLPKESM	4.37	645-655	96.1%	Biotin	DMSO
P2	LRSEYQADYES	4.14	1571-1581	96.9%	Biotin	DMSO
P3	QYIKDSYDLHD	4.41	2156-2166	92.6%	Biotin	DMSO
P4	GYTKDDKHEQD	4.66	712-722	96.6%	Biotin	Water
P5	LQEYFERNRQT	6.14	2050-2060	90.1%	Biotin	Water
apoB-48	ALTKKYRITEN	9.70	2117-2127	>90%	Biotin	Water
Site B	RLTRKRGLKLA	12.31	3359-3369	>90%	Biotin	Water

NOTE; P1-5 oligopeptides were synthesized by Genscript, USA. ApoB-48 and site B oligopeptides were synthesized by 1st BASE, Malaysia.



CHAPTER III

RESULTS

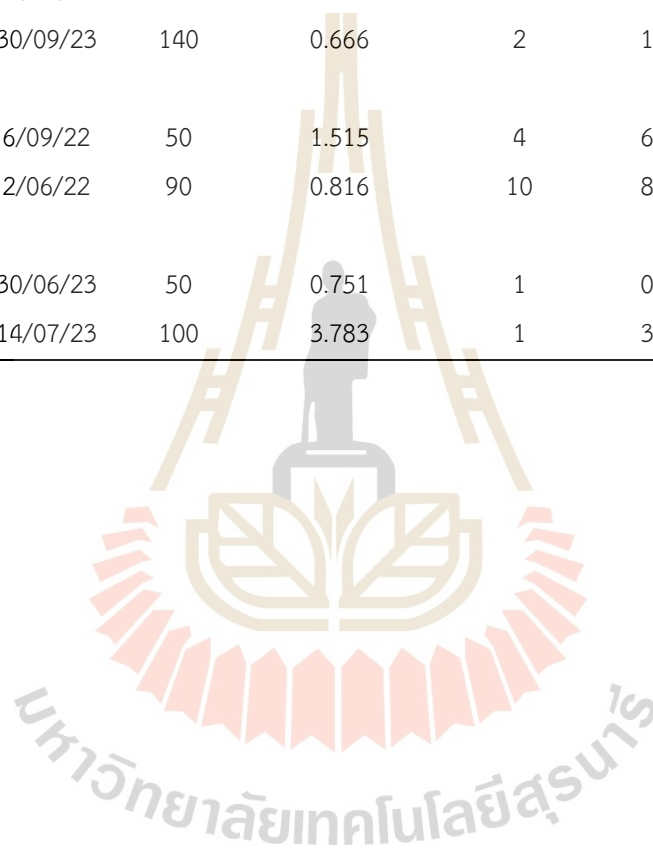
3.1 Production of the purified mAbs against human LDL

3.1.1 Purity of the generated mAbs against human LDL

High yields of the pure mAbs against human LDL were produced and used in this study. The mAbs clones hLDL-E8, hLDL-2D8 and hLDL-F5 were purified from culture supernatants by affinity chromatography using HiTrap® Protein G. The production yields of each purification lot are summarized in Table 3.1. The purity of the purified mAbs was examined by performing 10% SDS-PAGE under non-reducing and reducing conditions. According to the results shown in Figure 3.1, two protein bands of heavy chain and light chain were found under the reducing condition, at molecular weights of 55 and 25 kDa, respectively. Under non-reducing condition, only a band of whole molecule of antibody at a molecular weight about 150 kDa was observed. These results indicated that the purified mAbs are pure.

Table 3.1 Production yield of the purified hLDL-mAbs using HiTrap® protein G affinity chromatography.

Clone	Date	Starting volume (ml)	Concentration (mg/ml)	Total volume (ml)	Amount (mg)	Absorbance (OD 450 nm)
hLDL-E8	29/04/22	100	0.624	1.3	0.800	1.214
	30/09/23	140	0.666	2	1.332	1.941
hLDL-2D8	6/09/22	50	1.515	4	6.062	1.703
	2/06/22	90	0.816	10	8.166	0.912
hLDL-F5	30/06/23	50	0.751	1	0.751	0.815
	14/07/23	100	3.783	1	3.783	0.582



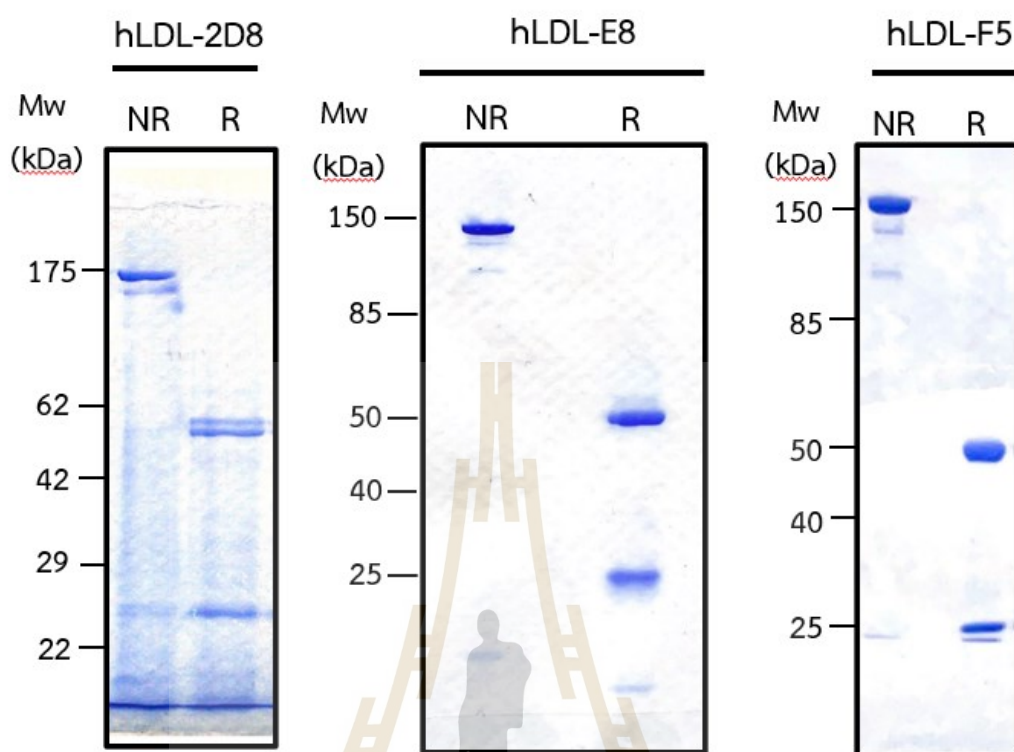


Figure 3.1 Purity of the purified mAbs against human LDL. The purified mAbs clone hLDL-2D8, hLDL-E8, and hLDL-F5 were resolved in 10% SDS-PAGE under reducing (R) and non-reducing (NR) conditions. Protein bands were visualized by staining with Coomassie Brilliant Blue R250. A representative result is one of three independent experiments.

3.1.2 Activity of the purified mAbs

The activity of the purified mAbs was analyzed by indirect ELISA. Commercial human apoB-100 (Merck, Germany) was used as an antigen for this study. The binding capacities of the purified mAbs to the human apoB-100 are shown in Figure 3.2. All purified mAbs clones (hLDL-2D8, hLDL-E8, and hLDL-F5) were able to bind to human apoB-100. This result suggests that the purified mAbs retained their binding activity after purification and can be used as a tool for further experiments.

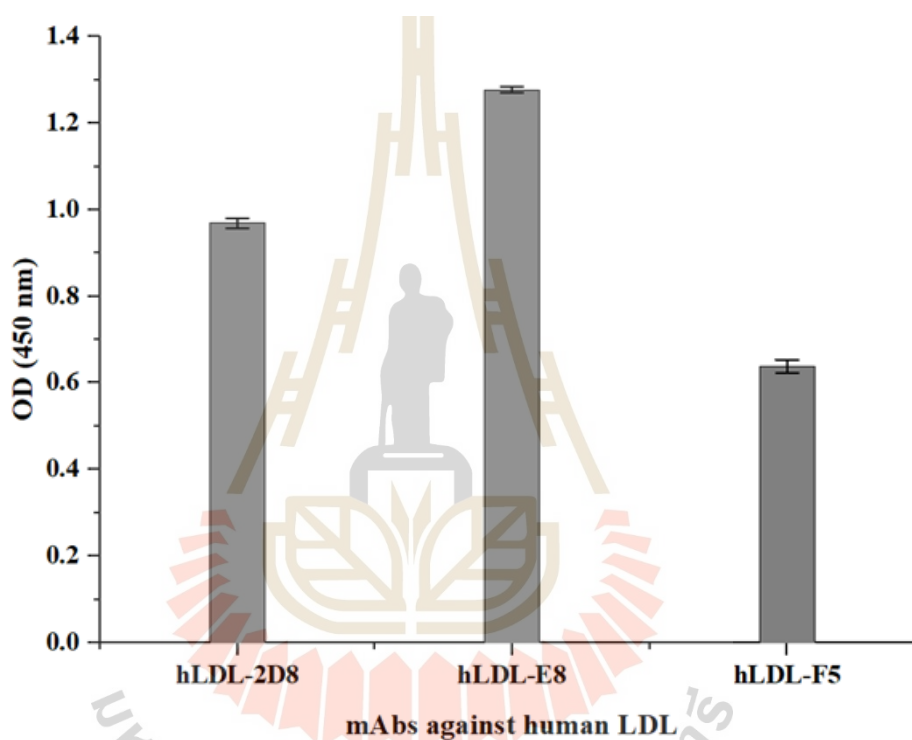


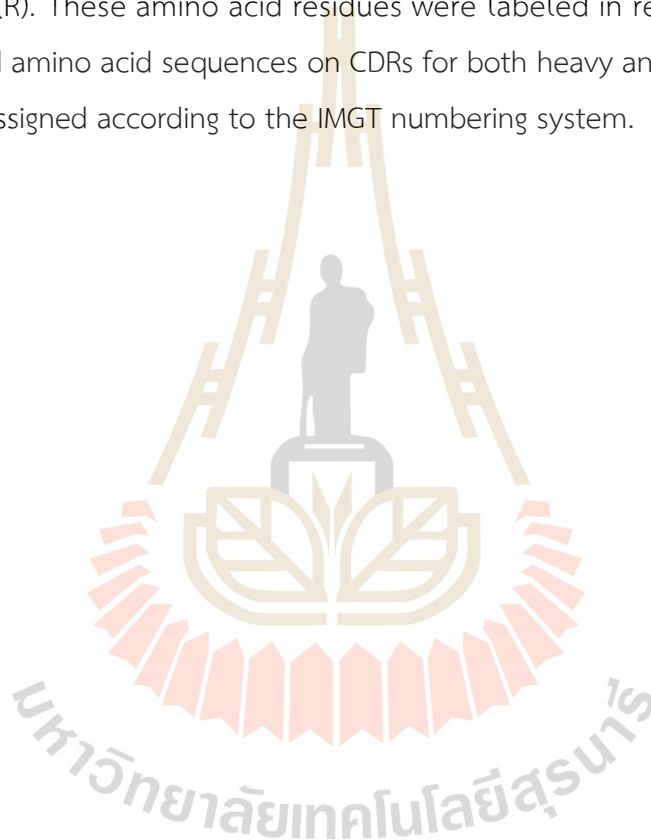
Figure 3.2 Binding activity of the purified mAbs against human LDL to human apoB-100. Five hundred nanogram of commercial human apoB-100 were immobilized on the ELISA plate wells. Purified mAbs (10 μ g/ml) were added and the binding activity was detected with HRP-anti-mouse-Ig at dilution 1:5,000. The optical density of the developed color was measured at wavelength 450 nm. A representative result from a means (\pm SD) of three independent experiments is shown.

3.2 Sequencing of the variable region of hLDL-mAbs

The total RNA was extracted from the hybridoma cells producing mAbs to human apoB-100 of clones hLDL-2D8, hLDL-E8, and hLDL-F5. The purity of the extracted RNA was analyzed using 1.5% agarose gel electrophoresis, which displayed clear bands of the 28s rRNA and 18s rRNA (Figure 3.3A). This suggests the high purity of the extracted RNA that can be used for amplification of the specific gene encoding the variable heavy (VH) and variable light chains (VL) of the mAbs, by performing RT-PCR using specific primers according to a previous report (Meyer et al., 2019). PCR product analysis by agarose gel electrophoresis revealed that the VL chain of all mAb clones are kappa light chain with the PCR product size of 550 bp, while VH chains were 900 bp (Figure 3.3B). The obtained PCR products were submitted for nucleotide sequencing by the Sanger method and the sequencing data was analyzed with available programs as shown in Table 2.2. Firstly, protein sequence alignment through MEGA-X with various reference nucleotide sequences. Then, IMGT was used for identifying the type of chain, sequence similarity, and CDRs before constructing the Fv structure by SWISS-MODEL.

Sequence analysis of three mAb clones, hLDL-2D8 (IgG_{2b} isotype), hLDL-E8 (IgG₁ isotype), and hLDL-F5 (IgG₁ isotype) revealed that the kappa light chain variable regions of all clones contain the same DNA sequence, whereas the heavy variable regions revealed different sequences. Moreover, the DNA sequences revealed that these mAb clones have a frameshift mutation in the V-gene region, resulting in an early stop codon. Therefore, chromatograms representing VH and VL sequences of the clones were then examined and adapted for sequencing errors compared to reference sequences (forty mouse immunoglobulin nucleotide sequences from NCBI databases). A consensus sequence was used to identify the percent identity of light and heavy variable regions. The results revealed that the average percentage identity of all frame regions and CDR residues of the light chain is 60% and the heavy chain ranges from 47.5% to 76.5% at the top-matched germline V genes. Amino acid alignment was performed in MEXGA-X software and the results are shown in Figure 3.4. Each residue in the alignment is assigned a color according to its profile (R group dependent). Considering CDRs based on a definition of a general protein-antibody

complex using consensus structural regions that interact with the antigens in all known complexes taken from Protein Data Bank (PDB) are concluded in Table 1.3. The CDRs of three clones showed some residues corresponding to the consensus compositions (Ofra et al., 2008), such as CDR-L1 contains Tyrosine (Y) and Histidine (H). CDR-L2 contains Tyrosine (Y), Serine (S) and Threonine (T). While CDR-L3 contains Histidine (H) and Arginine (R). For heavy chains, CDR-H1 and CDR-H2 contain all amino acids shown in Table 1.3. CDR-H3 contains Asparagine (N), Aspartic acid (D), Glycine (G), Arginine (R). These amino acid residues were labeled in red colors as shown in Table 3.4 and amino acid sequences on CDRs for both heavy and light chains of three mAbs were assigned according to the IMGT numbering system.



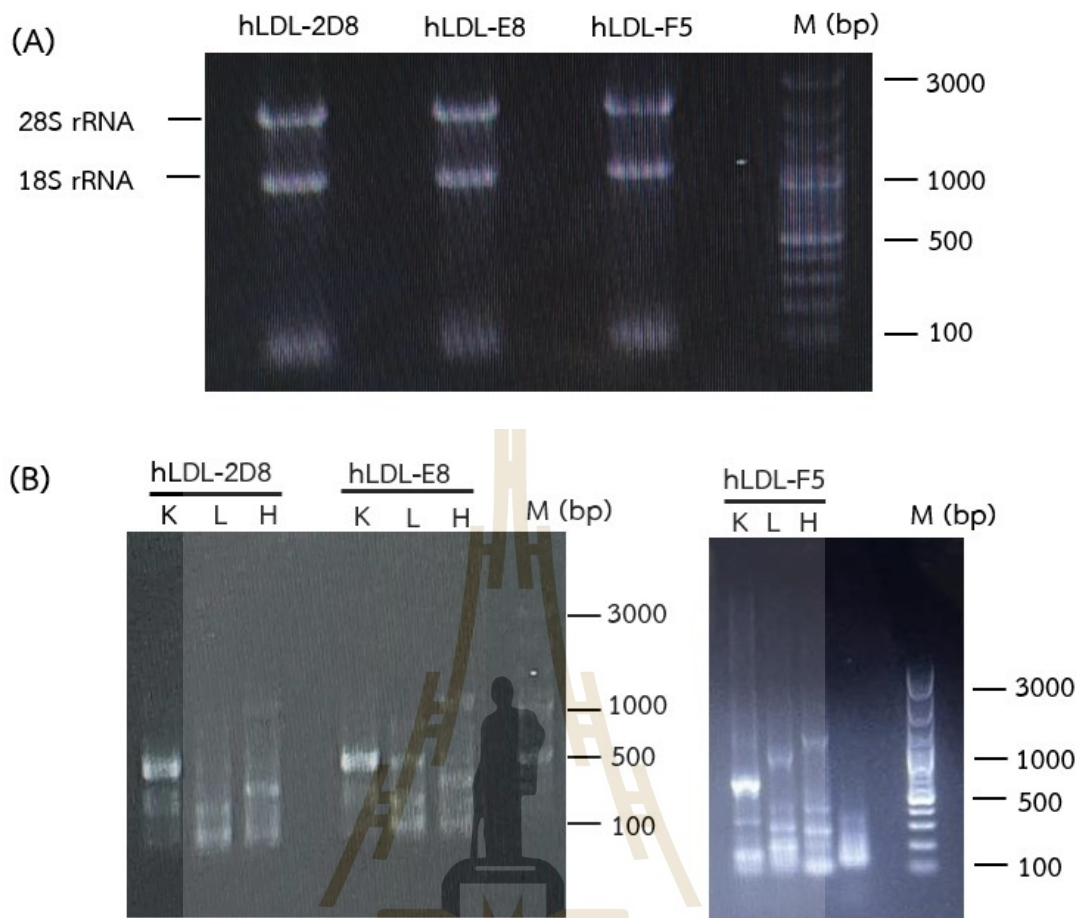


Figure 3.3 (A) Agarose gel electrophoresis (1.5%) of extracted RNA (2 µg/lane). (B) The PCR amplified products of heavy (H) and Light (L) chain genes. Immunoglobulin gene specific for variable heavy chain (VH) and variable light chain (VL) chain primers were used to amplify the cDNA. The PCR products were visualized on a 1.2% agarose gel electrophoresed at 100 volts for 35 min. K: Kappa (550 bp); L: Lambda (550 bp) and H: Heavy (900 bp).

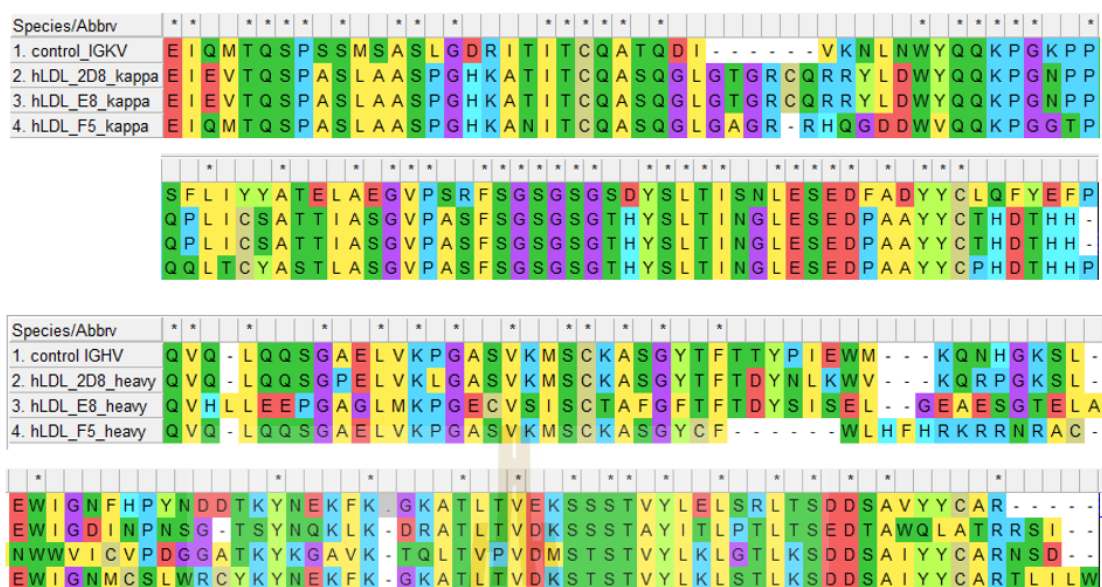


Figure 3.4 Amino acid sequence alignment of kappa (K) light chain and heavy (H) chain at variable fragment (Fv) of three different mAb clones compare to control mouse immunoglobulin variable chains (IGKV and IGHV) using MEGA-X software by muscle algorithm. (*) denotes identical amino acid, and (-) denotes non-conserved residues.

Table 3.2 Complementarity-determining regions (CDRs) of mAbs against human LDL heavy and light chains by IMGT numbering system.

Name	Type	CDR1	CDR2	CDR3
hLDL_2D8_KAPPA	VL	QQLGTGRCQRRY	SAT	THDTHHTRT
hLDL_E8_KAPPA	VL	QQLGTGRCQRRY	SAT	THDTHHTRT
hLDL_F5_KAPPA	VL	QQLGAGRRHQG	YAS	PHDTHHPH
hLDL_2D8_HEAVY	VH	GYTFTDYN	INPNSGT	TRRSITVQSGSKLS
hLDL_E8_HEAVY	VH	FGTFTDYSIS	ICVPDGGGA	CARNSD
hLDL_F5_HEAVY	VH	GYCFW	MCSLWRCY	ARTLILW

VL: variable light chain

VH: variable heavy chain.

3.3 Computational modeling of antibody Fv region

Modeling structures of the studied mAbs variable regions were constructed by a fully automated protein homology modeling server, SWISS-MODEL. The model quality was improved based on Qualitative Model Energy Analysis (QMEAN) and Quaternary Structure Quality Estimate (QSQE). The results revealed the existence of an individual immunoglobulin fold pattern with a sequence identity of about 50% compared to crystal structures. The RMSD value of three mAbs clones is about 2–3Å which explains the folding is likely the same with crystal structure except for some variable surface loops, the structural alignments are shown in Figure 3.5-3.7. The QSQE score value of hLDL-2D8 and hLDL-F5 is 0.74, while hLDL-E8 is 0.77 as reported in Table 3.3. The QSQE score value of about 0.7 can be considered reliable, thus the construct models are acceptable. Furthermore, the stereo-chemical accuracy of the model was evaluated by using the Ramachandran plot to visualize energetically allowed regions for the backbone dihedral angle, Ψ (Y axis) and Φ (X axis) of the amino acid in protein structure. The Ramachandran plot revealed that most amino acids exist in the accepting regions that are possible for amino acid residues in a protein structure, which are shown at the top left for beta-sheet, bottom left for right-handed alpha-helix and top right for left-handed alpha-helix forms. However, the plot showed some glycine residues that are located outside of the accepted regions. As this amino acid does not have the C β atom that can induce many steric clashes in the standard Ramachandran plot, thus these residues are not restricted to the common regions. In the plot, hLDL-2D8 analysis observed 99.5% in allowed regions while Ala at position 57 in the light chain was in a disallowed region. hLDL-E8 had 99.4% in allowed regions except for Ala at position 57 of the light chain. For hLDL-F5, 98.8% of amino acid residues were found in the allowed regions, except Ala at position 89 in the light chain and Leu at position 51 in the heavy chain that were in the disallowed region.

Table 3.3 SWISS-MODEL Homology Modelling Report.

Clone	Template	Seq Identity	QSQE	QMEAN	Method	Resolution	Seq Similarity	Coverage
hLDL- 2D8	3iy3.1	56.76	0.74	0.77	EM	-	0.46	0.97
hLDL- E8	6amj.1	49.28	0.77	0.73	X-ray	2.49Å	0.45	0.96
hLLD- F5	1bbj.1	57.51	0.74	0.73	X-ray	3.10Å	0.46	0.95



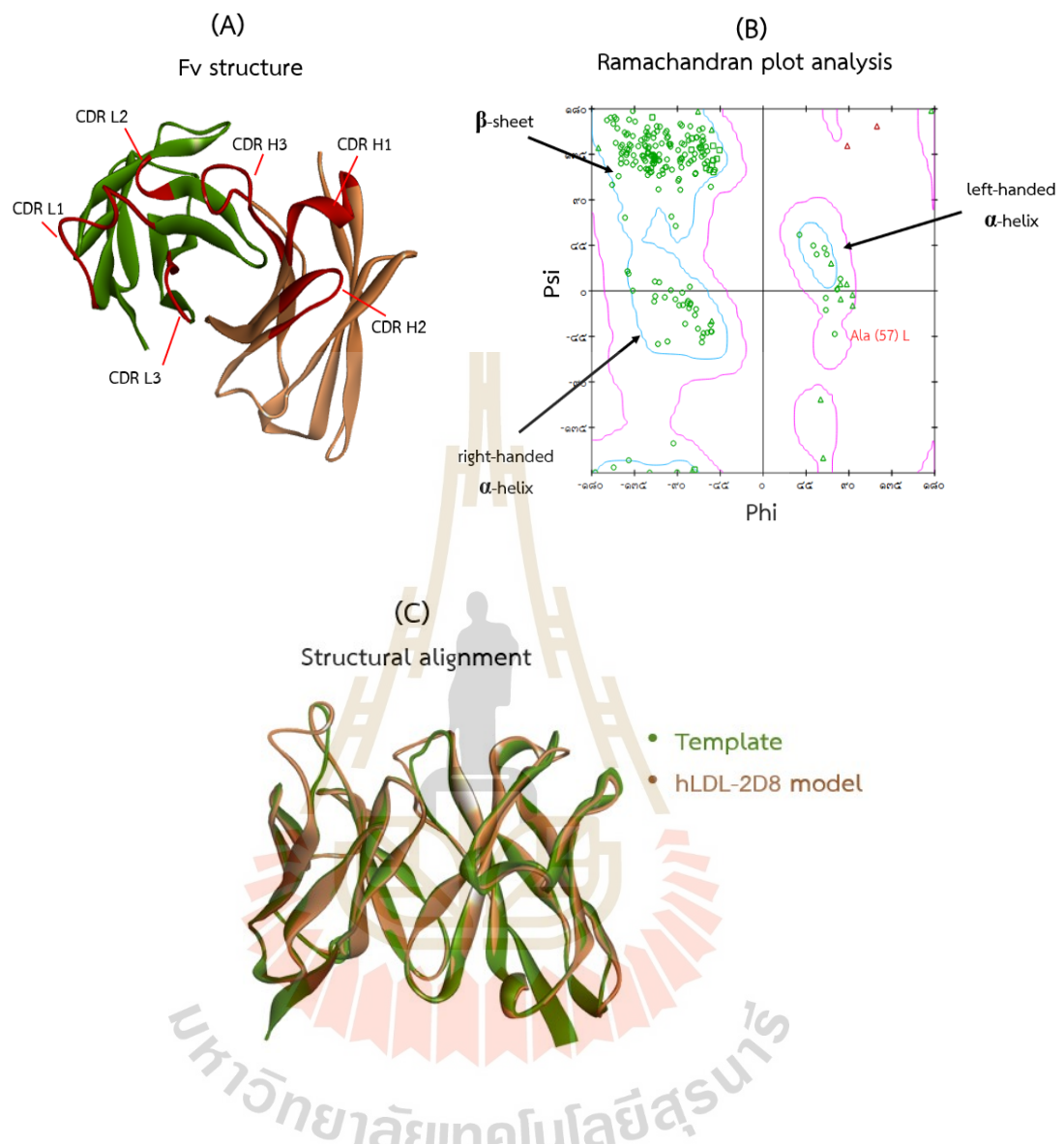


Figure 3.5 Computational modeling Fv structure of mAb hLDL-2D8 generated by SWISS-MODEL showing light (L) and heavy (H) chains with six complementarity-determining regions (CDRs) displayed by green color, orange color and red color, respectively (A). Ramachandran plot analysis shows phi-psi torsion angles of all residues in the Fv structure, and Glycine residues are separately identified by red triangles (B). Structural alignment between template structure (ID: [3iy3.1](#)) and structural model of hLDL-2D8 (C).

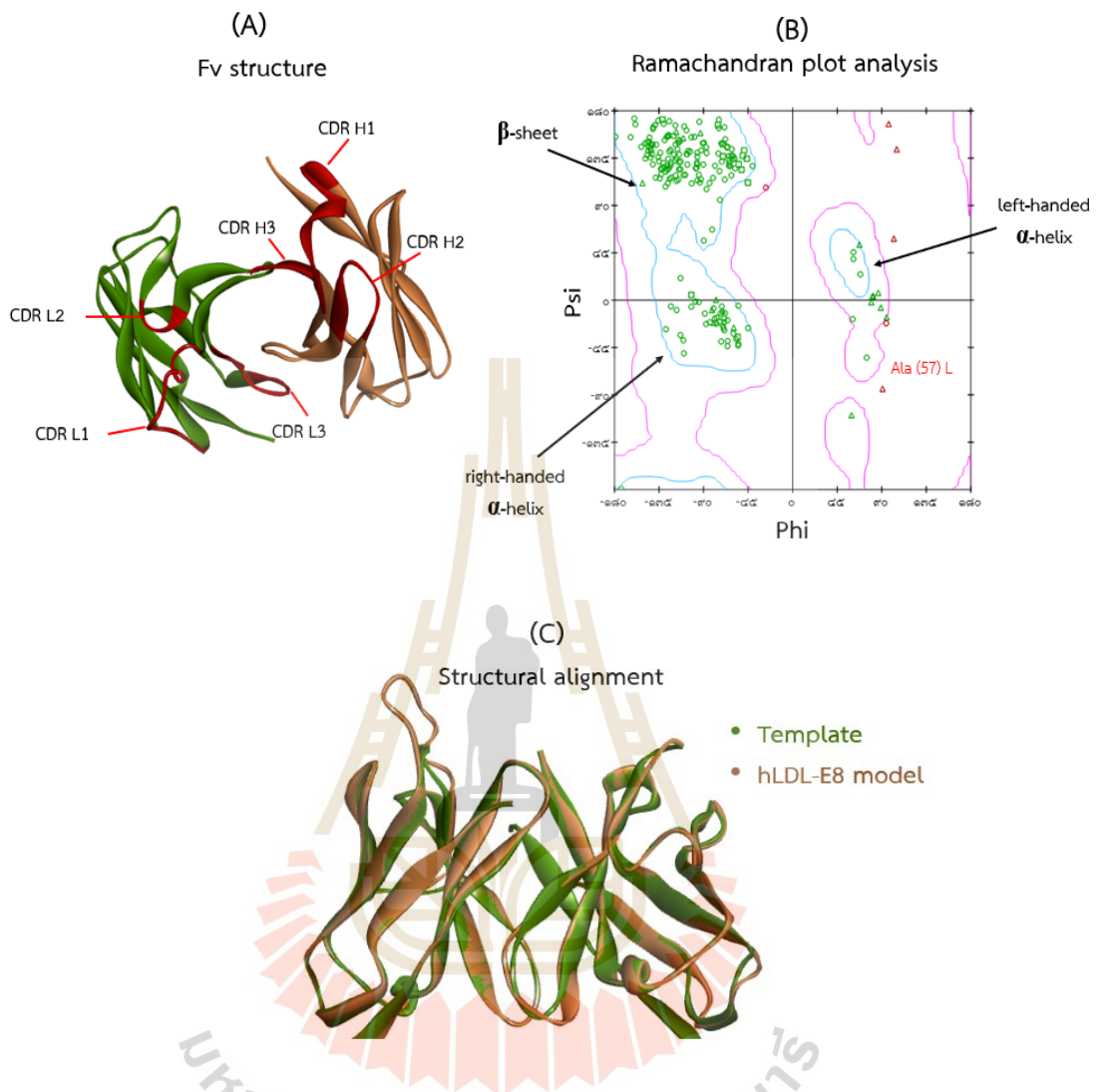


Figure 3.6 Computational modeling Fv structure of mAb hLDL-E8 generated by SWISS-MODEL showing light (L) and heavy (H) chains with six complementarity-determining regions (CDRs) displayed by green color, orange color and red color, respectively (A). Ramachandran plot analysis shows phi-psi torsion angles of all residues in the Fv structure, and Glycine residues are separately identified by red triangles (B). Structural alignment between template structure (ID: 6amj.1) and structural model of hLDL-E8 (C).

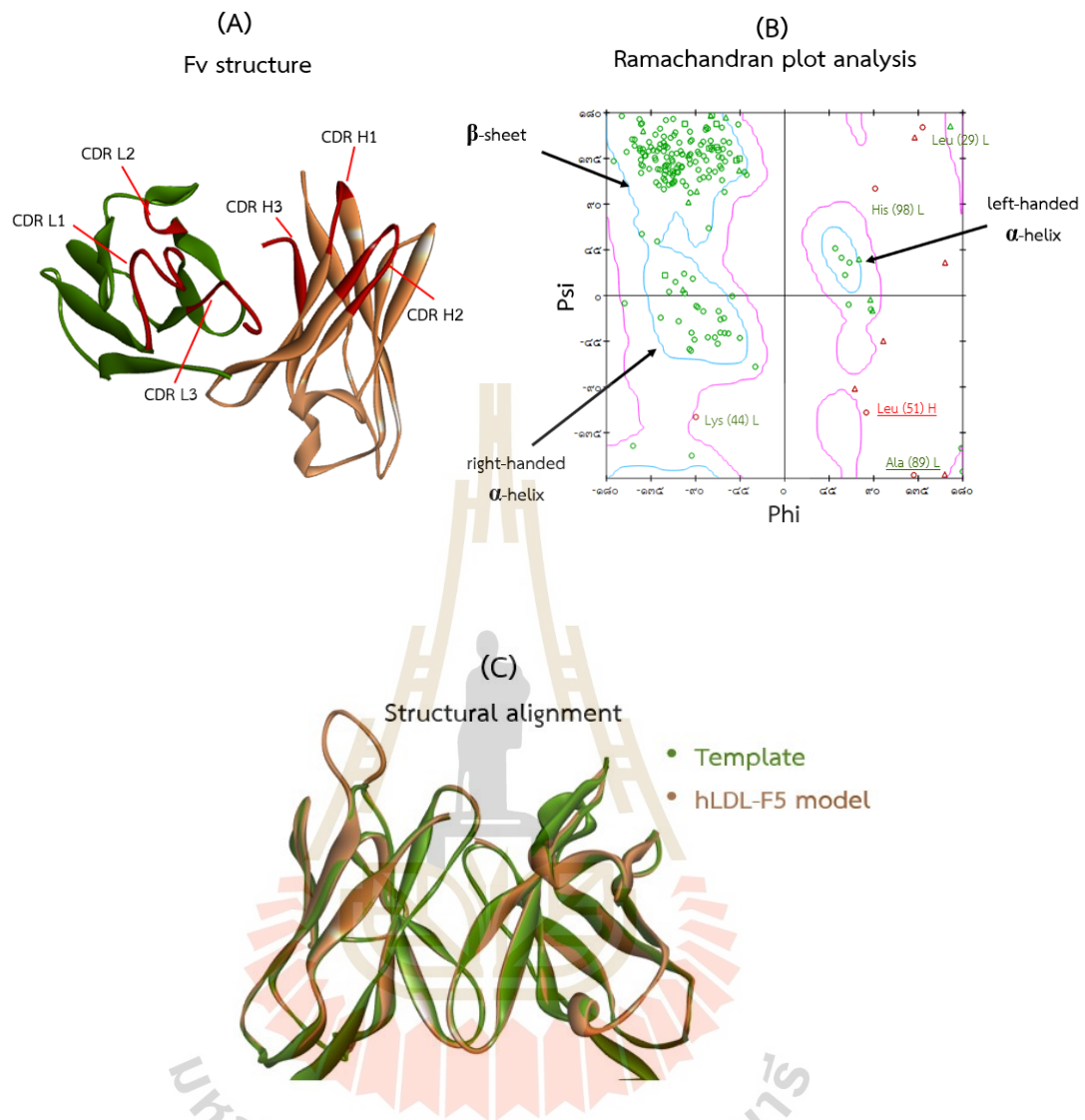


Figure 3.7 Computational modeling Fv structure of mAb hLDL-F5 generated by SWISS-MODEL showing light (L) and heavy (H) chains with six complementarity-determining regions (CDRs) displayed by green color, orange color and red color, respectively (A). Ramachandran plot analysis shows phi-psi torsion angles of all residues in the Fv structure, and Glycine residues are separately identified by red triangles (B). Structural alignment between template structure (ID: 1bbj.1) and structural model of hLDL-F5 (C).

3.4 Screening of mAbs binding regions by thrombin digestion and Immune Epitope Database (IEDB) prediction

Thrombin cleavage of apoB-100 has been reported to generate 4 different peptide fragments (Figure 3.8), called T1, T2, T3, and T4. T1 has cleavage site at amino acids (aa) 1297 and 3249 with molecular weight about 385 kDa, T2 (aa 3249-4536) (170 kDa). T1 can further be degraded to generate T3 fragment with a molecular size of 238 kDa (aa 1297-3249) and T4 fragment with a molecular size of 145 kDa ranging from 1 to 1297 amino acid residues (Corsini et al., 1987). In this study, thrombolytic cleavage of human apoB-100 was performed. Immunoblot was used to identify the mAb recognizing product fragments of the thrombolytic digestion and found that mAb clones hLDL-E8 and hLDL-F5 bind to the T1 and T3 fragments. However, mAb clone hLDL-2D8 reacted with T1, T4 of the NH₂-terminal fragments and other lower molecular weight fragments (Figure 3.9).

The Immune Epitope Database (IEDB) is an available server to predict the B cell linear epitope. This information provides a cluster of antigenicity residues for molecular docking of apoB-100 peptide fragments and Fv structure of mAbs. The IEDB prediction of apoB-100 results helped us to approach the accuracy of epitope prediction which knowing that the most optimal antigenic epitopes are flexible with hydrophilic located on the surface of the protein and antigenic determinants are preferably located at beta-turns or loops with amphipathic helices (Zobayer et al., 2019). (Figure 3.10, 3.11 and Table 3.4). The default value of linear epitope score is 0.35 and the normal range of surface accessibility is 1-6 but others are not mentioned.

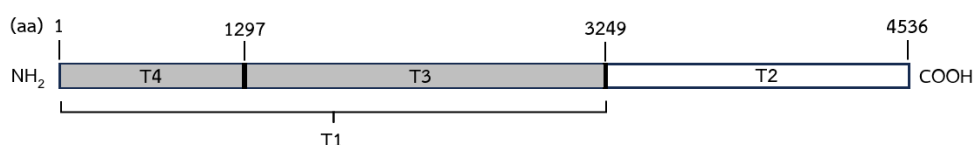


Figure 3.8 The amino acid residues corresponding to the major thrombin cleavage site on apoB-100 are indicated.

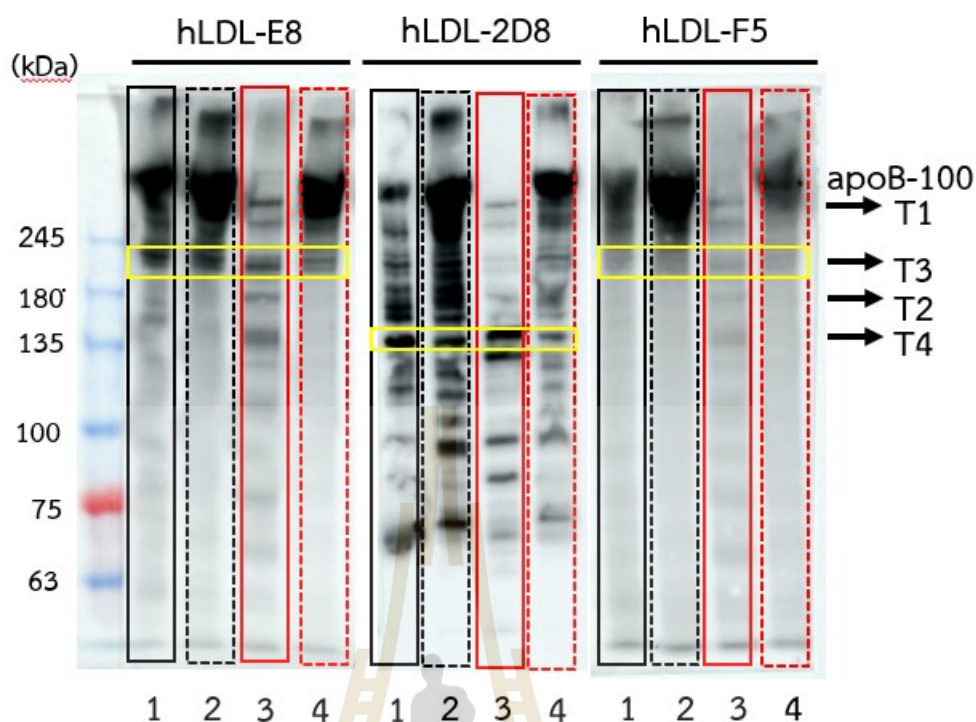


Figure 3.9 Immunoblots of thrombin digested of LDL and apoB-100. LDL and apoB-100 (150 μ g) were treated with plasma thrombin as described in Methods sections 2.7. The digested proteins (5 μ g proteins) were electrophoresed on 6% SDS-polyacrylamide and transferred to the PVDF membrane. The membranes were incubated with hLDL-E8 (2.5 μ g/ml), hLDL-2D8 (10 μ g/ml), and hLDL-F5 (5 μ g/ml). Lane: 1, commercial LDL; 2, commercial apoB-100; 3, digested LDL; 4, digested apoB-100. A representative result from one of three independent experiments is shown.

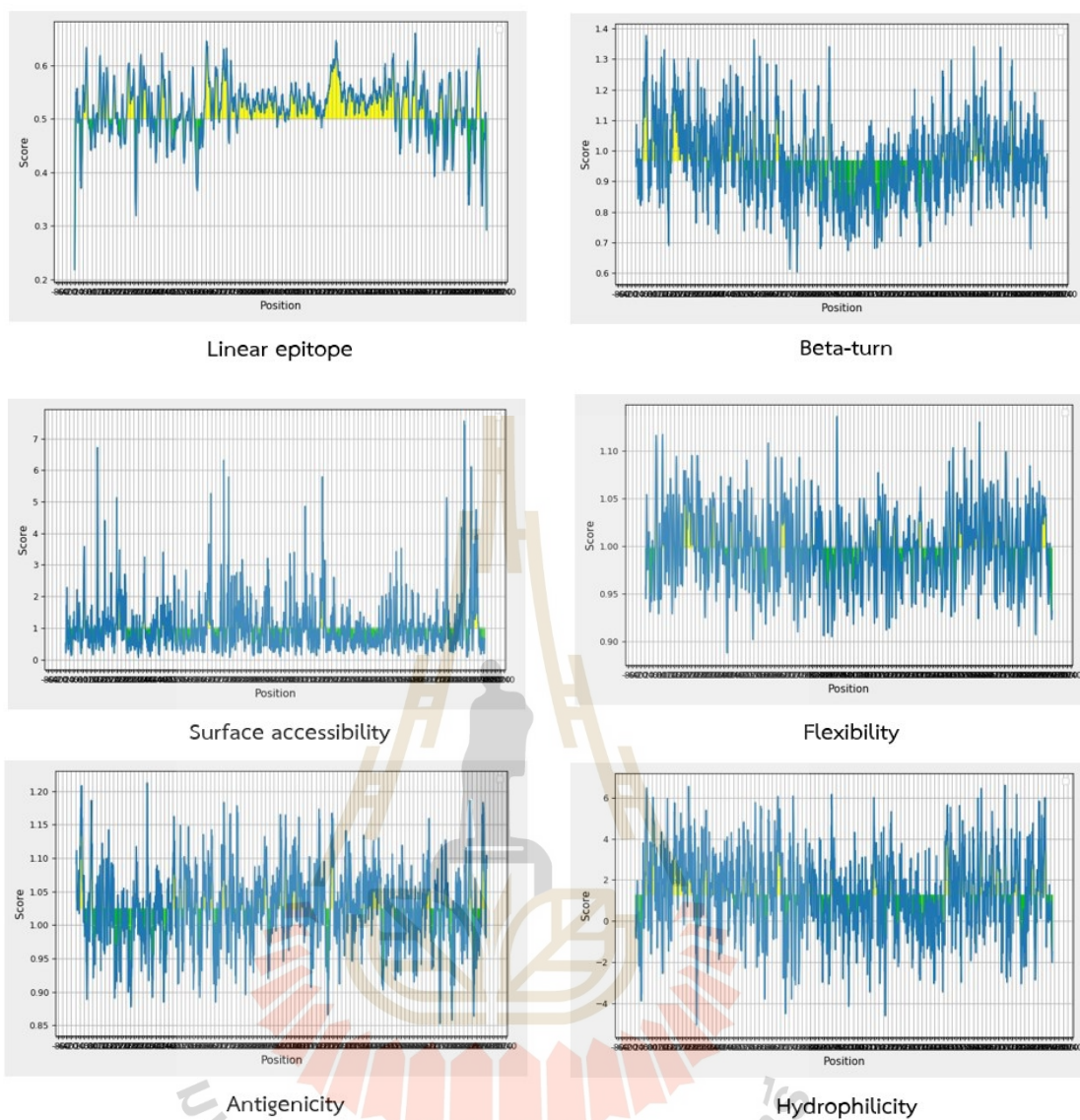


Figure 3.10 The linear epitope prediction generated by the IEDB server of T3 fragment apoB-100 (aa 1297-3249) based on sequence characteristics. The Y axis is the scoring value, and the X axis is the position of amino acid residues.

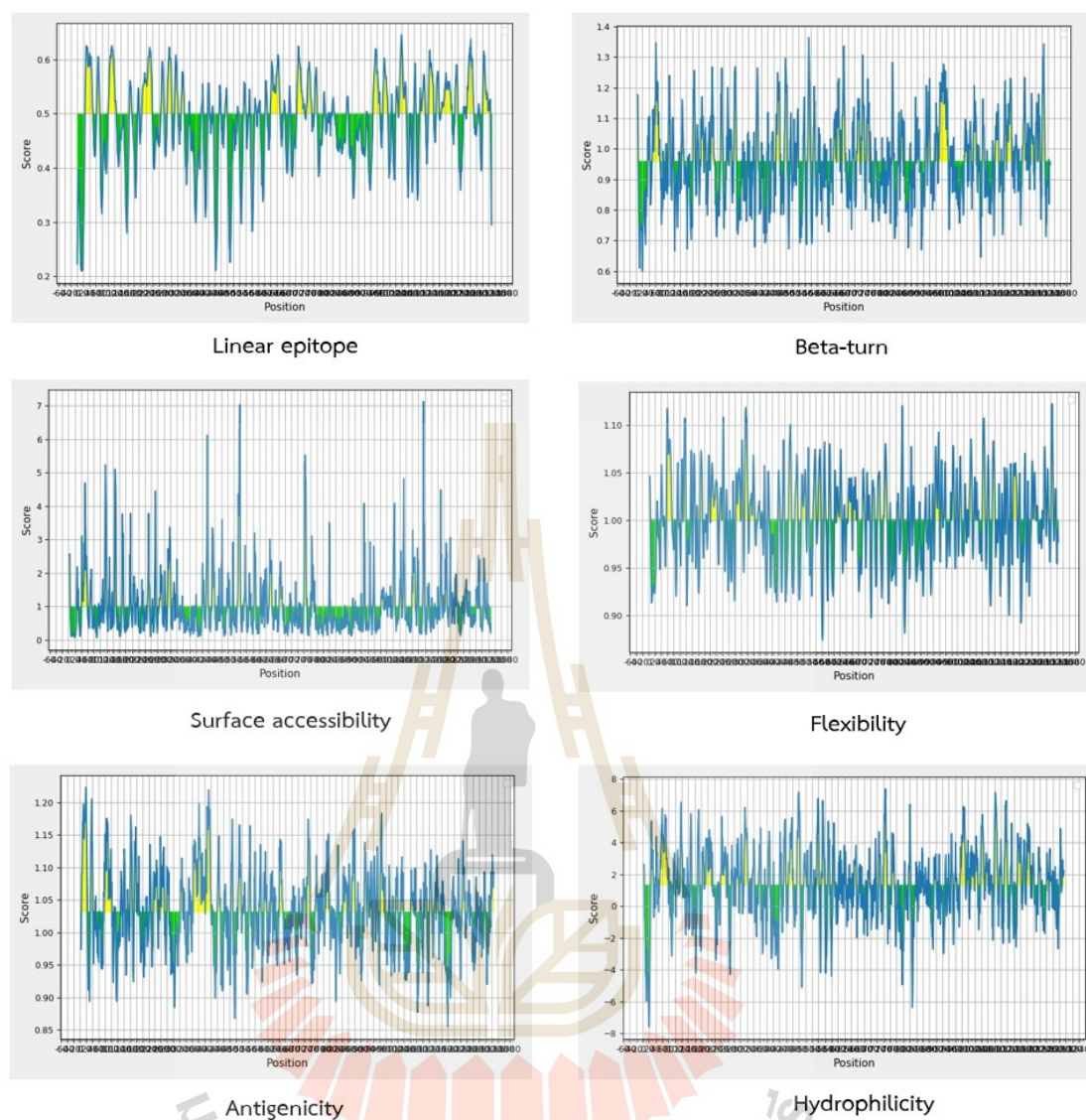


Figure 3.11 The linear epitope prediction generated by the IEDB server of T4 fragment apoB-100 (aa 1-1297) based on sequence characteristics. The Y axis is the scoring value, and the X axis is the position of amino acid residues.

Table 3.4 Scoring values of T3 and T4 apoB-100 fragments calculated according to amino acid properties from IEDB.

	T3	T4
Linear epitope score	0.218-0.66	0.210-0.645
Beta-turn score	0.604-1.377	0.6-1.364
Surface accessibility score	0.065-7.560	0.06-7.129
Flexibility score	0.888-1.136	0.874-1.122
Antigenicity score	0.853-1.212	0.855-1.223
Hydrophilicity score	-5.043-6.6	-7.586-7.371

3.5 Characterization of the mAb epitope binding

To determine the epitope binding region among the generated mAbs against human apoB-100, an inhibition ELISA was performed. Previous study (Lowhalidanon and Khunkaewla, 2021) suggested that hLDL-2D8 binds at a different compared epitope with hLDL-E8 but the new clone (hLDL-F5) has not been reported yet. In this work, each of the mAb clones were biotinylated and used as a detecting mAb, which was added after adding unconjugated primary mAb of each clone. Negative reactivity is observed if the unconjugated primary mAb (blocking mAb) prevents binding of the biotinylated mAb and indicates that these mAbs have the same or neighboring epitope binding site. Positive reactivity means that the biotinylated mAb can bind to the human apoB-100, indicating that the binding epitope of the mAb is different from that of the unconjugated primary mAb. Percent inhibitions of the biotinylated mAbs by the blocking mAbs are shown in Figure 3.12 and Table 3.5. The reactivity of biotinylated mAb binding to apoB-100 was used as a positive control in calculation and a negative control is unconjugated mAb binding to apoB-100 detected by HRP-streptavidin as in the inhibition assay.

The result shows that self-blocking of mAb hLDL-2D8 and hLDL-E8 are 78.9% and 70.8%, respectively. The percentage of inhibition was significantly reduced while different clones were applied as blocking antibodies. The results suggested that binding epitopes of mAb hLDL-2D8 and hLDL-E8 on apoB-100 are located at different

sites. While blocking hLDL-E8 can reduce the reactivity of conjugated hLDL-F5 about 33%. In addition, self-blocking of mAb clone hLDL-F5 was 34%, indicating low binding affinity to apoB-100 compared to other clones.

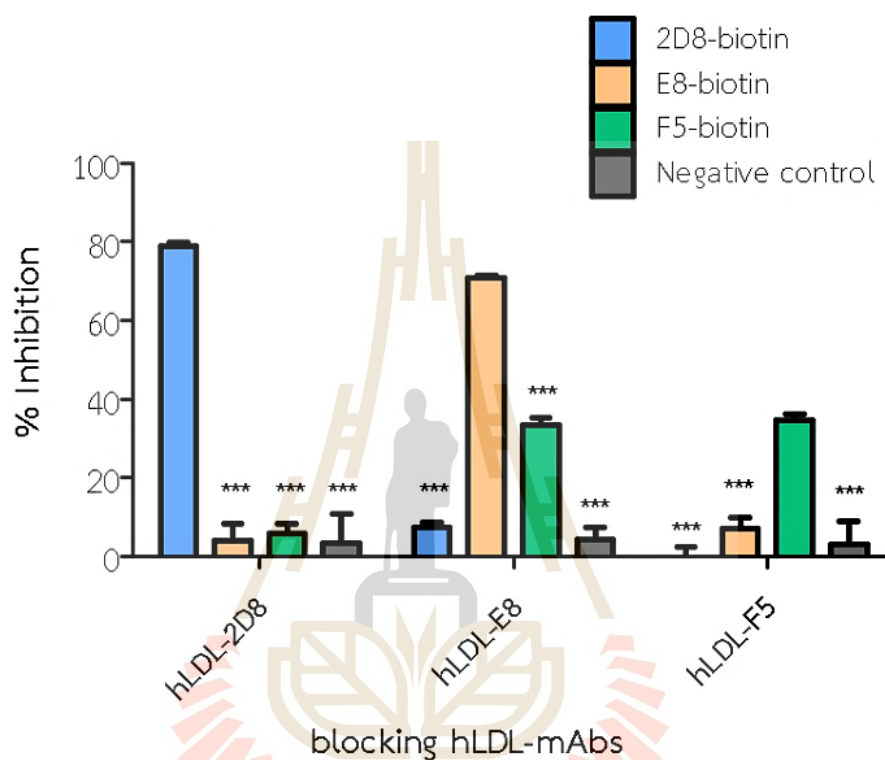


Figure 3.12 Percent binding inhibition among each mAb analyzed by inhibition ELISA. ApoB-100 protein was precoated on the ELISA plate and then reacted with either hLDL-2D8, hLDL-E8, or hLDL-F5. The data represents means (\pm SD), *** indicated $p < 0.001$ when comparing to each self-blocking.

Table 3.5 Summary of inhibition analysis of the generated mAbs against human LDL.

Unlabeled mAbs (blocking mAbs)	% Inhibition		
	Biotinylated mAbs		
	hLDL-2D8	hLDL-E8	hLDL-F5
hLDL-2D8	78.9	4.1	5.6
hLDL-E8	7.4	70.8	33.3
hLDL-F5	0.08	7.2	34.7

3.6 Computational docking and simulations of mAbs Fv region with apoB-100

Fv homology models were constructed and docked with apoB-100 peptides using the Autodock Vina and GOLD programs to investigate and screen for their binding regions according to the score values. The selected regions of amino acid residues for screening were based on the location of epitopes recognized by these mAbs to the thrombolytic fragments of apoB-100 and IEDB prediction. The docking scores were plotted and shown in Figure 3.13. The results revealed that mAb hLDL-E8 showed almost the same highest binding score as hLDL-F5 at -8.3 and -9.3 kcal/mol for Autodock Vina and GOLD score at 112.38 and 106.31, respectively. A group docking score of hLDL-2D8 showed lower free energy for both screening platforms at -6.9 kcal/mol and a GOLD score is 91.57.

Molecular docking revealed ¹⁵⁷⁴EYQADYE¹⁵⁸⁰ and ²¹⁵⁷YIKDSYD²¹⁶³ might be binding epitopes of hLDL-E8 and hLDL-F5 that the predicted binding sites of mAb hLDL-E8 and hLDL-F5 provide the same predicted Autidock Vina score values are -7.8 and -8.1 kcal/mol, for hLDL-F5 are -9 and -8.2 kcal/mol, respectively. For GOLD docking, the score values of mAb hLDL-E8 are 96.81 and 95.05, while mAb hLDL-F5 are 93.05 and 95.05, respectively. The highest GOLD score value for mAb hLDL-2D8 was found at the amino acid residues ⁶⁴⁵DPNNYLPKES⁶⁵⁴ and Autodock Vina at -6.4 kcal/mol. According to the obtaining scores, linear mapping of the epitope binding

sites for each mAb on the apoB-100 were assigned. Fv of hLDL-F5 and hLDL-E8 interact with same residues of two peptides, ¹⁵⁷⁴EYQADYE¹⁵⁸⁰ and ²¹⁵⁷YIKDSYD²¹⁶³, which were labeled as blue color according to the highest score with $\text{RMSD} \leq 1$ from both predictions as shown in Figure 3.15.



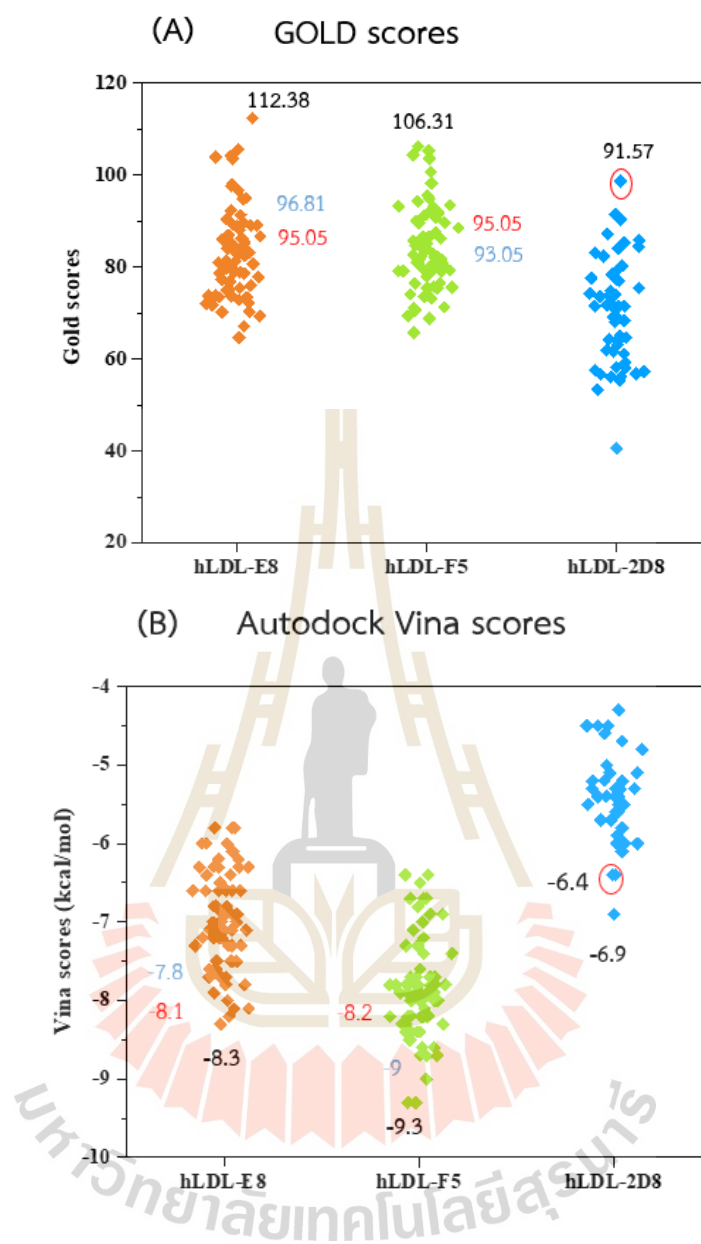


Figure 3.13 The docking score of mAbs hLDL-E8 (n=70), hLDL-F5 (n=70), and hLDL-2D8 (n=53) with $\text{RMSD} \leq 1$. (A) GOLD score function; (B) Autodock Vina score function. The labeling with a black color number represents the highest score value, red and blue colors represent the same predicted scores for both programs.

3.7 Confirmation of the epitope binding sites on apoB-100 by ELISA

In order to validate the computational prediction, an indirect ELISA technique was used to confirm binding epitopes of the studies mAbs on apoB-100. Streptavidin was coated on the well surface to capture the biotinylated peptides before detection with mAbs hLDL-2D8, or hLDL-E8 or hLDL-F5 followed by addition of HRP-conjugated anti-mouse-Ig. The positive reactivity of the tested peptides was observed by optical density measurement at wavelength 450 nm at 0–0.3. While mAbs bind to a coating apoB-100 acts as a positive control was observed a high signal in range 1.3–2.5. The signals of tested peptide for clone hLDL-2D8 was about 0.0873 for P4 whereas for P1 it was 0.0537. For clone hLDL-E8, tested peptides were observed at P3 and P5 with OD values about 0.24343 and 0.3134, respectively. When hLDL-F5 was tested under the same conditions, it had no significant signal over the background (Figure 3.14). However, this result suggested that hLDL-E8 showed the binding region in the range of amino acid residues 2050 to 2166 of P3 and P5 oligopeptides on full-length apoB-100. Considering the secondary structure apoB-100 that was taken from PDB, the amino acid sequence of P3 neighboring to P5 may have some overlapping in this area as shown in Figure 3.16. hLDL-2D8 seemed to bind at P4 (aa 712–722) more than P1 (aa 645–655). Unfortunately, hLDL-F5 still needs to be confirmed to a specific binding region by other techniques.

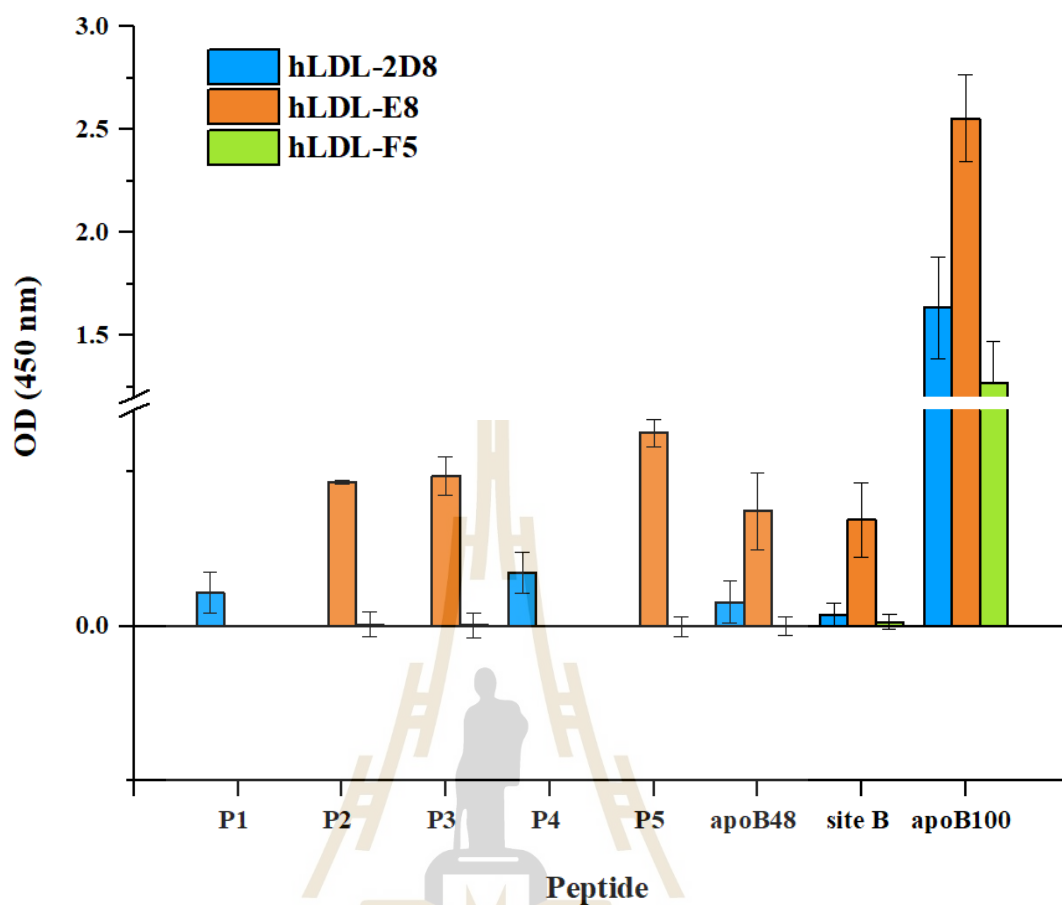


Figure 3.14 Epitope binding region confirmation was performed by ELISA assay. Plate coated with streptavidin-peptide (20 $\mu\text{g}/\text{ml}$) to capture with hLDL-mAbs (10 $\mu\text{g}/\text{ml}$) and then detected using the HRP-anti-mouse-Ig (1:5,000), OD at 450 nm was measured. The data represents the means ($\pm\text{SD}$) of three independent experiments.

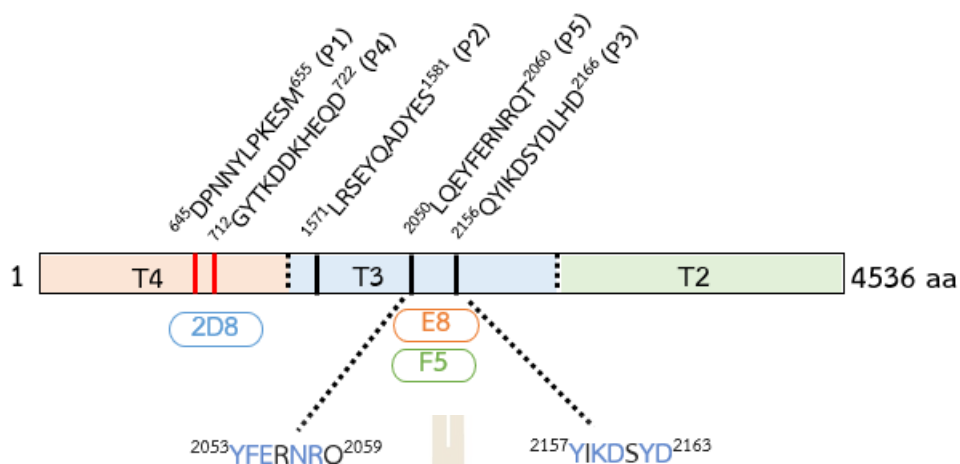


Figure 3.15 Linear map of apoB-100 and assignment of epitopes according to IEDB, docking score function and ELISA result. Amino acid sequence and range recognition on full-length apoB-100 (aa 4536) were labeled. Solid black lines were assigned for the same binding region of hLDL-E8 and hLDL-F5 and the same binding residues according to computational prediction were labeled a blue color.

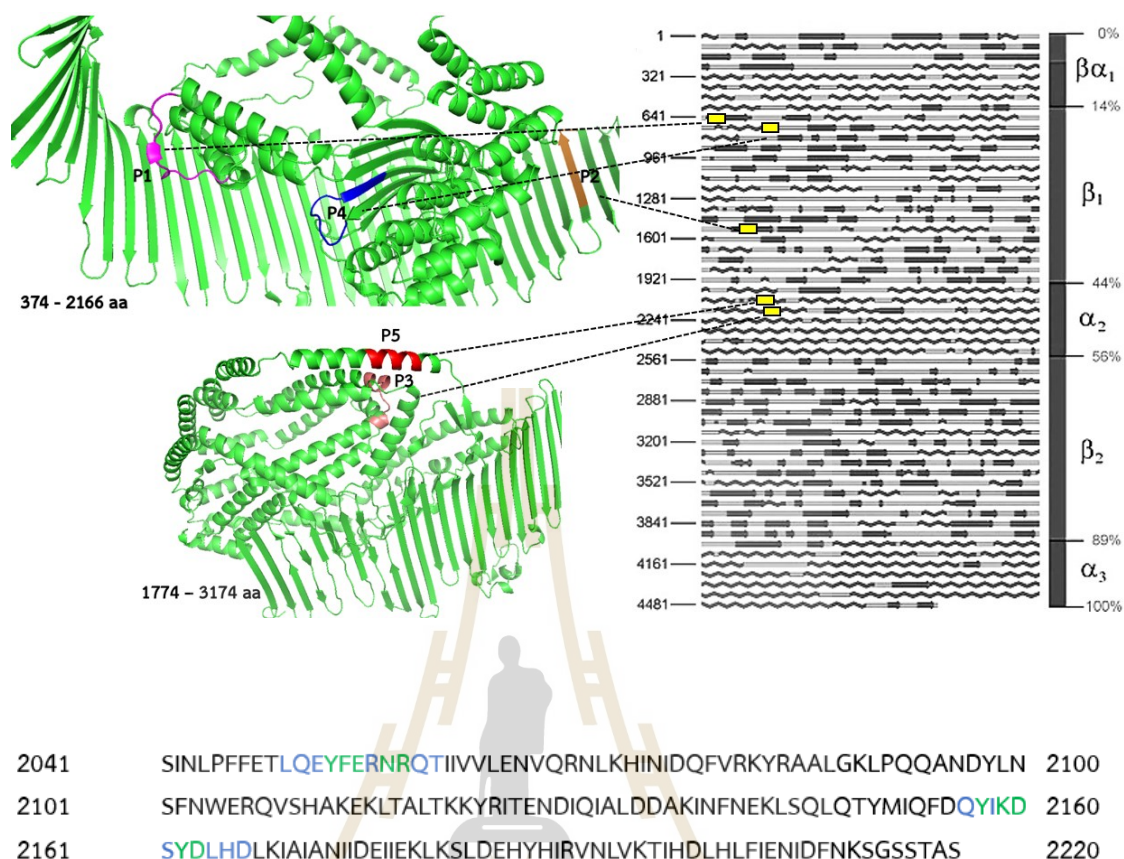


Figure 3.16 Epitopes assignment on secondary structure fragment from PDB (left) and linear diagram with different five domains (right) of full-length apoB-100, adapted from (SMALL, 2006). The amino acid sequence of oligopeptide P5 (2050-2060 aa) and P3 (2156-2166 aa) were assigned as blue color. Overlapping residues from a computational prediction of hLDL-E8 and hLDL-F5 by Autodock Vina and GOLD were assigned in as green color.

3.8 Binding affinity determination of apoB-100-specific mAbs by indirect ELISA

To evaluate the affinity constant (K_{aff}) based on the Law of Mass Action by indirect ELISA, serial dilution of both antigen (coating the plate) and antibody were performed. Various concentrations of human apoB-100 ranging from 0.039-40 $\mu\text{g/ml}$ were tested with an excess concentration of the mAbs at 80 $\mu\text{g/ml}$. According to the sigmoidal curve shown in Figure 3.17, four concentrations of apoB-100 at 1.25, 2.5, 5, and 10 $\mu\text{g/ml}$ that represent a linear portion of the curve are appropriate values and were chosen for further binding affinity tests. These concentrations were used to perform indirect ELISA with a serial four-fold dilution of a different mAb concentration range, hLDL-E8 (0.0009-15 $\mu\text{g/ml}$), hLDL-2D8 (0.0003-5 $\mu\text{g/ml}$), and hLDL-F5 (0.00048-500 $\mu\text{g/ml}$). To investigate how antibody affinity affected the sigmoidal dose-response curve's measurement of the affinity constant of three hLDL-mAbs, the sigmoidal curve of the obtained OD values (Y-axis) versus the logarithm of antibody concentrations (X-axis) were plotted (Figure 3.18-3.20). The affinity constant of mAbs was calculated by the general equation given in the 'Method (2.10.3)' and the results are shown in Table 3.6-3.8.

The results showed that at an OD-50 of each coated apoB-100 concentration (2.5, 5, and 10 $\mu\text{g/ml}$), there was approximately a one-fold increase in the antibody concentration that could be observed in the hLDL-2D8 clone experiment. The graph indicated that the concentration of Ab, [Ab] at OD-50 moved to the right hand when the concentration of the coated apoB-100 was decreased. Antibody concentration at OD-50 values of clone hLDL-E8 moved to the right hand, which is clearly seen with all concentrations of the coated apoB-100. For clone hLDL-F5, [Ab] at OD-50 showed varying antibody concentration for all experiments when apoB-100 concentration was 2-fold decreased may be caused by an unsaturated point of the range antibody concentration. However, most [Ab] tends to decrease 1.5 times, making the OD-50 values shift to the left hand. This information suggested that the binding affinity of the antibody tends to decrease as the antigen concentration decreases. Moreover, hLDL-2D8 shows the strong binding and specificity to apoB-100 with low antibody concentration to assess a saturation point compared to hLDL-E8 and hLDL-F5.

According to the characteristic of the OD-50 value and the affinity constant obtained by the Beatty equation calculation, the behavior of the hLDL-F5 corresponds to theoretical curve-response as shown in Figure 1.10. This result suggested that apoB-100 has two epitopes recognized by hLDL-F5. On the other hand, clones hLDL-2D8 and hLDL-E8 can be described by the Law of Mass action, the antibody concentration at equilibrium increased by decreasing of antigen to maintain an equilibrium constant (K_{eq}) at ratio of antigen: antibody is 1:1. This suggestion can assume that one part of an antigen is recognized by the mAb (Reverberi and Reverberi, 2007).



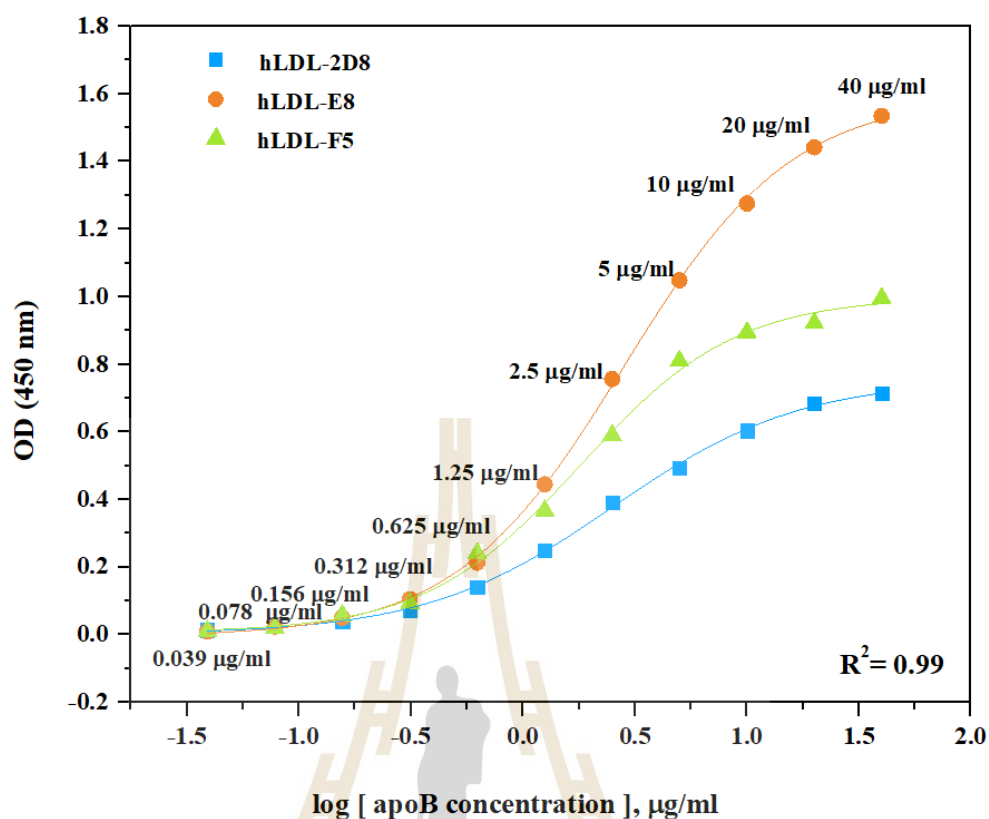


Figure 3.17 Dose dependence binding of mAbs with apoB-100 using serial dilutions of coated apoB-100 ranging from (apoB-100) 0.039-40 µg/ml. Excess concentration of the mAbs; hLDL-2D8, hLDL-E8, and hLDL-F5 at 80 µg/ml were used for saturation. A representative result from one of three independent experiments is shown.

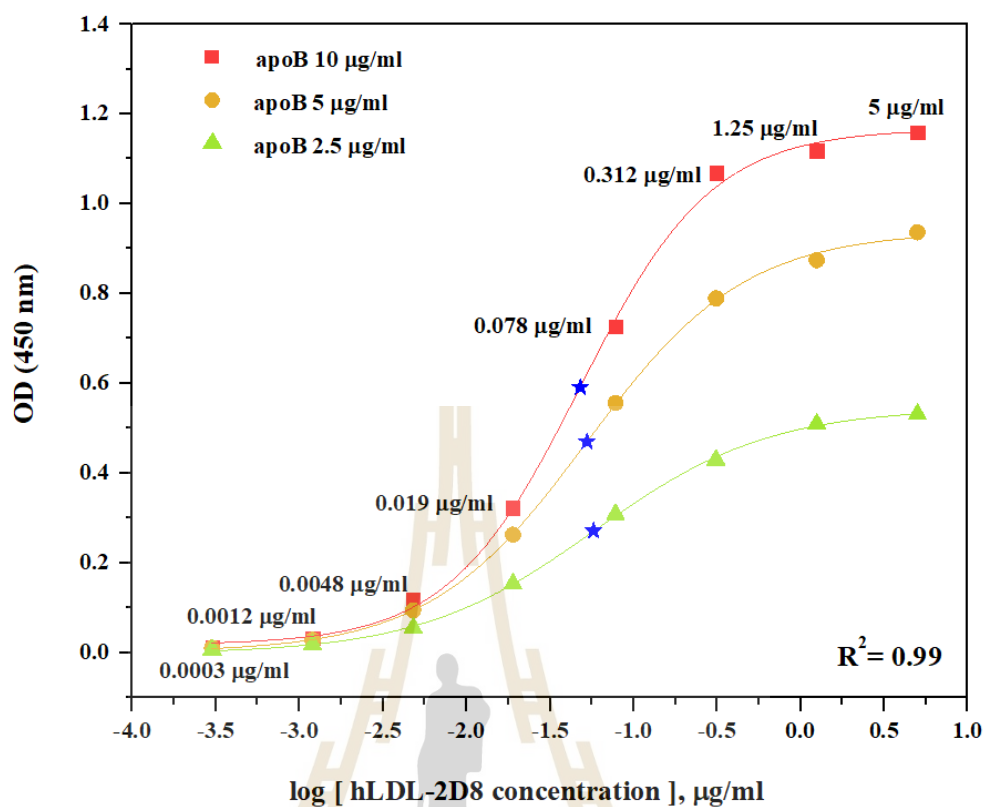


Figure 3.18 Experimental dose-response curve for mAb hLDL-2D8 (0.0003-5 $\mu\text{g/ml}$) at three different human apoB-100 concentrations, (*) denotes antibody concentration at OD-50. A representative result from one of three independent experiments is shown.

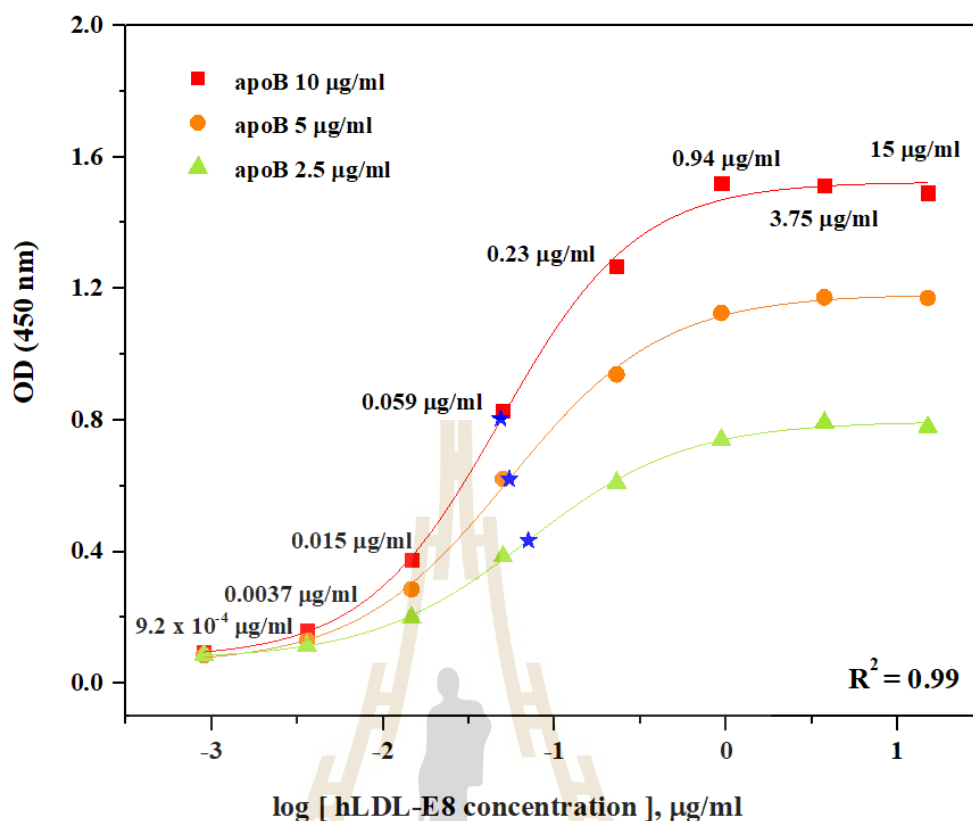


Figure 3.19 Experimental dose-response curve for mAb hLDL-E8 (0.0009-15 µg/ml) at three different human apoB-100 concentrations, (*) denotes antibody concentration at OD-50. A representative result from one of three independent experiments is shown.

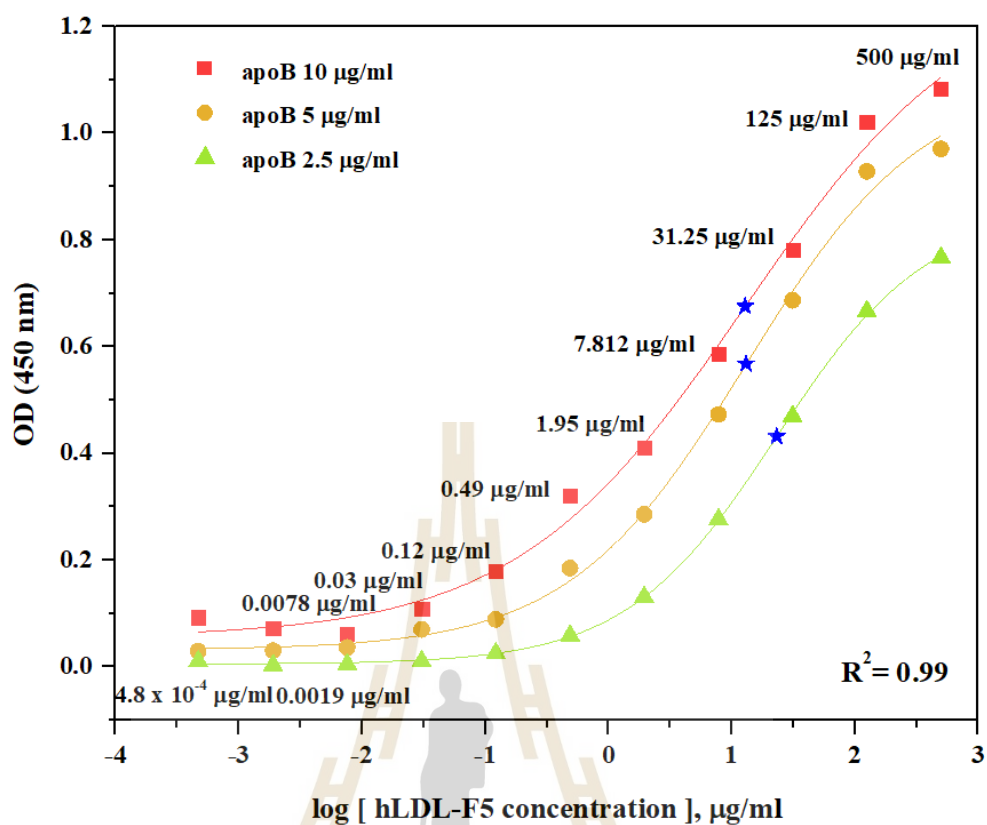


Figure 3.20 Experimental dose-response curve for mAb hLDL-F5 (0.00048-500 $\mu\text{g/ml}$) at three different human apoB-100 concentrations, (*) denotes antibody concentration at OD-50. A representative result from one of three independent experiments is shown.

Table 3.6 Calculated affinity constants (K_{aff}) of mAb hLDL-2D8 from experimental dose-response curve value determined by indirect ELISA.

mAbs	[apoB] (ng/ml)	[Ab] at OD-50 (ng/ml)	K _{aff} (M ⁻¹)	Average K _{aff} (M ⁻¹)	Average K _{aff} (M ⁻¹)
hLDL-2D8	10,000	10.09	3.2 × 10 ⁹	2.27±0.95 × 10 ⁹	1.51±0.69 × 10 ⁹
		39.31	2.3 × 10 ⁹		
		47.99	1.3 × 10 ⁹		
	5,000	16.79	0.83 × 10 ⁹	1.33±0.59 × 10 ⁹	
		35.78	1.98 × 10 ⁹		
		52.66	1.18 × 10 ⁹		
	2,500	53.21	1.7 × 10 ⁹	0.93±0.71 × 10 ⁹	
		36.85	0.8 × 10 ⁹		
		58.02	0.3 × 10 ⁹		

Table 3.7 Calculated affinity constants (K_{aff}) of mAb hLDL-E8 from experimental dose-response curve value determined by indirect ELISA.

mAbs	[apoB] (ng/ml)	[Ab] at OD-50 (ng/ml)	K_{aff} (M^{-1})	Average K_{aff} (M^{-1})	Average K_{aff} (M^{-1})
hLDL-E8	10,000	44.62	10.71×10^8	$10.88 \pm 1.51 \times 10^8$	$7.25 \pm 3.56 \times 10^8$
		48.46	12.46×10^8		
		46.09	9.46×10^8		
	5,000	57.33	5.76×10^8	$7.12 \pm 1.49 \times 10^8$	
		54.31	8.72×10^8		
		62.7	6.89×10^8		
	2,500	93.74	2.80×10^8	$3.76 \pm 1.30 \times 10^8$	
		70.15	5.24×10^8		
		85.78	3.23×10^8		



Table 3.8 Calculated affinity constants (K_{aff}) of mAb hLDL-F5 from experimental dose-response curve value determined by indirect ELISA.

mAbs	[apoB] (ng/ml)	[Ab] at OD-50 (ng/ml)	K _{aff} (M ⁻¹)	Average K _{aff} (M ⁻¹)	Average K _{aff} (M ⁻¹)
hLDL-F5	10,000	18,444	4.75 × 10 ⁶	7.08±3.34 × 10 ⁶	4.39±2.63 × 10 ⁶
		18,551	10.9 × 10 ⁶		
		12,856	5.58 × 10 ⁶		
	5,000	17,114	5.53 × 10 ⁶	4.25±1.74 × 10 ⁶	
		12,693	4.96 × 10 ⁶		
		13,145	2.27 × 10 ⁶		
	2,500	15,335	1.86 × 10 ⁶	1.83±0.22 × 10 ⁶	
		13,910	2.03 × 10 ⁶		
		23,101	1.59 × 10 ⁶		

Table 3.9 Conclusion of characteristics of three mAbs on apoB-100.

Clone name	Thrombin fragment	Inhibition assay	Affinity			Confirmation epitope site
			Docking score		ELISA	
			Autodock Vina	GOLD		
hLDL-2D8	T4	Inhibit other clones	*	*	***	⁷¹² GYTKDDKHEQD ⁷²²
hLDL-E8	T3	Inhibit hLDL-F5 33%	**	***	**	²⁰⁵⁰ LQEYFERNRQT ²⁰⁶⁰ ²¹⁵⁶ QYIKDSYDLHD ²¹⁶⁶
hLDL-F5	T3	Self-inhibition with low affinity	***	**	*	-

Note; * indicates the relative docking score value and ELISA results between hLDL-2D8, hLDL-E8, and hLDL-F5, *** is the highest value.

CHAPTER IV

DISCUSSION AND CONCLUSION

The antigen-antibody interaction involves non-covalent interaction between the binding site of the antigen (Ag) epitope and the complementary site on the antibody (Ab). Knowing the ability of an Ab bind to a surface antigen with specificity and high affinity is important to immunity and makes Abs a valuable tool in biomedical research, diagnostics, and therapy. Several studies have tried to map the binding epitope of mAb on apoB-100 molecule. Thrombolytic cleavage has been used to generate different fragments of apoB-100 with limited cleavage patterns of four fragments. In combination with protein expression in *E.coli* system, protein fragments representing the complete apoB-100 cDNA was used to assign the possibility of unambiguous assignment of epitopes. Some reports revealed mAbs specific for an epitope on the LDL receptor binding region, lead to blocking LDL binding to the LDL receptor resulting in an atheroprotective effect. However, some mAbs have been reported to have poor access to receptor-bound LDL. This suggests that mAbs against human LDL can bind inside and outside of LDL receptor regions. (Triplett and Fisher, 1978; Cardin et al., 1984; Marcel et al., 1987; Krul et al., 1988; Milne et al., 1989; Pease et al., 1990; Chatterton et al., 1991; Fantappie et al., 1992).

In this study, three mAbs against human LDL (hLDL-2D8, hLDL-E8, hLDL-F5), which were known to bind on the apoB-100 of LDL particles were selected to identify their critical binding epitopes. Firstly, DNA sequences of the variable region from extracted RNA hybridoma cell line expressing these antibodies were identified. RT-PCR, a basic method used for amplifying DNA variable regions with specific primers was performed following a previous paper (Meyer et al., 2019).

After Sanger Sequencing, the obtained DNA sequence needed to be corrected by comparing it with the available nucleotide immunoglobulin sequence from NCBI. Then, translating DNA to protein sequence was performed by IMGT for complement Ab or CDRs identification. The result suggests that the heavy chain is the main chain to identify an individual mAb against human LDL by showing the different amino acid residues on their CDRs. The accurate sequences of light and heavy variable chains were checked by IMGT with an acceptable percentage more than 50% on average.

To assess the accuracy antibody structure for computational docking, the models were selected by focusing on suitable Fv structure using SWISS-MODEL servers compared to crystal structure with an acceptable QSQE score value above 0.7. Then, the amino acid residues of the model were analyzed by Ramachandran plot, the results revealed more than 99% amino acid residues in the favored region that retains the fold pattern of Fv immunoglobulin structure (Janeway et al., 2001). The variable regions of both heavy and light chain immunoglobulin are in direct interaction with the antigen and frequently mutated to allow diverse antigenic specificities to be recognized. This region is called hypervariable region or CDRs. Amino acid sequence alignment of the tested mAb variable regions using IMGT tool revealed the hypervariable regions containing charged side chains of Arg (R), His (H), Asp (D), hydrophobic side chain of Ala (A), Tyr (W), Trp (Y) and uncharged side chain of Ser (S), Thr (T), Gln (Q) and Asn (N). The finding corresponded to a previous report indicating that 55% of four amino acids found in CDR residues including tyrosine (24%), serine (12%), asparagine (10%), and tryptophan (9%) and less than 10% of the other ten amino acids in the CDR (C, M, Q, K, A, P, V, E, H, L) (Ofra et al., 2008). This finding assists in computational antibody modeling design and molecular docking of CDR-epitope complexes prediction between mAbs Fv structure and apoB-100.

To characterize the binding epitope for each human LDL mAbs, an inhibition assay was performed. Percent inhibitions of binding of the biotinylated mAbs by the blocking mAbs are shown in Figure 3.12. as summarized in Table 3.5, which suggested that binding epitope of hLDL-F5 on apoB-100 overlaps with the mAb hLDL-E8 binding sites. hLDL-E8 can inhibit hLDL-F5 33% whereas hLDL-2D8 binds to different epitope with hLDL-F5 and hLDL-E8.

ApoB-100 is a large protein with high susceptibility to be degraded by proteolysis (Chapman and Kane, 1975). Shortening of the protein to define the specific linear binding site is the process to reduce the difficulty for mAb binding epitope screening. Thrombolytic digestion was applied for apoB-100 digestion to obtain the different fragments including T1 (385 kDa), T2 (170 kDa), T3 (238 kDa) and T4 (145 kDa). As shown in Figure 3.9, mAbs hLDL-E8 and hLDL-F5 mAbs bound specifically to T3 fragment, while hLDL-2D8 strongly reacted with T4 fragment. Note that all tested mAbs preferentially bind to undigested LDL rather than undigested apoB-100. This result supports the inhibition assay that hLDL-2D8 binds at different fragment with hLDL-F5 and hLDL-E8. Some bands of the digested product at low molecular weight were also recognized by all mAbs, which may be caused by continuous digestion of the protein after 8 hours of incubation. Although we can scope the binding region by thrombolytic digestion, in which there are thousands of amino acid residues in range. There are still a lot of peptide ligands that are difficult to predict by molecular docking. Therefore, free epitope databases, IEDB prediction server, was used to reduce the number of epitope binding sites to ten amino acids according to amino acid properties. The peptide ligand was selected by their ability of antigenicity such as a high score of flexibility, hydrophilicity, accessibility on the surface of the protein. Then, the rapid method, molecular docking was derived according to the different docking score functions to find the interaction details of mAbs and oligopeptides apoB-100. Preparation of molecular docking, CDRs region of antibody was accounted as a boundary for docking process and ligands were generated by the Discovery software with optimizing structure. Two molecular docking programs that are available in our lab, including GOLD and Autodock Vina were used. The GOLD score is reported in terms of fitness value which higher the fitness shown better docked interaction of the complexes. Contrasting, the Autodock Vina score is reported in terms of the docking energy score, the lower the score the better the interaction. As shown in Figure 3.13, mAbs hLDL-E8 and hLDL-F5 have same binding region with high interacting score of amino acid sequence ¹⁵⁷⁴EYQADYE¹⁵⁸⁰ and ²¹⁵⁷YIKDSYD²¹⁶³ of full-length apoB-100. This sequence is located near the glycosaminoglycan binding region at aa 2117-2127 (Flood et al., 2002). The

predicted binding site of mAb hLDL-2D8 indicated at a sequence ⁶⁴⁵DPNNYLPKES⁶⁵⁴, which corresponds to the highest score docking and IEDB prediction. Molecular docking is a powerful computational method to study the binding mode of small molecules to proteins, protein-protein interaction, include Ab-Ag interaction. Nevertheless, one must keep in mind that the result obtained from this platform is based on the binding mode prediction, which may not be true with the physiological interaction of the proteins. Therefore, the generated interaction model is strongly recommended to be refined using experimental data to obtain an accurate result. This study predicted binding epitope of the mAbs hLDL-E8, hLDL-2D8 and hLDL-F5 on apoB-100 were validated by performing indirect ELISA. As the coating antigens are small oligopeptides with 11 amino acid residues, binding efficiency of the mAbs to these peptides can be lower than the native protein. As shown in the results, low binding signal was observed for interaction of mAb hLDL-E8 with apoB-100 and oligopeptides P3 and P5 at aa 2050 to 2166. The mAb hLDL-2D8 tends to bind oligopeptide P4 at aa 712-722. No interacting signal to any oligopeptide was observed while using mAb hLDL-F5, which can cause by either misprediction or the antibody itself has low binding affinity even with the native apoB-100, which is supported by the inhibition assay shown in Figure 3.12 and its affinity constant shown in Table 3.8.

To access the antibody-apoB-100 interaction in term of kinetic, the affinity constant was investigated by immunoassay. The main advantage of this technique is it is easy to perform, relatively cheap, rapid, and practical for routine use. This approach relies upon the measurement of the use of total antibody concentration added per well [Ab], by performing a serial dilution of antibody against logarithm of concentration to provide dose-response curve and then calculate the affinity constant according to Beatty equation (Beatty et al., 1987). The result showed a strong binding affinity of mAb hLDL-2D8 bound to apoB-100 at $1.51 \pm 0.69 \times 10^9 \text{ Mol}^{-1}$ and calculated affinity constant of mAb hLDL-E8 is $7.25 \pm 3.56 \times 10^8 \text{ Mol}^{-1}$. While mAb hLDL-F5 displayed a lower affinity constant ($4.39 \pm 2.63 \times 10^6 \text{ Mol}^{-1}$). In this study, molecular docking was used to evaluate the affinity of potential antigens screened among peptide apoB-100 and Fv antibody against human LDL. There is an opposite result of binding affinity with immunoassay which clone hLDL-F5 and hLDL-E8 show

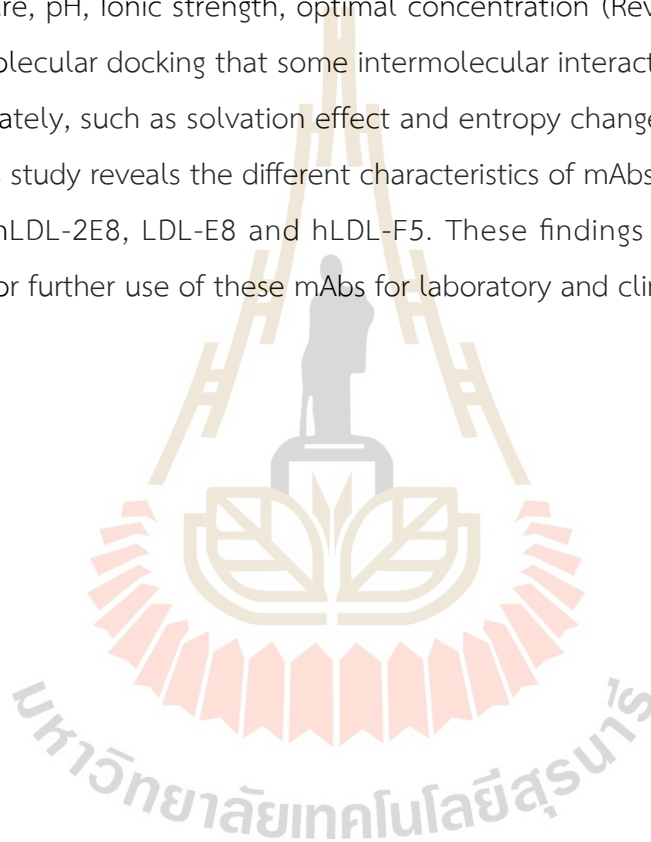
high binding score by molecular docking, whereas the ELISA result displayed a low affinity constant including hLDL-2D8 also displayed the same opposite result as the conclusion in Table 3.9.

Performing ELISA assay to investigate the binding region and binding affinity is still not sufficient to confirm the accurate results. Generally, the ELISA method was described that some antibodies display disproportionately increased binding at high antigen densities compared to low antigen densities and Ab avidity enhancement effect strongly depends on the density of antigens, since the reach of the two binding sites of IgG is about 150 Å (Hadzhieva et al., 2017). So, the distribution pattern of epitopes at the surface of pathogens has a profound impact on antigen-antibody interaction. Additionally, a low affinity of antibodies permits higher dynamics during the antigen recognition process (Janin, 1995; Stites, 1997). While docking procedure cannot access the total affinity of conformational apoB-100 protein docking because there is no full-length structure reported in the database. Besides, the three-dimensional structure of a protein-protein docking is difficult to determine binding interaction. The important consideration is that the protein shape, reflecting the protein fold, a large ligand-receptor area to a large extent determines the docking solution (Vakser, 2013).

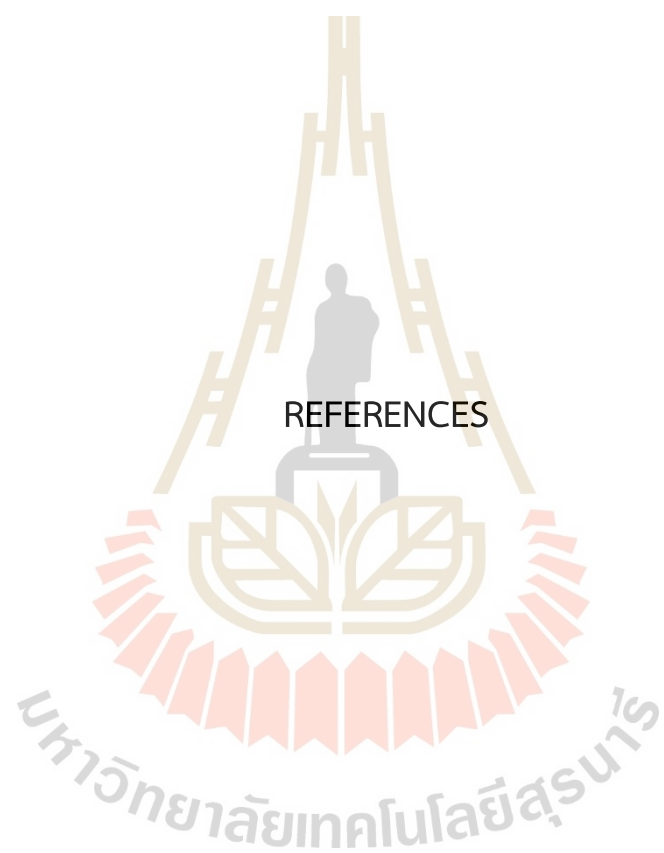
Overall results are challenging due to the apoB-100 is a large protein. The role of conformational and linear epitopes are also critical for binding affinity investigation. Furthermore, the binding efficiency of mAbs to conformationally sensitive epitopes might be expected to change with antigen surface density. Several methods have been previously reported site of apoB-100, for example, using of the digestive enzyme to generate epitope site of apoB-100, using bacterial expression clone to map epitopes, or mapping mAbs using electron microscopy to visualize pairs of mAbs binding to LDL surface (Chatterton et al., 1991).

In conclusion, CDRs of the in-house mAbs against human LDL clones hLDL-2D8, hLDL-E8, and hLDL-F5 were identified by DNA sequencing analysis. The epitope prediction was carried out by computational and experimental methods. Thrombolytic digestion and IEDB prediction were performed to narrow down the epitope position full-length apoB-100 and the result reveals a specific binding region

for each clone of hLDL-mAbs. For the molecular docking suggests that five oligopeptides with high docking scores (P1-P5) bind to different epitopes in response to GAGs regions as previously reported. Confirmation by ELISA assay reveals epitope binding site of hLDL-E8 was assumed to be in a range of 2050 to 2166 amino acids. Additionally, the binding affinity of monoclonal antibodies against apoB-100 performed by immunoassay has the opposite results with molecular docking. The problem can occur from many factors that affecting antigen-antibody interaction such as temperature, pH, ionic strength, optimal concentration (Reverberi and Reverberi, 2007) and molecular docking that some intermolecular interaction terms are hard to predict accurately, such as solvation effect and entropy change (Yuriev et al., 2011). However, this study reveals the different characteristics of mAbs against human apoB-100 clones hLDL-2E8, LDL-E8 and hLDL-F5. These findings contribute valuable information for further use of these mAbs for laboratory and clinical research.



REFERENCES



REFERENCES

- Abanades, B., Wong, W. K., Boyles, F., Georges, G., Bujotzek, A. and Deane, C. M. (2022). ImmuneBuilder: Deep-Learning models for predicting the structures of immune proteins. *bioRxiv*, 2022.2011. 2004.514231.
- Adolf-Bryfogle, J., Xu, Q., North, B., Lehmann, A. and Dunbrack Jr, R. L. (2015). PylgClassify: a database of antibody CDR structural classifications. *Nucleic acids research* 43(D1), D432-D438.
- Ambrosetti, F., Olsen, T. H., Olimpieri, P. P., Jiménez-García, B., Milanetti, E., Marcatilli, P. and Bonvin, A. M. (2020). proABC-2: PRediction of AntiBody contacts v2 and its application to information-driven docking. *Bioinformatics* 36(20), 5107-5108.
- Amzel, L. M. and Poljak, R. J. (1979). Three-dimensional structure of immunoglobulins. *Annual review of biochemistry* 48(1), 961-997.
- Beatty, J. D., Beatty, B. G. and Vlahos, W. G. (1987). Measurement of monoclonal antibody affinity by non-competitive enzyme immunoassay. *Journal of immunological methods* 100(1-2), 173-179.
- Behbodikhah, J., Ahmed, S., Elyasi, A., Kasselmann, L. J., De Leon, J., Glass, A. D. and Reiss, A. B. (2021). Apolipoprotein B and cardiovascular disease: biomarker and potential therapeutic target. *Metabolites* 11(10), 690.
- Biasini, M., Bienert, S., Waterhouse, A., Arnold, K., Studer, G., Schmidt, T., . . . Bordoli, L. (2014). SWISS-MODEL: modelling protein tertiary and quaternary structure using evolutionary information. *Nucleic acids research* 42(W1), W252-W258.
- Cardin, A. D., Witt, K., Chao, J., Margolius, H., Donaldson, V. and Jackson, R. (1984). Degradation of apolipoprotein B-100 of human plasma low density lipoproteins by tissue and plasma kallikreins. *Journal of Biological Chemistry* 259(13), 8522-8528.

- Chaffey, N. (2003). Alberts, B., Johnson, A., Lewis, J., Raff, M., Roberts, K. and Walter, P. Molecular biology of the cell. 4th edn, *Oxford University Press*
- Chapman, M. J. and Kane, J. P. (1975). Stability of the apoprotein of human serum low density lipoprotein: Absence of endogenous endopeptidase activity. *Biochemical and Biophysical Research Communications* 66(3), 1030-1036.
- Chatterton, J. E., Phillips, M., Curtiss, L., Milne, R., Marcel, Y. and Schumaker, V. (1991). Mapping apolipoprotein B on the low density lipoprotein surface by immunoelectron microscopy. *Journal of Biological Chemistry* 266(9), 5955-5962.
- Chiu, M. L., Goulet, D. R., Teplyakov, A. and Gilliland, G. L. (2019). Antibody structure and function: the basis for engineering therapeutics. *Antibodies* 8(4), 55.
- Cooper, A. D. (1997). Hepatic uptake of chylomicron remnants. *Journal of lipid research* 38(11), 2173-2192.
- Corsini, A., Spilman, C., Innerarity, T., Arnold, K., Rall Jr, S., Boyles, J. and Mahley, R. (1987). Receptor binding activity of lipid recombinants of apolipoprotein B-100 thrombolytic fragments. *Journal of lipid research* 28(12), 1410-1423.
- Dunbar, J. and Deane, C. M. (2016). ANARCI: antigen receptor numbering and receptor classification. *Bioinformatics* 32(2), 298-300.
- Esser, V., Limbird, L., Brown, M. S., Goldstein, J. L. and Russell, D. W. (1988). Mutational analysis of the ligand binding domain of the low density lipoprotein receptor. *Journal of Biological Chemistry* 263(26), 13282-13290.
- Fantappie, S., Corsini, A., Sidoli, A., Uboldi, P., Granata, A., Zanelli, T., . . . Catapano, A. (1992). Monoclonal antibodies to human low density lipoprotein identify distinct areas on apolipoprotein B-100 relevant to the low density lipoprotein-receptor interaction. *Journal of lipid research* 33(8), 1111-1121.
- Feingold, K. R. (2021). Introduction to lipids and lipoproteins. *endotext [internet]*.
- Flood, C., Gustafsson, M., Richardson, P. E., Harvey, S. C., Segrest, J. P. and Borén, J. (2002). Identification of the proteoglycan binding site in apolipoprotein B48. *Journal of Biological Chemistry* 277(35), 32228-32233.
- Frasca, V. (2016). Biophysical characterization of antibodies with isothermal titration calorimetry. *Journal of Applied Bioanalysis* 2(3), 827.

- Giudicelli, V., Duroux, P., Rollin, M., Aouinti, S., Folch, G., Jabado-Michaloud, J., . . . Kossida, S. (2022). IMGT® Immunoinformatics Tools for Standardized V-DOMAIN Analysis. *Methods and Protocols*, 477.
- Goldberg, I. J., Wagner, W. D., Pang, L., Paka, L., Curtiss, L. K., DeLozier, J. A., . . . Pillarisetti, S. (1998). The NH2-terminal region of apolipoprotein B is sufficient for lipoprotein association with glycosaminoglycans. *Journal of Biological Chemistry* 273(52), 35355-35361.
- Hadzhieva, M., Pashov, A. D., Kaveri, S., Lacroix-Desmazes, S., Mouquet, H. and Dimitrov, J. D. (2017). Impact of antigen density on the binding mechanism of IgG antibodies. *Scientific reports* 7(1), 3767.
- Huey, R., Morris, G. M. and Forli, S. (2012). Using AutoDock 4 and AutoDock vina with AutoDockTools: a tutorial. *The Scripps Research Institute Molecular Graphics Laboratory* 10550(92037), 1000.
- Janeway, C., Travers, P., Walport, M. and Shlomchik, M. J. (2001). Immunobiology: the immune system in health and disease, *Garland Pub. New York*.
- Janin, J. (1995). Principles of protein-protein recognition from structure to thermodynamics. *Biochimie* 77(7-8), 497-505.
- Ji, E. and Lee, S. (2021). Antibody-based therapeutics for atherosclerosis and cardiovascular diseases. *International Journal of Molecular Sciences* 22(11), 5770.
- Johnson, G. and Wu, T. T. (2000). Kabat database and its applications: 30 years after the first variability plot. *Nucleic acids research* 28(1), 214-218.
- Jumper, J., Evans, R., Pritzel, A., Green, T., Figurnov, M., Ronneberger, O., . . . Potapenko, A. (2021). Highly accurate protein structure prediction with AlphaFold. *Nature* 596(7873), 583-589.
- Kim, S. D., Shin, K.-R. and Zhang, B.-T. (2003). Molecular immunocomputing with application to alphabetical pattern recognition mimics the characterization of ABO blood type. The 2003 Congress on Evolutionary Computation, 2003. CEC'03., *IEEE*.

- Krawczyk, K., Baker, T., Shi, J. and Deane, C. M. (2013). Antibody i-Patch prediction of the antibody binding site improves rigid local antibody–antigen docking. *Protein Engineering, Design & Selection* 26(10), 621-629.
- Krawczyk, K., Liu, X., Baker, T., Shi, J. and Deane, C. M. (2014). Improving B-cell epitope prediction and its application to global antibody-antigen docking. *Bioinformatics* 30(16), 2288-2294.
- Krul, E. S., Kleinman, Y., Kinoshita, M., Pflieger, B., Oida, K., Law, A., . . . Schonfeld, G. (1988). Regional specificities of monoclonal anti-human apolipoprotein B antibodies. *Journal of Lipid Research* 29(7), 937-947.
- Kumar, S., Stecher, G., Li, M., Knyaz, C. and Tamura, K. (2018). MEGA X: molecular evolutionary genetics analysis across computing platforms. *Molecular biology and evolution* 35(6), 1547.
- Kunik, V., Ashkenazi, S. and Ofra, Y. (2012). Paratome: an online tool for systematic identification of antigen-binding regions in antibodies based on sequence or structure. *Nucleic acids research* 40(W1), W521-W524.
- Leem, J., Dunbar, J., Georges, G., Shi, J. and Deane, C. M. (2016). ABodyBuilder: Automated antibody structure prediction with data–driven accuracy estimation. *MAbs, Taylor & Francis*.
- Lefranc, M.-P., Giudicelli, V., Ginestoux, C., Jabado-Michaloud, J., Folch, G., Bellahcene, F., . . . Lane, J. m. (2009). IMGT®, the international ImMunoGeneTics information system®. *Nucleic acids research* 37(suppl_1), D1006-D1012.
- Li, H., Li, D.-q., Li, X.-x. and Wang, L.-q. (2016). The association between oxidized low-density lipoprotein antibodies and hematological diseases. *Lipids in health and disease* 15, 1-10.
- Li, L., Chen, S., Miao, Z., Liu, Y., Liu, X., Xiao, Z. X. and Cao, Y. (2019). AbRSA: a robust tool for antibody numbering. *Protein Science* 28(8), 1524-1531.
- Lowhalidanon, K. and Khunkaewla, P. (2021). Discrimination between minimally modified LDL and fully oxidized LDL using monoclonal antibodies. *Analytical biochemistry* 619, 114103.

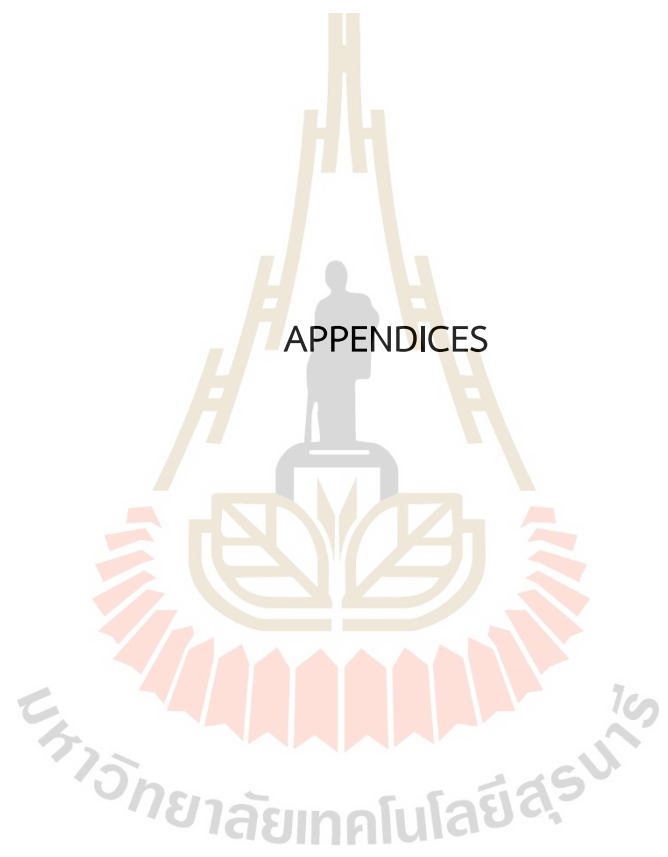
- Mahley, R. W., Innerarity, T. L., Rall Jr, S. C. and Weisgraber, K. H. (1984). Plasma lipoproteins: apolipoprotein structure and function. *Journal of lipid research* 25(12), 1277-1294.
- Marcel, Y. L., Innerarity, T. L., Spilman, C., Mahley, R. W., Protter, A. A. and Milne, R. W. (1987). Mapping of human apolipoprotein B antigenic determinants. *Arteriosclerosis: An Official Journal of the American Heart Association, Inc.* 7(2), 166-175.
- McComb, S., Thiriot, A., Akache, B., Krishnan, L. and Stark, F. (2019). Introduction to the immune system. *Immunoproteomics: Methods and Protocols*, 1-24.
- Meyer, L., López, T., Espinosa, R., Arias, C. F., Vollmers, C. and DuBois, R. M. (2019). A simplified workflow for monoclonal antibody sequencing. *PloS one* 14(6), e0218717.
- Milne, R., Theolis Jr, R., Maurice, R., Pease, R., Weech, P., Rassart, E., . . . Marcel, Y. (1989). The use of monoclonal antibodies to localize the low density lipoprotein receptor-binding domain of apolipoprotein B. *Journal of Biological Chemistry* 264(33), 19754-19760.
- Morita, S.-y. (2016). Metabolism and modification of apolipoprotein B-containing lipoproteins involved in dyslipidemia and atherosclerosis. *Biological and Pharmaceutical Bulletin* 39(1), 1-24.
- Morita, S.-y., Kawabe, M., Nakano, M. and Handa, T. (2003). Pluronic L81 affects the lipid particle sizes and apolipoprotein B conformation. *Chemistry and physics of lipids* 126(1), 39-48.
- Narciso, J. E. T., Uy, I. D. C., Cabang, A. B., Chavez, J. F. C., Pablo, J. L. B., Padilla-Concepcion, G. P. and Padlan, E. A. (2011). Analysis of the antibody structure based on high-resolution crystallographic studies. *New biotechnology* 28(5), 435-447.
- Ofran, Y., Schlessinger, A. and Rost, B. (2008). Automated identification of complementarity determining regions (CDRs) reveals peculiar characteristics of CDRs and B cell epitopes. *The Journal of Immunology* 181(9), 6230-6235.

- Olimpieri, P. P., Chailyan, A., Tramontano, A. and Marcatili, P. (2013). Prediction of site-specific interactions in antibody-antigen complexes: the proABC method and server. *Bioinformatics* 29(18), 2285-2291.
- Olofsson, S.-O., Wiklund, O. and Borén, J. (2007). Apolipoproteins AI and B: biosynthesis, role in the development of atherosclerosis and targets for intervention against cardiovascular disease. *Vascular health and risk management* 3(4), 491-502.
- Pease, R., Milne, R., Jessup, W., Law, A., Provost, P., Fruchart, J.-C., . . . Scott, J. (1990). Use of bacterial expression cloning to localize the epitopes for a series of monoclonal antibodies against apolipoprotein B100. *Journal of Biological Chemistry* 265(1), 553-568.
- Reverberi, R. and Reverberi, L. (2007). Factors affecting the antigen-antibody reaction. *Blood transfusion* 5(4), 227.
- Robbio, L. L., Uboldi, P., Marcovina, S., Revoltella, R. P. and Catapano, A. L. (2001). Epitope mapping analysis of apolipoprotein B-100 using a surface plasmon resonance-based biosensor. *Biosensors and Bioelectronics* 16(9-12), 963-969.
- Roselaar, S. E., Kakkanathu, P. X. and Daugherty, A. (1996). Lymphocyte populations in atherosclerotic lesions of apoE^{-/-} and LDL receptor^{-/-} mice: decreasing density with disease progression. *Arteriosclerosis, thrombosis, and vascular biology* 16(8), 1013-1018.
- Schroeder Jr, H. W. and Cavacini, L. (2010). Structure and function of immunoglobulins. *Journal of allergy and clinical immunology* 125(2), S41-S52.
- Schwede, T., Kopp, J., Guex, N. and Peitsch, M. C. (2003). SWISS-MODEL: an automated protein homology-modeling server. *Nucleic acids research* 31(13), 3381-3385.
- Sela-Culang, I., Kunik, V. and Ofran, Y. (2013). The structural basis of antibody-antigen recognition. *Frontiers in immunology* 4, 302.
- Shoenfeld, Y., Harats, D. and Wick, G. (2001). Atherosclerosis and autoimmunity, *Elsevier*.
- SMALL, L. R. M. R. B. (2006). Modular Structure of Solubilized Human Apolipoprotein B-100. *THE JOURNAL OF BIOLOGICAL CHEMISTRY* 281(28), 19732-19739.

- Smeets, D., Gisterå, A., Malin, S. G. and Tsiantoulas, D. (2022). The spectrum of B cell functions in atherosclerotic cardiovascular disease. *Frontiers in Cardiovascular Medicine* 9.
- Snapkov, I., Chernigovskaya, M., Sinitcyn, P., Lê Quý, K., Nyman, T. A. and Greiff, V. (2022). Progress and challenges in mass spectrometry-based analysis of antibody repertoires. *Trends in Biotechnology* 40(4), 463-481.
- Šrámková, V. (2017). Regulation of lipogenesis in human adipose tissue: Effect of metabolic stress, dietary intervention and aging.
- Stites, W. E. (1997). Protein–protein interactions: interface structure, binding thermodynamics, and mutational analysis. *Chemical reviews* 97(5), 1233-1250.
- Studio, D. (2008). Discovery studio. *Accelrys* [2.1].
- Tian, K., Xu, Y., Sahebkar, A. and Xu, S. (2020). CD36 in atherosclerosis: pathophysiological mechanisms and therapeutic implications. *Current Atherosclerosis Reports* 22, 1-10.
- Triplett, R. B. and Fisher, W. R. (1978). Proteolytic digestion in the elucidation of the structure of low density lipoprotein. *Journal of Lipid Research* 19(4), 478-488.
- Vakser, I. A. (2013). Low-resolution structural modeling of protein interactome. *Current opinion in structural biology* 23(2), 198-205.
- van Leeuwen, E. M., Emri, E., Merle, B. M., Colijn, J. M., Kersten, E., Cougnard-Gregoire, A., . . . de Jong, E. K. (2018). A new perspective on lipid research in age-related macular degeneration. *Progress in retinal and eye research* 67, 56-86.
- Vattepu, R., Sneed, S. L. and Anthony, R. M. (2022). Sialylation as an important regulator of antibody function. *Frontiers in Immunology* 13, 818736.
- Verdonk, M. L., Cole, J. C., Hartshorn, M. J., Murray, C. W. and Taylor, R. D. (2003). Improved protein–ligand docking using GOLD. *Proteins: Structure, Function, and Bioinformatics* 52(4), 609-623.
- Vita, R., Mahajan, S., Overton, J. A., Dhanda, S. K., Martini, S., Cantrell, J. R., . . . Peters, B. (2019). The immune epitope database (IEDB): 2018 update. *Nucleic acids research* 47(D1), D339-D343.

- Waterhouse, A., Bertoni, M., Bienert, S., Studer, G., Tauriello, G., Gumienny, R., . . . Bordoli, L. (2018). SWISS-MODEL: homology modelling of protein structures and complexes. *Nucleic acids research* 46(W1), W296-W303.
- Wu, T. T. and Kabat, E. A. (1970). An analysis of the sequences of the variable regions of Bence Jones proteins and myeloma light chains and their implications for antibody complementarity. *The Journal of experimental medicine* 132(2), 211-250.
- Ye, J., Coulouris, G., Zaretskaya, I., Cutcutache, I., Rozen, S. and Madden, T. L. (2012). Primer-BLAST: a tool to design target-specific primers for polymerase chain reaction. *BMC bioinformatics* 13, 1-11.
- Ye, J., Ma, N., Madden, T. L. and Ostell, J. M. (2013). IgBLAST: an immunoglobulin variable domain sequence analysis tool. *Nucleic acids research* 41(W1), W34-W40.
- Young, S., Bertics, S., Scott, T., Dubois, B., Curtiss, L. and Witztum, J. (1986). Parallel expression of the MB19 genetic polymorphism in apoprotein B-100 and apoprotein B-48. Evidence that both apoproteins are products of the same gene. *Journal of Biological Chemistry* 261(7), 2995-2998.
- Yuriev, E., Agostino, M. and Ramsland, P. A. (2011). Challenges and advances in computational docking: 2009 in review. *Journal of Molecular Recognition* 24(2), 149-164.
- Zobayer, N., Hossain, A. A. and Rahman, M. A. (2019). A combined view of B-cell epitope features in antigens. *Bioinformation* 15(7), 530.

APPENDICES



APPENDIX A

PERMISSION LETTER



This is a License Agreement between Miss Tariga Srirakarn, School of Chemistry, Institute of Science, Suranaree University of Technology 30000, Thailand ("User") and Copyright Clearance Center, Inc. ("CCC") on behalf of the Rightsholder identified in the order details below. The license consists of the order details, the Marketplace Permissions General Terms and Conditions below, and any Rightsholder Terms and Conditions which are included below.

All payments must be made in full to CCC in accordance with the Marketplace Permissions General Terms and Conditions below.

Order Date	21-Dec-2023	Type of Use	Republish in a thesis/dissertation
Order License ID	1428530-1	Publisher	PERGAMON
ISSN	1350-9462	Portion	Image/photo/illustration

LICENSED CONTENT

Publication Title	PROGRESS IN RETINAL AND EYE RESEARCH	Rightsholder	Elsevier Science & Technology Journals
Article Title	A new perspective on lipid research in age-related macular degeneration.	Publication Type	Monographic Series
Date	01/01/1994	Start Page	56
Language	English	End Page	86
Country	United Kingdom of Great Britain and Northern Ireland	Volume	67

REQUEST DETAILS

Portion Type	Image/photo/illustration	Distribution	Worldwide
Number of Images / Photos / Illustrations	1	Translation	Original language of publication
Format (select all that apply)	Print, Electronic	Copies for the Disabled?	No
Who Will Republish the Content?	Author of requested content	Minor Editing Privileges?	No
Duration of Use	Life of current edition	Incidental Promotional Use?	No
Lifetime Unit Quantity	Up to 499	Currency	USD
Rights Requested	Main product		

NEW WORK DETAILS

Title	IDENTIFICATION OF EPITOPES AND BINDING AFFINITY OF MONOCLONAL ANTIBODIES AGAINST HUMAN APOLIPOPROTEIN B-100	Institution Name	Suranaree University of Technology
Instructor Name	Associate Prof. Dr. Panida Khunkaewla	Expected Presentation Date	2024-02-19

ADDITIONAL DETAILS

Order Reference Number	N/A	The Requesting Person / Organization to Appear on the License	Miss Tariga Srirakarn, School of Chemistry, Institute of Science, Suranaree University of Technology 30000, Thailand
------------------------	-----	---	--

REQUESTED CONTENT DETAILS

Title, Description or Numeric Reference of the Portion(s)	Figure 1.1 Composition and main physical-chemical properties of major lipoprotein classes.	Title of the Article / Chapter the Portion Is From	A new perspective on lipid research in age-related macular degeneration.
Editor of Portion(s)	N/A	Author of Portion(s)	Elisabeth M. van Leeuwen, Eszter Emri
Volume / Edition	67	Issue, if Republishing an Article From a Serial	N/A
Page or Page Range of Portion	56-86	Publication Date of Portion	2018-11-01

This is a License Agreement between Miss Tariga Sritrakarn, School of Chemistry, Institute of Science, Suranaree University of Technology 30000, Thailand ("User") and Copyright Clearance Center, Inc. ("CCC") on behalf of the Rightsholder identified in the order details below. The license consists of the order details, the Marketplace Permissions General Terms and Conditions below, and any Rightsholder Terms and Conditions which are included below.

All payments must be made in full to CCC in accordance with the Marketplace Permissions General Terms and Conditions below.

Order Date	21-Dec-2023	Type of Use	Republish in a thesis/dissertation
Order License ID	1428530-2	Publisher	ELSEVIER IRELAND LTD
ISSN	0009-3084	Portion	Image/photo/illustration

LICENSED CONTENT

Publication Title	Chemistry and physics of lipids	Publication Type	Journal
Article Title	Pluronic L81 affects the lipid particle sizes and apolipoprotein B conformation.	Start Page	39
Date	01/01/1966	End Page	48
Language	English	Issue	1
Country	Ireland	Volume	126
Rightsholder	Elsevier Science & Technology Journals		

REQUEST DETAILS

Portion Type	Image/photo/illustration	Distribution	Worldwide
Number of Images / Photos / Illustrations	2	Translation	Original language of publication
Format (select all that apply)	Print, Electronic	Copies for the Disabled?	No
Who Will Republish the Content?	Author of requested content	Minor Editing Privileges?	No
Duration of Use	Life of current edition	Incidental Promotional Use?	No
Lifetime Unit Quantity	Up to 499	Currency	USD
Rights Requested	Main product		

NEW WORK DETAILS

Title	IDENTIFICATION OF EPITOPES AND BINDING AFFINITY OF MONOCLONAL ANTIBODIES AGAINST HUMAN APOLIPOPROTEIN B-100	Institution Name	Suranaree University of Technology
Instructor Name	Associate Prof. Dr. Panida Khunkaewla	Expected Presentation Date	2024-02-19

ADDITIONAL DETAILS

Order Reference Number	N/A	The Requesting Person / Organization to Appear on the License	Miss Tariga Sritrakarn, School of Chemistry, Institute of Science, Suranaree University of Technology 30000, Thailand
-------------------------------	-----	--	---

REQUESTED CONTENT DETAILS

Title, Description or Numeric Reference of the Portion(s)	Figure 1.2 and 1.5	Title of the Article / Chapter the Portion Is From	Pluronic L81 affects the lipid particle sizes and apolipoprotein B conformation.
Editor of Portion(s)	Morita, Shin-ya; Kawabe, Misa; Nakano, Minoru; Handa, Tetsuro	Author of Portion(s)	Morita, Shin-ya; Kawabe, Misa; Nakano, Minoru; Handa, Tetsuro
Volume / Edition	126	Issue, if Republishing an Article From a Serial	1
Page or Page Range of Portion	39-48	Publication Date of Portion	2003-11-01



This is a License Agreement between Miss Tariga Sritrakarn, School of Chemistry, Institute of Science, Suranaree University of Technology 30000, Thailand ("User") and Copyright Clearance Center, Inc. ("CCC") on behalf of the Rightsholder identified in the order details below. The license consists of the order details, the Marketplace Permissions General Terms and Conditions below, and any Rightsholder Terms and Conditions which are included below.

All payments must be made in full to CCC in accordance with the Marketplace Permissions General Terms and Conditions below.

Order Date	21-Dec-2023	Type of Use	Republish in a thesis/dissertation
Order License ID	1428530-3	Publisher	ELSEVIER LTD.
ISSN	0167-7799	Portion	Image/photo/illustration

LICENSED CONTENT

Publication Title	Trends in biotechnology	Publication Type	Journal
Article Title	Progress and challenges in mass spectrometry-based analysis of antibody repertoires	Start Page	463
		End Page	481
Date	01/01/1983	Issue	4
Language	English, English	Volume	40
Country	United Kingdom of Great Britain and Northern Ireland		
Rightsholder	Elsevier Science & Technology Journals		

REQUEST DETAILS

Portion Type	Image/photo/illustration	Distribution	Worldwide
Number of Images / Photos / Illustrations	1	Translation	Original language of publication
Format (select all that apply)	Print, Electronic	Copies for the Disabled?	No
Who Will Republish the Content?	Author of requested content	Minor Editing Privileges?	No
Duration of Use	Life of current edition	Incidental Promotional Use?	No
Lifetime Unit Quantity	Up to 499	Currency	USD
Rights Requested	Main product		

NEW WORK DETAILS

Title	IDENTIFICATION OF EPITOPES AND BINDING AFFINITY OF MONOCLONAL ANTIBODIES AGAINST HUMAN APOLIPOPROTEIN B-100	Institution Name	Suranaree University of Technology
		Expected Presentation Date	2024-02-19
Instructor Name	Associate Prof. Dr. Panida Khunkaewla		

ADDITIONAL DETAILS

Order Reference Number	N/A	The Requesting Person / Organization to Appear on the License	Miss Tariga Sritrakarn, School of Chemistry, Institute of Science, Suranaree University of Technology 30000, Thailand
------------------------	-----	---	---

REQUESTED CONTENT DETAILS

Title, Description or Numeric Reference of the Portion(s)	Figure 1.6	Title of the Article / Chapter the Portion Is From	Progress and challenges in mass spectrometry-based analysis of antibody repertoires
Editor of Portion(s)	Snapkov, Igor; Chernigovskaya, Maria; Sinitcyn, Pavel; Lê Quý, Khang; Nyman, Tuula A.; Greiff, Victor	Author of Portion(s)	Snapkov, Igor; Chernigovskaya, Maria; Sinitcyn, Pavel; Lê Quý, Khang; Nyman, Tuula A.; Greiff, Victor
Volume / Edition	40	Issue, if Republishing an Article From a Serial	4
Page or Page Range of Portion	463-481	Publication Date of Portion	2022-04-01

APPENDIX B

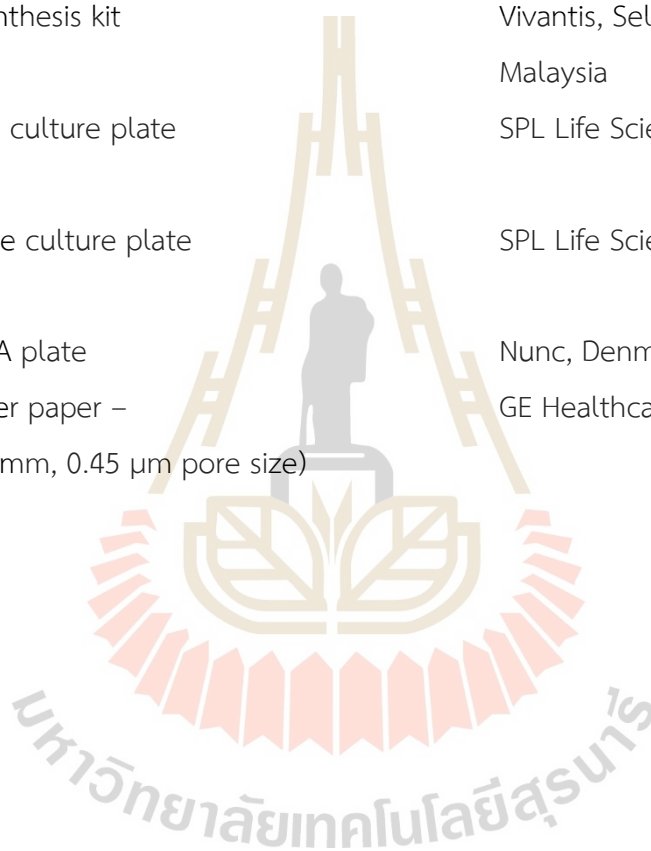
LIST OF CHEMICALS AND MATERIALS USED IN THIS STUDY

Chemicals/Materials	Source
Agarose gel	Norgen, Biotek Corp., Thorold, ON, Canada
Ammonium chloride (NH ₄ Cl)	Carlo Erba, Milan, Italy
Ammonium (II) sulfate (NH ₄) ₂ SO ₄	Carlo Erba, Milan, Italy
Bis-acrylamide	Acros Organics, New Jersey, USA
Bromophenol blue	Carlo Erba, Milan, Italy
Calcium chloride (CaCl ₂)	Carlo Erba, Milan, Italy
Chloroform	Carlo Erba, Milan, Italy
Coomassie brilliant blue R250	AppliChem, Damstadt, Germany
Dimethylsulfoxide (DMSO)	Vivantis, Malaysia
Disodium hydrogen phosphate (Na ₂ HPO ₄)	Carlo Erba, Milan, Italy
Ethanol	Carlo Erba, Milan, Italy
Ethylenediaminetetraacetic acid - disodium salt dehydrate (EDTA)	Amersham Biosciences, Uppsala, Sweden
EZ-Link® NHS-Biotin reagents	Thermo Scientific, Rockford, USA
Fetal Bovine Serum (FBS)	Gibco, Gran Island, N.Y., USA
Fungizone (Amphotericin B)	Gibco, Gran Island, N.Y., USA
GENEzol reagent	Geneaid, Taiwan
Glycerol	Carlo Erba, Milan, Italy
Glycine	Vivantis, Malaysia
Glacial acetic acid	Carlo Erba, Milan, Italy
HiTrap™ Protein G HP column	GE Healthcare, Uppsala, Sweden



Horseradish peroxidase conjugated – rabbit anti-mouse immunoglobulins – antibody	Dako, Glostrup, Denmark
Horseradish peroxidase conjugated – streptavidin	Invitrogen, Thermo Scientific, USA
Hydrochloric acid (HCl)	Carlo Erba, Milan, Italy
Isocove's Modified Dulbecco's – Medium (IMDM)	Gibco, Gran Island, N.Y., USA
Isopropanol	Tedia, USA
Isotypic determination kit	Sigma, St. Louis, MO, USA
Low Density, Human (LDL)	Merck, Germany
2-Mercaptoethanol	Acros Organics, New Jersey, USA
Methanol	Carlo Erba, Milan, Italy
Pierce™ BCA protein assay kit	Thermo Scientific, Rockford, USA
Polyoxyethylenes orbitan monolaurate – (Tween 20)	Scharlau Chemie, S.A., Barcelona, Spain
Potassium chloride (KCl)	Carlo Erba, Milan, Italy
Potassium hydrogen carbonate (KHCO ₃)	Carlo Erba, Milan, Italy
Potassium hydrogen phosphate (KH ₂ PO ₄)	Carlo Erba, Milan, Italy
Serum-free media for hybridoma – culture (ISF-1)	Biochrom AG, Berlin, Germany
Skim milk	Himedia, Mumbai, India
Sodium carbonate (Na ₂ CO ₃)	Carlo Erba, Milan, Italy
Sodium chloride (NaCl)	Carlo Erba, Milan, Italy
Sodium hydrogen carbonate (NaHCO ₃)	Carlo Erba, Milan, Italy
Sodium hydrogen phosphate (NaH ₂ PO ₄)	Carlo Erba, Milan, Italy
Sodium hydroxide (NaOH)	Carlo Erba, Milan, Italy
Sodium lauryl sulfate (SDS)	Carlo Erba, Milan, Italy
SYBR Safe DNA Gel Stain	Thermo Fisher Scientific,
Massachusetts,	USA

3, 3', 5, 5'-Tetramethylbenzidine – substrate (TMB)	Merck, Darmstadt, Germany
N, N, N', N'-Tetramethyl – ethylenediamine (TEMED)	AppliChem, Darmstadt, Germany
10 cm diameter tissue culture dish	SPL Life Science, Gyeonggi-do, Korea
Tri-sodium citrate	Carlo Erba, Milan, Italy
Viva cDNA synthesis kit	Vivantis, Selangor Darul Ehsan, Malaysia
6-wells tissue culture plate	SPL Life Science, Gyeonggi-do, Korea
12-wells tissue culture plate	SPL Life Science, Gyeonggi-do, Korea
96-wells ELISA plate	Nunc, Denmark
Whatman filter paper – (diameter 90 mm, 0.45 µm pore size)	GE Healthcare, Uppsala, Sweden



APPENDIX C

LIST OF INSTRUMENTS USED IN THIS STUDY

Instruments	Source
AKTA start protein purification system	GE Healthcare, Uppsala, Sweden
Automatic high-pressure autoclave – Hirayama	Artisan Technology Group, USA
Autopipettes for tissue culture	Thermo Scientific, USA
Autopipettes – Research plus	Eppendorf, Germany
Biohazard safety cabinet class II	ESCO, Singapore
Brushless microcentrifuge	Denville Scientific, Canada
CO ₂ incubator – Forma series II water jacket	Thermo Scientific, USA
Electrophoresis and electrotransfer unit	Cosmo Bio, Tokyo, Japan
Gene Amp PCR System – 9700	Applied Biosystems, Singapore
Himac compact refrigerated centrifuge – RXII series	Hitachi, Japan
Light microscope – CX21	Olympus, Japan
Microplate spectrophotometer	Tecan, Switzerland
Multichannel pipette – ACURA855	Socorex, Switzerland
Multichannel pipette for tissue culture	Biohit, Finland
Nanodrop spectrophotometer – ND 1000	Thermo Scientific, USA
pH meter	Satorius, Germany
Rapid-Flow sterile disposable Rochester,	Thermo Fisher Scientific,
Refrigerated microcentrifuge – 5415R	Eppendorf, Germany

Sodium Dodecyl Sulfate – (SDS-PAGE) apparatus	BIO-RAD, USA
Trans-blot semi-dry transfer cell	BIO-RAD, USA
Ultra-sonicator	Crest, Pennsylvania
Versatile refrigerated centrifuge – CT15RT	Techcomp, Kowloon, Hong Kong



APPENDIX D

REAGENTS AND BUFFER PREPARATION

1. Reagents for cell culture

1.1 Incomplete Isocove's modified dulbecco's medium (IMDM)

IMDM	powder 1 pack
NaHCO ₃	3.024 g
Gentamycin (40 mg/ml)	1 ml
Dissolve in deionized water and adjust volume to	1,000 ml
Filtrate through 0.2 µm membrane filter	
Add Fungizone (250 µg/ml)	1 ml
Determine the sterility before use and store at 4 °C	

1.2 Complete IMDM medium

Incomplete IMDM medium	90 ml
Heat-inactivated fetal bovine serum	10 ml
Determine the sterility before use and store at 4 °C	

2. Reagents for Enzyme-linked immunosorbent assay (ELISA)

2.1 Coating buffer (0.1 M carbonate-bicarbonate buffer pH 9.6)

Na ₂ CO ₃	1.06 g
NaHCO ₃	1.26 g
H ₂ O	200 ml

Mix and adjust pH to 9.6 with concentrated HCl

Adjust final volume to 250 ml with deionized water

2.2 0.05% Tween-PBS

PBS pH 7.2	500 ml
Tween 20	250 μ l
Mix and store at RT	

2.3 Blocking solution (2% skim milk-PBS)

Skim milk	2 g
PBS pH 7.2	100 ml
Freshly prepare before use	

2.4 Stop reaction solution (1N HCl)

Concentrated HCl	8.3 ml
H ₂ O	91.7 ml
Slowly dropwise HCl to H ₂ O	
Store at RT	

2.5 10X Phosphate buffer saline (PBS) pH 7.2

NaCl	80 g
KCl	2 g
Na ₂ HPO ₄	11.5 g
KH ₂ PO ₄	2 g
H ₂ O	700 ml
Adjust pH to 7.2 with NaOH or HCl	
Adjust volume with H ₂ O to	1,000 ml

2.6 1X PBS pH 7.2

10x PBS pH 7.2	100 ml
H ₂ O	900 ml
Store at RT	

3. Reagents for Sodium Dodecyl Sulfate – Poly Acrylamide Gel Electrophoresis (SDS-PAGE)

3.1 1.5 M Tris-HCl pH 8.8

Tris-base	9.08 g
H ₂ O	20 ml
Adjust pH to 8.8 with HCl	
Adjust volume with H ₂ O to	50 ml
Store at 4 °C	

3.2 0.5 M Tris-HCl pH 6.8

Tris-base	3 g
H ₂ O	25 ml
Adjust pH to 6.8 with HCl	
Adjust volume with H ₂ O to	50 ml
Store at 4 °C	

3.3 30% Monomer (30.8% acrylamide, 2.7% bis-acrylamide)

Acrylamide	15 g
Bis-acrylamide	0.4 g
H ₂ O to	50 ml
Filtrate through 0.45 µm filter paper	
Store in the dark at 4 °C	

3.4 10X Running buffer

Glycine	144.13 g
Tris-base	30.28 g
SDS	10 g
H ₂ O to	1,000 ml
Store at RT	

3.5 1X Running buffer

10X Running buffer	100 ml
--------------------	--------

H ₂ O	900 ml
Store at RT	

3.6 10% Ammonium persulfate (APS)

Ammonium persulfate	0.05 g
H ₂ O	0.5 ml
Mix well, aliquot to 100 µl/tube, and store at -20 °C	

3.7 10% Sodium dodecyl sulfate (SDS)

SDS	0.1 g
H ₂ O	1 ml
Mix well, aliquot to 150 µl/tube, and store at -20 °C	

3.8 Stacking gel (4% gel, 0.125 M Tris pH 6.8)

H ₂ O	1.5 ml
0.5 M Tris-HCl pH 6.8	625 µl
Acrylamide/bis (30.8%/2.7%)	332.5 µl
10% SDS	25 µl
10% APS	12.5 µl
TEMED	5 µl
Total volume	2.5 ml

3.9 Resolving gel (10% gel, 0.375 M Tris pH 8.8)

H ₂ O	4 ml
1.5 M Tris-HCl pH 8.8	2.5 ml
Acrylamide/bis (30.8%/2.7%)	3.3 ml
10% SDS	100 µl
10% APS	50 µl
TEMED	10 µl
Total	10 ml

3.10 10X non-reducing buffer (NRB)

H ₂ O	1.25 ml
1 M Tris-HCl pH 6.8	0.625 ml
Glycerol	1 ml
10% SDS	2 ml
1% Bromophenol blue	125 µl
Aliquot to 300 µl/tube and keep at -20 °C	

3.11 5X reducing buffer (RB)

10X NRB	250 µl
2-ME	25 µl
H ₂ O	225 µl
Aliquot to 100 µl/tube and keep at -20 °C	

3.12 0.025% Coomassie brilliant blue R250 (40% methanol; 7% acetic acid)

Coomassie brilliant blue R250	0.25 g
Methanol	400 ml
Glacial acetic acid	70 ml
Add H ₂ O to	1,000 ml
Mix well until dissolved and store at RT	

3.13 De-staining gel solution I (40% methanol, 7% acetic acid)

Methanol	400 ml
Glacial acetic acid	70 ml
Add H ₂ O to	1,000 ml
Mix well until dissolved and store at RT	

3.14 De-staining gel solution II (5% methanol, 7% acetic acid)

Methanol	50 ml
Glacial acetic acid	70 ml

Add H₂O to 1,000 ml
Mix well until dissolved and store at RT

4. Reagents for Western blot

4.1 Towbin buffer (25 mM Tris; 192 mM Glycine; 20% Methanol)

Tris-base 3.03 g
Glycine 14.4 g
Methanol 200 ml
Adjust volume with H₂O to 1,000 ml
Mix well until dissolved and store at RT

4.2 5% Skim milk

Skim milk 2.5 g
1X PBS pH 7.2 50 ml
Mix well until dissolved (Freshly prepared before use)

4.3 0.1% Tween-PBS

Tween 20 0.5 ml
1x PBS pH 7.2 500 ml
Mix well and store at RT

5. Reagents for immunoglobulin G purification

5.1 Binding buffer (20 mM Sodium phosphate; pH 7.0)

1M Na₂HPO₄ 11.56 ml
1M NaH₂PO₄ 8.4 ml
H₂O 800 ml
Adjust pH to 7.0 with 1N HCl
Adjust volume with H₂O to 1,000 ml
Filtrate through 0.45 µm Whatman filter paper (GE Healthcare, Uppsala, Sweden) and degas by sonication before use

5.1.1 1 M Na₂HPO₄

Na ₂ HPO ₄	2.84 g
H ₂ O	20 ml

5.1.2 1M NaH₂PO₄

NaH ₂ PO ₄	2.76 g
H ₂ O	20 ml

5.2 Elution buffer (0.1 M Glycine pH 2.7)

Glycine	0.7506 g
H ₂ O	50 ml

Adjust pH to 2.7 with 1N HCl

Adjust volume with H₂O to 100 ml

Filtrate through 0.45 µm Whatman filter paper (GE Healthcare, Uppsala, Sweden) and degas by sonication before use

Store at RT

5.3 Neutralizing buffer (1 M Tris-HCl pH 9.0)

Tris-base	6.05 g
H ₂ O	20 ml

Adjust pH to 9.0 with 1N HCl

Adjust volume with H₂O to 50 ml

Store at RT

5.4 20% Ethanol

Absolute ethanol	200 ml
H ₂ O	800 ml

Filtrate through 0.45 µm Whatman filter paper (GE Healthcare, Uppsala, Sweden) and degas by sonication before use

Store at RT

6. Reagents for agarose gel electrophoresis

6.1 50X TAE buffer (0.04 M Tris-base, 0.002 M EDTA, and 0.02 M Acetic acid)

Tris-base	242 g
Disodium EDTA	18.61 g
Glacial acetic acid	57.1 ml
Add H ₂ O to	1,000 ml
Store at RT	

6.2 1X TAE buffer

50X TAE buffer	20 ml
H ₂ O	980 ml
Store at RT	

6.3 1% Agarose gel

Agarose	0.3 g
Add 1X TAE buffer to	30 ml
Melt until agarose well dissolve using microwave	
Cool down at RT	
Add SYBR green	1 μ l
Pour the mixture into the gel cassette, place the combs, and let the gel polymerize at RT	

7. 100 mM Tris-HCl pH 8, 100 ml

Tris-base	1.21 g
H ₂ O to	100 ml
Adjust pH with 6 M HCl to pH 8	

8. Electrophoresis sample buffer, 25 ml

5% (w/v) SDS (289.43 g/mol)	1.25 g
-----------------------------	--------

40% (w/v) sucrose (342.24 g/mol)	10 g
10% (v/v) 2-mercaptoethanol	2.5 ml
0.01% (w/v) bromophenol blue	2.5 μ l
H ₂ O to	25 ml

9. 100 mM EDTA, 25 ml

EDTA (372.24 g/mol)	0.93 g
H ₂ O to	25 ml



CURRICULUM VITAE

Name : Miss Tariga Srirakarn
Date of birth : Aug 20, 1998
Nationality : Thai
Current address : School of Chemistry, Institute of Science, Suranaree
University of Technology, Nakhon Ratchasima, 30000, Thailand
Tel. +66-879481072, E-mail: ging.tarigar3@gmail.com

EDUCATION

2021, B.Sc. (Chemistry), 1st Class honor, School of Chemistry, Institute of Science, Suranaree University of Technology.

SCHOLARSHIP (2017 – 2023)

Development and Promotion of Science and Technology Talent project (DPST) student

EXTRA-CURRICULAR ACTIVITIES:

Attending a workshop Molecular docking at Kasetsart University during June 7-8, 2023.

POSTER PRESENTATION

Srirakarn T., Lowhalidanon K., Khunkaewla P. Epitope mapping and binding affinity of the monoclonal antibodies against human apoB-100. The 17th International Symposium of the Protein Society of Thailand (PST2022). At Khum Kham International Convention Centre, Chiang Mai, Thailand during November 9-11, 2022. For poster presentation.

ORAL PRESENTATION

Srirakarn T., Lowhalidanon K., Khunkaewla P. Epitope mapping and binding affinity of the monoclonal antibodies against human apoB-100. Science Postgrad Annual Research Conference: SPARC 2023 Institute of Science, Suranaree University of Technology. At Suranaree University of Technology, Nakhon Ratchasima, Thailand on March 18, 2022. For oral presentation.